INSTITUTO SUPERIOR DE ENGENHARIA DE LISBOA

Área Departamental de Engenharia de Eletrónica e Telecomunicações e de computadores

IoT Network – Design and Implementation

Bruno Alexandre Duarte Santos Costa

Licenciado

Dissertação para obtenção do Grau de Mestre
em Engenharia Eletrónica e de Telecomunicações

Orientador: Prof. Doutor Pedro Renato Tavares Pinho

Júri:

Presidente: Prof. Nuno António Fraga Juliano Cota

Vogais: Prof. Doutor Nuno Miguel Abreu Luís

Prof. Doutor Pedro Renato Tavares Pinho

Dezembro, 2018

INSTITUTO SUPERIOR DE ENGENHARIA DE LISBOA

Área Departamental de Engenharia de Eletrónica e Telecomunicações e de computadores

IoT Network – Design and Implementation

Bruno Alexandre Duarte Santos Costa

Licenciado

Dissertação para obtenção do Grau de Mestre
em Engenharia Eletrónica e de Telecomunicações

Orientador: Prof. Doutor Pedro Renato Tavares Pinho

Júri:

Presidente: Prof. Nuno António Fraga Juliano Cota

Vogais: Prof. Doutor Nuno Miguel Abreu Luís

Prof. Doutor Pedro Renato Tavares Pinho

Dezembro, 2018

Agradecimentos

Em primeiro lugar gostaria de agradecer ao meu Orientador, o professor Pedro Pinho, que para além de me ter aceite enquanto orientando sobre um tema que sempre achei aliciante, sempre me prestou bastante auxílio e me deu todo o suporte e confiança para a realização do trabalho. Obrigado professor por nunca ter deixado de acreditar em mim. Em segundo lugar gostaria de agradecer ao Instituto de Telecomunicações de Aveiro e aos alunos Felizberto Pereira e Rui Oliveira, que para além dos concelhos que me foram dando para a realização da dissertação, despenderam do seu tempo várias vezes para me acompanharem nos resultados medidos.

Gostaria de agradecer também à minha namorada Patrícia, por todo o apoio que me foi dando ao longo deste ano bastante complicado, mesmo estando a vários kms de distância, nunca deixou de acreditar em mim e sempre me deu motivação. A toda a minha família, em especial aos meus pais, aos meus irmãos, aos meus amigos e colegas, por tudo o que contribuíram, não só para a realização da dissertação, mas também durante todo o meu percurso académico e profissional.

Finalmente, gostaria de deixar um agradecimento especial a todos os meus colegas da Nokia no Reino Unido, principalmente às pessoas que me facilitaram bastante as viagens a Portugal e que também tornaram a realização desta dissertação possível. Obrigado Bobby, Sanjeev, Vijay e Vinoth.

Resumo

Nos últimos anos um novo conceito conhecido na linguagem anglo-saxónica como IoT *(Internet of Things)* ganhou destaque no mundo da tecnologia. A IoT tem como principal objetivo permitir que diversos tipos de objetos físicos, como por exemplo carros, casas e cidades consigam transmitir a informação que obtêm de forma autónoma através de sensores, para plataformas que as recebem e as utilizam de forma inteligente, moldando assim uma rede de objetos interligados, sem existir qualquer tipo de intervenção humana.

Para se perceber este conceito, foi efetuado um estudo às redes que servem de base a este conceito, as redes LPWA *(Low Power Wide Area)*, e em mais detalhe à tecnologia LoRa. De forma a estimar a cobertura desta tecnologia, foi efetuado um planeamento teórico utilizando o modelo de OH *(Okumura-Hata)*, e com base nos resultados obtidos, recorreu-se a um simulador electromagnético, o *CloudRF*, que permitiu estimar mais em detalhe a cobertura para a zona de Aveiro. De forma a validar os resultados obtidos teoricamente e por simulação, foi efetuado um conjunto de medidas em campo em alguns pontos da cidade de Aveiro.

Da análise global de resultados obtidos, concluiu-se que a tecnologia LoRa é de facto bastante viável para ser utilizada numa implementação de uma rede IoT num ambiente urbano. O modelo de OH quando adaptado com as margens de cobertura adequadas para o tipo de ambiente em estudo permite obter uma boa aproximação em termos de cobertura outdoor. Apesar de ser bastante sensível a movimentações, a tecnologia LoRa através das medidas realizadas permitiu obter coberturas até 2 km num ambiente de propagação maioritariamente urbano, e superiores a 5 km numa área mais aberta e com uma maior linha de vista.

Palavras-Chave: IoT, LPWA, LoRa, planeamento, cobertura, *Okumura-Hata*, simulação, *CloudRF*, medidas, Aveiro

Abstract

In recent years a new concept known in the anglo-saxonic language as IoT (*Internet of Things*) has gained prominence in the world of technology. IoT's main objective is to allow various types of physical objects, such as cars, houses and cities to transmit the information they obtain autonomously through sensors, to platforms that receive and use them intelligently, forming a network of interconnected objects, without any kind of human intervention.

To understand this concept, a study was made of the networks that underlie this concept, LPWA (*Low Power Wide Area Networks*), and in more detail to LoRa technology. In order to estimate the coverage of this technology, a theoretical planning was performed using the OH model (*Okumura-Hata*), and based on the results obtained, an electromagnetic simulator *(CloudRF)*, was used, which allowed to estimate in more detail the coverage in the area of study. In order to validate the results obtained theoretically and by simulation, a set of measurements was made in the field in some points of the city of Aveiro.

From the global analysis of the obtained results, it was concluded that LoRa technology is in fact quite feasible to be used in an implementation of an IoT network in an urban environment. The OH model when adapted with the appropriate coverage margins for the type of study environment allows a good approximation in terms of outdoor coverage. Despite being very sensitive to movements, it was possible to obtain distances up to 2 km in a mostly urban propagation environment, and more than 5 km in a more open area with a greater line of sight.

***Keywords*:** IoT, LPWA, LoRa, planning, coverage, *Okumura-Hata*, simulation, *CloudRF*, measurements, Aveiro

Contents

List of Figures

List of Tables

List of Acronyms

3GPP – 3rd Generation Partnership Project

ADR – Adaptive Data Rate

AES – Advanced Encryption Suite

AppEUI – Application Identifer

Appskey – Application Session Key

BER – Bit Error Rate

BL – Boby Loss

BLE – Bluetooth Low Energy

BPL – Building Penetration Loss

BW – Bandwidth

CDF – Cumulative Density Function

CF – Carrier Frequency

CIoT – Celular IoT

CPL – Car Penetration Loss

CR – Coding Rate

CRC – Cyclic Redundancy Check

CSS – Chirp Spread Spectrum

dB – Decibel

dBm – Decibel Miliwatt

DBPSK – Differential Binary Phase Shift Keying

DE – Data Rate Optimization

DEM – Digital Elevation Models

DH – Diffie-Hellman

DL – Downlink

DSS – Direct Spread Spectrum

DevAddr – Device Address

EC – European Commission

EC-GSM – Extended Coverage GSM

ECC – Electronic Communications Committee

EDGE – Enhanced Data Rates for GSM Evolution

EIRP – Effective Isotropic Radiated Power

ERP – Effective Radiated Power

ETSI – European Telecommunications Standards Institute

FCnt – Frame Counter

FCtrl – Frame Control

FEC – Forward Error Correction

FHDR – Frame Header

FHSS – Frequency Hopping Spread Spectrum

FOpts – Frame Options

FPort – Port Field

FRMPayload – Frame Payload

GMSK – Gaussian Minimum Shift Keying

GPRS – General Packet Radio Service

GPS – Global Positioning System

GSM – Groupe Speciale Mobile

IF – Interference

IH – Implicit Header

IT – Instituto de Telecomunicações

ITU – International Telecommunication Union

IoT – Internet of Things

KML – Keyhole Markup Language

LBT – Listen Before Talk

LIDAR – Light Detection and Ranging

LNF – Log-Normal Fading

LPWA – Low Power Wide Area

LTE-M – Long Term Evolution for Machines

M2M – Machine-2-Machine

MAC – Media Access Control

MCG – Multi Channel Gateway

MHDR – MAC Header

MIC – Message Integrity Code

MMSE – Minimum Mean Square Error

Mtype – Message Type

NASA – National Aeronautics and Space Administration

NB-IoT – Narrowband-IoT

NS – Network Server

NwkSKey – Network Session Key

OH – Okumura-Hata

OQPSK – Offset Quadrature Phase Shift Keying

OTAA – Over-the-air-activation

PDF – Probability Density Function

PL – Path Loss

PSR – Packet Success Rate

RF – Rayleigh Fading

RFID – Radio-Frequency Identification

RPMA – Random Phase Multiple Access

RSA – Rivest-Shamir-Adleman

SCG – Single Channel Gateway

SF – Spreading Factor

SIG – Special Interest Group

SNR – Signal-To-Noise Ratio

SRD – Short Range Devices

SRTM – Shuttle Radar Topography Mission

TTN – The Things Network

ToA – Time-on-Air

UL – Uplink

UMTS – Universal Mobile Telecommunications System

UNB – Ultra Narrow Band

WPAN – Wireless Personal Area Network

WSN – Wireless Sensor Network

List of Symbols

$\boldsymbol{\gamma}$ – Threshold value

$\boldsymbol{\lambda}$ – Wavelength

$\boldsymbol{\mu}$ – Mean value

$\boldsymbol{\sigma}$ – Standard deviation

$\boldsymbol{\alpha(h_{Sensor})}$ – Correction factor for the sensor height

$\boldsymbol{A_{Gateway}}$ – Area served by one gateway

$\boldsymbol{A_{Total}}$ – Total area in study

$\boldsymbol{BL_{Marg}}$ – Body Loss margin

$\boldsymbol{BPL_{Marg}}$ – Building Penetration Loss margin

$\boldsymbol{BW_n}$ – Noise Bandwidth

$\boldsymbol{B_D}$ – Doppler spread

$\boldsymbol{B_S}$ – Signal bandwidth

$\boldsymbol{c}$ – Speed of light in vacuum

$\boldsymbol{CPL_{Marg}}$ – Car Penetration Loss margin

$\boldsymbol{d}$ – Distance between the transmitter and the receiver

$\boldsymbol{d_0}$ – Reference distance between the transmitter and the receiver

$\boldsymbol{d_{GW-GW}}$ – Relative distance between two gateways

$\boldsymbol{d_{máx}}$ – Maximum distance between the transmitter and the receiver

$\boldsymbol{E_b}$ – Energy of bit

$\boldsymbol{f_c}$ – Frequency of the link

$\boldsymbol{f_m}$ – Doppler shift

$\boldsymbol{G_{Gateway}}$ – Gain of the gateway's antenna

$\boldsymbol{G_{RX}}$ – Receiver antenna gain

$\boldsymbol{G_{Sensor}}$ – Gain of the sensor's antenna

$\boldsymbol{G_{TX}}$ – Transmitter antenna gain

$\boldsymbol{h_{Gateway}}$ – Height of the gateway

$\boldsymbol{h_{Sensor}}$ – Height of the sensor

IF_{Marg} – Interference margin

k – Boltzmann's constant

LNF_{Marg} – Log-Normal Fading margin

$L_{Connectors}$ – Attenuation caused by the connectors

L_{Feeds} – Attenuation caused by the feeds

L_p – Propagation loss

$L_{p_{50\%}}$ – Propagation loss at 50% of the coverage

$L_{p_{95\%}}$ – Propagation loss at 95% of the coverage

n – Path loss decay

$n_{payload}$ – Payload length

$n_{preamble}$ – Preamble length

NF – Noise Figure

N_0 – Noise Power spectral density

N_b – Number of bits/symbol

$N_{Gateways}$ – Number of necessary gateways

PL – Path loss

$\overline{PL}$ – Mean path loss

P_{RX} – Received power

$Prob$ – Probability

P_{TX} – Transmitted power

Q – Q-function

R – Radius of the cell

RF_{Marg} – Rayleigh Fading margin

R_C – Chip-rate

R_S – Symbol rate

R_b – Data rate

$SS_{Design_{UL_{in-car}}}$ – Design Signal Strength Uplink In-Car

$SS_{Design_{UL_{indoor}}}$ – Design Signal Strength Uplink Indoor

$SS_{Design_{UL_{outdoor}}}$ – Design Signal Strength Uplink Outdoor

$SS_{Req_{DL}}$ – Signal Strength Required Downlink

$SS_{Req_{UL}}$ – Signal Strength Required Uplink

SS_{LoRa} – Sensitivity of a LoRa device

$\boldsymbol{T}$ – Room temperature

$\boldsymbol{T_C}$ – Coherence time

$\boldsymbol{T_S}$ – Symbol time

$\boldsymbol{T_{packet}}$ – Packet duration

$\boldsymbol{T_{payload}}$ – Payload duration

$\boldsymbol{T_{preamble}}$ – Preamble duration

$\boldsymbol{U}$ $(\boldsymbol{\gamma})$ – Useful service area

$\boldsymbol{v}$ – Relative velocity

$\boldsymbol{X_\sigma}$ – Gaussian random variable

1

Introduction

This chapter introduces the developed dissertation, where the motivation and its objectives are described. The structure of this report is also presented with a brief description of the various chapters.

1.1. Motivation

With the sustained fast digitalization of everyday life, existing communication technologies are faced with new challenges. With the rapid growth of M2M (Machine-to-Machine) communications, a new concept called IoT *(Internet of Things)* has emerged. The paradigm of IoT relies on the deployment of billions of objects having the capability of transmitting information about their context and environment and to create a real-time, secured and efficient interaction between the real and the virtual worlds. As an exponential growth of connected things is expected in the incoming years, a new range of protocols and technologies has arisen: LPWAN's (Low Power Wide Area Networks).

In order to address the various requirements of the IoT applications, LPWA technologies presents better trade-offs between range, power consumption and cost, when compared to the traditional cellular and short range wireless technologies, such as Wi-Fi or Bluetooth, making them the most suitable technology for IoT connectivity. Among various LPWA technologies, LoRa (Long Range) is one of most relevant due to its unique modulation, which makes it a very versatile technology that can adapt to different type of environments and applications, and therefore the focus on this thesis.

1.2. Objectives

With IoT being the future, IT (Instituto de Telecomunicações) and its research departments have started to deploy a Smart City network using LoRa technology in the city of Aveiro, Portugal. In this way, the objective of this dissertation focuses on the evaluation and estimation of coverage to deploy in a near-future an efficient urbanized Smart City, with emphasis on the city of Aveiro, but also applicable to other cities that share the same environment characteristics.

For that, first a theoretical network planning is proposed to estimate the link budget and consequently the coverage for the area in study. Posteriorly, a simulation of a LoRa network with a Radio Planning Software is performed, and finally the performance of the network is evaluated based on a set of measurements collected in the field.

1.3. Document Organization

This document is organized as follows:

Chapter 1 details the dissertation's motivation and its objectives are described. The organization of the document is also presented.

Chapter 2 provides an overview about the IoT, mainly it's concept, forecasts and challenges. To fulfil the IoT requirements, LPWAN's have emerged, and therefore their characteristics are explained, as well a comparation between them and the existing networks.

Chapter 3 presents a detailed description of the LoRa technology, mainly it's physical layer and MAC layer.

Chapter 4 proposes the utilization of some concepts that are necessary for the realization of the network planning. The steps and the solutions adopted for the proposed solution are explained and the theoretical calculations are done, namely, the link budget.

Chapter 5 provides simulation results using a radio planning Software adapted to LoRa technology, accordingly to the calculations obtained from the previous chapter.

Chapter 6 presents the analysis carried in the real-life deployment, in terms of reliability and availability and provides the comparation with the expected results.

Chapter 7 summarizes the work performed in this dissertation, the main conclusions and suggests possible future improvements.

2

Introduction to IoT

This chapter aims to describe the concepts and technologies addressed and necessary for the understanding of the elaborated dissertation. An introduction to the M2M (Machine-2-Machine) concept, namely its definition, architecture and growth potential, is made initially. It then describes in detail what is the IoT *(Internet of Things)*, how it came about, and all its potential for growth. Due to all its potential and the advantages that IoT introduces, many sectors and industries use this technology. Therefore, some examples of applications are identified and described, as well as some challenges that IoT will have to overcome when it grows, namely in terms of the security and privacy of its users.

The study of wireless networks, namely short and long-range networks, is shown, where examples of technologies and the characteristics associated with each are shown. Taking into account the main requirements of IoT, i.e the need to interconnect devices with a low energy consumption, but with a wide area of coverage. The LPWA (Low Power Wide Area) networks are described in more detail, namely the modulation used, the explanation of the physical layer and how the access to the medium is performed by the various technologies classified as LPWA.

Finally, a comparison is made between the various existing LPWA technologies in the market, as well as the solutions presented by 3GPP (3rd Generation Partnership Project) for this type of networks, taking advantage of existing cellular networks.

2.1 Internet of Things

New technologies play an increasingly dominant role in the daily lives of the human being. Over the last few years, a new concept has gained prominence in the world of technologies. With an increasingly important role in our day, IoT is a revolutionary technology that is changing our lives. The integration of intelligent devices into the everyday life of the human being is becoming more frequent since they contribute in a very significant way to a better quality of life of its users. IoT appears in this context, in order to allow the interconnection of all these devices through the Internet, in order to share information with each other and automatically. Each IoT device has its own way of working, but there is one common feature to everyone: they are all interconnected with each other over the Internet. For this communication between devices to be established, IoT had as its principle an already existing concept, consisting essentially of communication between machines, which is called M2M, described in the next subchapter.

2.2 Machine-2-Machine

M2M denotes several concepts, for example: Man-to-Machine, Machine-to-Man, Machine-to-Mobile and Mobile-to-Machine. However, the most common and most used concept is Machine-to-Machine.

M2M is a general concept that can be used to describe any technology that allows certain networked devices, such as computers, sensors and mobile devices, to share information and perform certain actions without the need for human being.

Applications that support M2M provide benefits to individuals, businesses, communities and organizations across industries, as they can reduce production costs, optimize processes, and increase the efficiency of multiple applications.

2.2.1 Architecture and data management

Although each implementation of this concept is unique, the overall architecture of an M2M network is usually common to the various applications. Figure 2.1 shows an example of an

M2M architecture, which is essentially divided into three parts: M2M device local network, communication network and operator network.

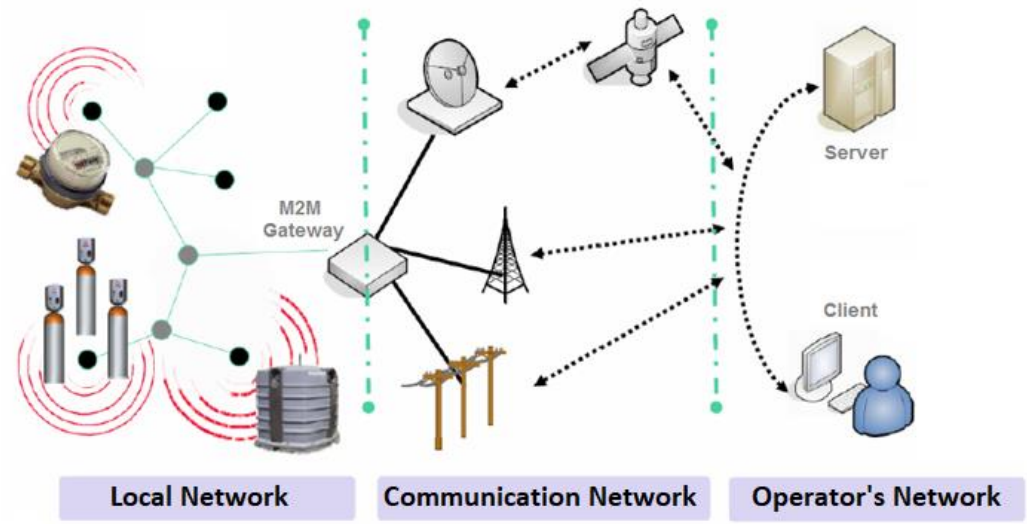

Figure 2.1 –M2M Architecture example [1]

The Local Network is formed by communication between all M2M devices. In this, all acquisitions and data sharing between devices is performed. Normally these are sensors, meters, RFID devices (Radio Frequency Identification) and other related devices. The local network formed by these devices, interconnected with a suitable gateway, allows the data to be forwarded to the communication network, which then redirects them to the corresponding operator.

The Communication Network consists of the infrastructure that allows communication between the M2M devices and the applications that handle them, at a high distance. For this purpose, technologies characterized by enabling long range communication such as for example mobile cellular networks, satellite links and fibre optic communications are commonly used.

The Operator's Network allows the data sent by the M2M devices to be received by M2M servers and applications, which are then in charge of evaluating the received data and consequently performing certain actions based on the data analysis performed.

2.2.2 Potential and growth

As can be seen from Figure 2.2, the number of M2M connections has grown exponentially over the various sectors that use this technology.

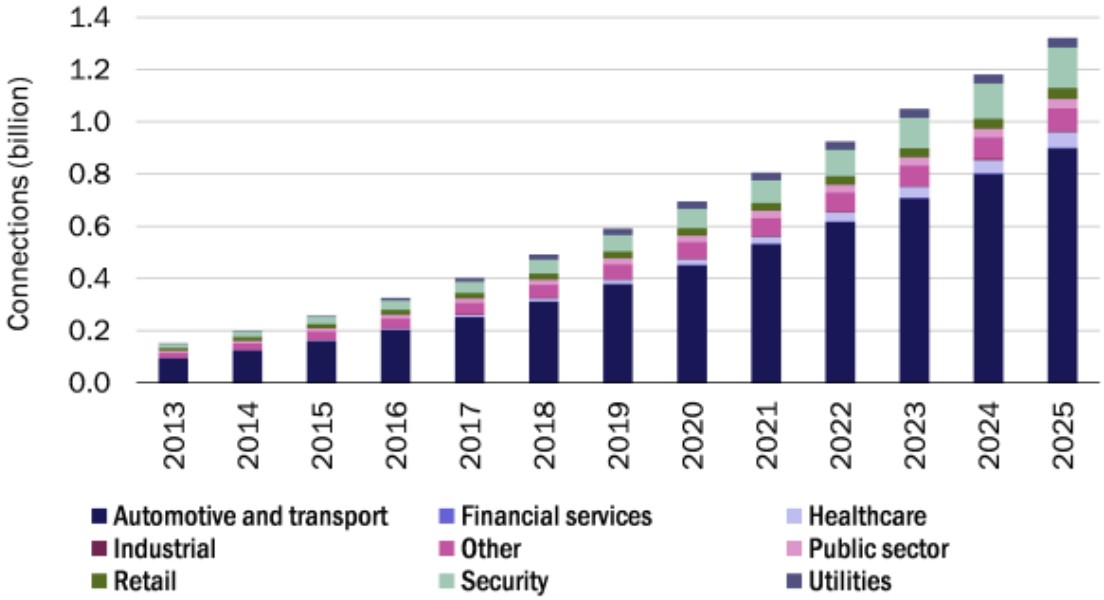

Figure 2.2 – Prevision of the M2M connecivity worlwide between 2013 and 2015 [2]

According to Analysis Mason in [2], the number of connections between M2M devices worldwide is expected to grow to more than 1.3 billion by 2025. This increase will be driven mainly by the continued growth of embedded and aftermarket connectivity in the automation industry and transport, which is increasingly introducing more links between devices over the years, while also highlighting the contribution of the other sectors to this forecast.

2.3 Definition of IoT

IoT is, syntactically speaking, formed by two terms: "Internet" and "Things". The first term defines the basis upon which IoT is sustained, and through which it is possible that the "things", identified by the second term, can share information with one another. IoT aims to bring the real world as close as possible to information systems, where simple everyday objects, vehicles or even buildings are equipped with sensors, and enables these objects to intelligently capture and share the most varied information (i.e temperature reading, humidity, brightness, etc.) and

can be used in different business areas. In other words, IoT includes any type of physical object or entity that can be made addressable and has the capability to transmit data without human intervention, and as such, Machine-2-Machine (M2M) communications are required to support it. The concept is to connect to the Internet all the things that are possible and useful to connect, including things that initially when they were produced were never intended to connect to the internet.

As with M2M technology, the IoT concept is constantly expanding and rapidly in the coming years this convergence will unleash a new dimension of services that improve the quality of life of consumers and the productivity of companies.

Although the concept of IoT is becoming more common these days and is undergoing a major evolution worldwide, its integration in the telecommunications market took several years to take place, as explained below.

2.3.1 Historic evolution of the concept

In 1990, John Romkey and Simon Hackett created the first device to be connected to the Internet without being a computer, a toaster. This was presented during an INTEROP conference, in which it was remotely controlled by a computer and was a tremendous success during it. However, during their demonstrations at the conference, bread was manually added to the toaster, which stripped them of their independence. A year later, a robot was added to the toaster to put bread into the toaster, making the system completely autonomous, as shown in Figure 2.3.

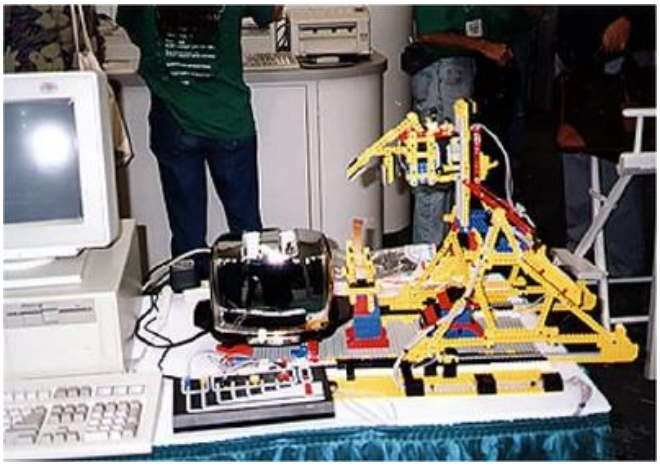

Figure 2.3 – Autonomous toaster [3], [4]

Although already existing a device belonging to the world of IoT, the concept itself emerged, fruit of the work developed by the Auto-ID Center. Kevin Ashton, co-founder and CEO of the company, presented to Procter & Gamble in 1999 a new technology, Radio Frequency Identification (RFID), and gave the title "Internet of Things" as its title. RFID technology quickly became a success and began to be used primarily in the pharmaceutical industry because of the ease with which articles were monitored. However, only 10 years later, the IoT concept began to be praised, particularly in the summer of 2010 when information emerged that Google Street View had not only taken 360-degree photos but also stored tons of data of people's Wi-Fi networks, giving rise to social debate about whether this was the beginning of a new Go-ogle strategy, not only to index the Internet but also to index the entire physical world [4].

The concept of IoT emerged in such a way that in 2012, the theme of the largest Internet conference in Europe, LeWeb, was IoT.

2.3.2 Potential and growth of IoT

As mentioned in the previous subchapter, the term IoT had its first appearance in 1999. Today, the term IoT is quite broad and diversified in terms of applications, as will be described in the next subchapter, in such a way that it is estimated that the number of devices connected to the Internet by the IoT networks is superior to other technological devices, such as smartphones, tablets, laptops and computers, as shown by the Figure 2.4.

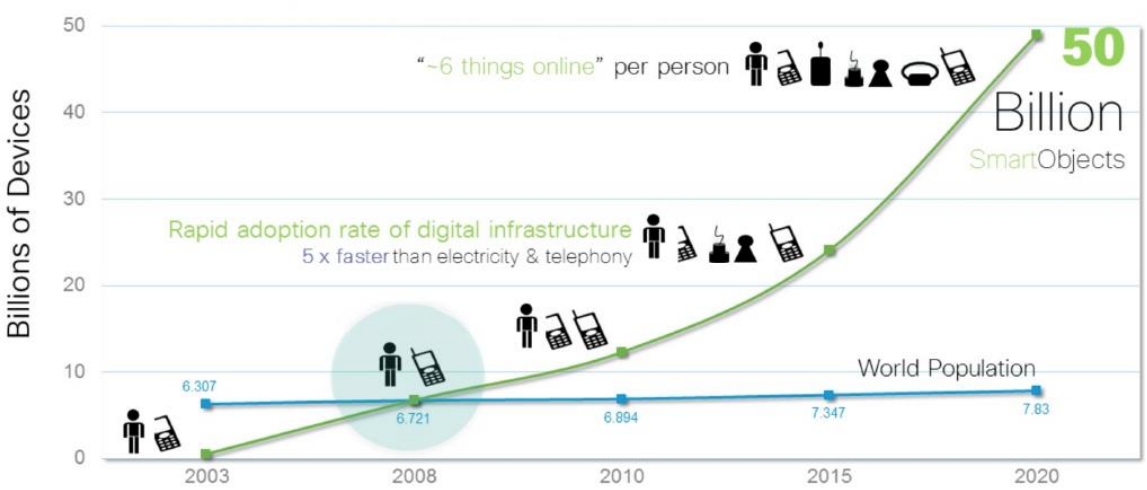

Figure 2.4 –IoT growth – Number of devices vs. Worldwide population [5]

The number of objects connected to the Internet continues to grow, and in 2008 even exceeded the number of the total population of the planet.

It should be noted that the exponential increase that has occurred in recent years has been such that if there are currently around 30 billion devices, in 2020 it is anticipated that there will be about 50 billion devices, about 6 per person, contrary to that which happened 10 years ago, when each person usually had only one device [5].

More optimistically, Gartner estimated that only about 26 billion devices would be connected to the Internet by 2020 [6].

It will be effectively from 2020 that IoT will begin to reach its full potential, according to the chart in the Figure 2.5.

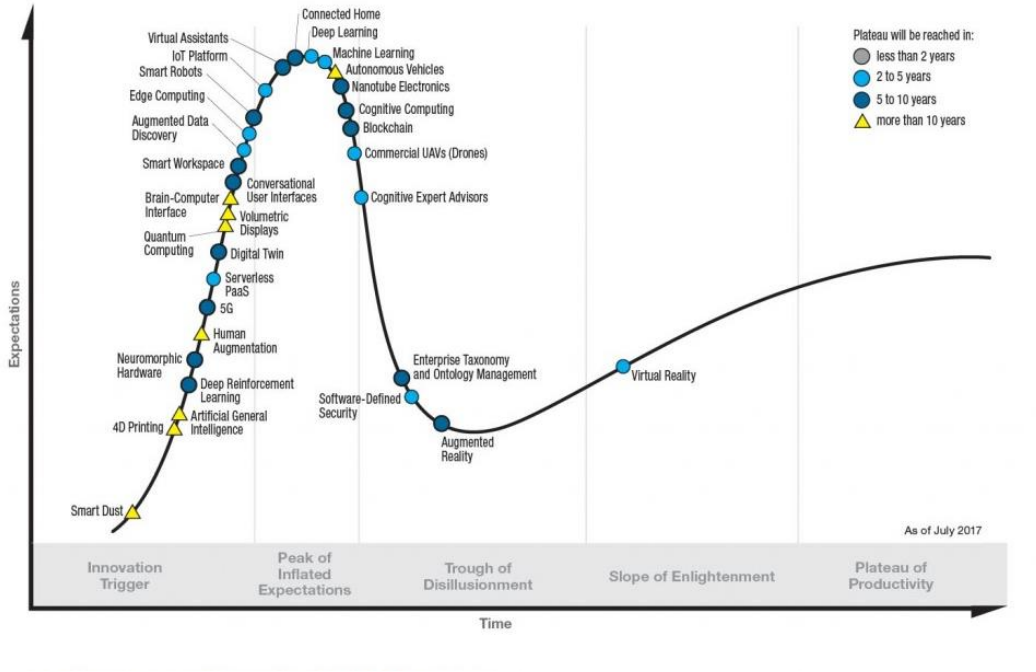

Figure 2.5 – Lifecycle of new technologies [7]

More recently, Gartner predicts that 8.4 billion connected things will be used worldwide by 2017 [8], which represents an increase of about 31% over the year 2016 [9], and consequently an expense total of 2 trillion dollars in IoT equipment and services.

There will be many companies supplying this technology, so the end users will be the biggest beneficiaries. Together, the regions of Greater China, North America and Western Europe will hold over 67% of IoT devices installed worldwide in 2017.

Gartner in the same publication subdivided the IoT market into three broad categories:

- Consumers - Devices used by private consumers;
- Enterprises: multiple industries - Devices used by companies in multiple industries;
- Enterprises: private industry - Devices used by companies in a particular industry.

The consumer sector is the one with the greatest number of devices installed compared to the business sectors. By 2020 this sector is expected to hold more than 63% of what represents the total number of IoT devices, as Table 2.1 shows.

Category	2016	2017	2018	2020
Consumers	3,963.0	5,244.3	7,036.3	12,863.0
Companies: Multiple Industries	1,102.1	1,501.0	2,132.6	4,381,4
Companies: Private Industry	1,316.6	1,635.4	2,027.7	3,171.0
Total	**6,381.8**	**8,380.6**	**11,196.6**	**20,415.4**

Table 2.1 – Number of IoT devices per category (Millions of users) [8]

As consumers buy more and more devices, companies are investing more and more in the IoT market. By 2017, investment in the business sector is expected to exceed $964 billion, much higher than consumer investment of about $725 billion. It is notorious that initially the investment by the companies is much higher compared to the consumers, however, in the following years, the companies start to obtain the expected return, as indicated in Table 2.2.

Category	2016	2017	2018	2020
Consumers	532,515	725,696	985,348	1,494,466
Companies: Multiple Industries	212,069	280,059	372,989	567,659
Companies: Private Industry	634,921	683,817	736,543	863,662
Total	**6,381.8**	**8,380.6**	**11,196.6**	**20,415.4**

Table 2.2 – Investment of IoT devices per category (Millions of dollars) [8]

2.3.3 IoT challenges

As discussed in the previous subchapter, IoT will bring many benefits in different areas of application. However, as the IoT market evolves, there are some issues that need to be addressed. Today, the IoT market is going through (or will pass in the future) the following challenges [5]:

- Security;
- Privacy;
- Interoperability;
- Treatment of the data.

Security in IoT networks is very important as it can cause potential privacy breaches in the case of a consumer or represent security risks in the case of companies. The fact that each device can send or receive information through Internet raises many concerns. One of the main reasons for this concern is that most of the devices are in vulnerable locations and therefore more easily susceptible to external attacks. In this way, it will be necessary to apply some security techniques, and cryptography is often used in this sense. Methods such as AES (*Advanced Encryption Suite*), RSA (*Rivest-Shamir-Adleman*) and DH (*Diffie-Hellman*) would be plausible to use, however, due to the small size and limited processing of many devices attached to this type as well as the limited transmission rate, may inhibit encryption and other more robust security measures to be used.

Interoperability of the various IoT devices is also a challenge in the IoT market. As will be described in the next subchapter, there are several technologies and consequently several manufacturers of IoT devices. Thus, it is to be expected that there are several different communication protocols for each entity, and consequently incompatibility between the IoT devices of each of them. The existence of interoperability between the various entities will allow that there is only one global standard that defines the rules regarding the operation of the IoT devices.

Finally, IoT devices may have to generate large amounts of information, sometimes even in real time, depending on the type of application. The processing and analysis of large amounts of data implies that a greater capacity is required for the gateways who receive all this information. In this way, companies will have to be safeguarded to ensure the correct preparation for the growth of the IoT market.

2.4 IoT technology overview

In the past, conventional communication protocols evolved to offer higher data rates with each generation, trying gather the user needs that were using bandwidth-heavy applications like video streaming or large file downloads. In the IoT though, the senders and receivers of data are mostly sensors that, depending on the application, may not require high uplink or downlink speeds, since they communicate sparingly and transmit only a few kBits/s.

There are various architectures attempting to represent how IoT devices will operate. However, the most basic model can be identified in a stack consisting of three components, each one corresponding to a different high-level task, as depicted in the Figure 2.6:

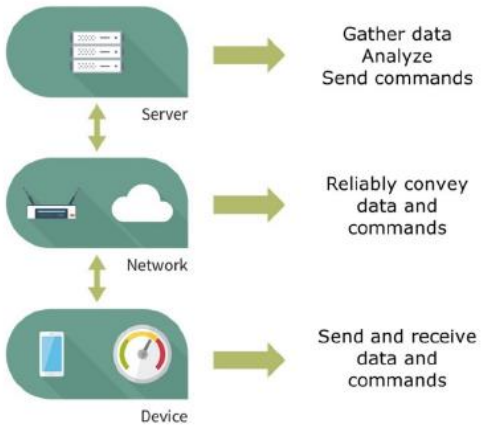

Figure 2.6 – The IoT layer structure [10]

1) A Perception layer collects data from sensors and controls actuators;
2) A Network layer interconnects devices so that they can share information between themselves or with a centralized data sink;
3) An Application layer stores, interprets and makes use of the collected data.

The IoT scenario poses some key requirements that needs to be tackled and solved by any technology operating at the Network layer, such as [11]:

Low Power Consumption: Most of IoT applications require long battery life devices, once that in most IoT deployments, due to the accessibility restrictions, manually batteries replacing leads to an enormous logistical expense. Typically, the IoT devices are supposed to sporadically transmit small size packets with simplified protocol stacks and improved sensitivities, which lead to a low power consumption. For that, a battery lifetime of 10 years or more with AA or coin cell batteries is desirable to bring the maintenance cost down. [12]

Scalability: The technology that will support the IoT infrastructure needs to achieve the best possible efficiency, handling at the same time with frequent network congestion and packets collision caused by the massive number of connected devices, and consequently, their rapid growth. It is forecasted that the device density will be in the order of 60000 devices per km^2 [10].

Low Device cost: To have a reliable and profitable business case for IoT, the devices cost needs to be as cheap as possible, typically 1-2€, to help vendors gain an edge in the market by reducing the price for a device [13]. Furthermore, the network installation and maintenance should also follow the same constraints.

Long Range and Deep-Indoor Coverage: The IoT infrastructures are designed for large coverage ranges and deep indoor coverage, by enhancing link budget for 15-20 dB [14]. Thus, it should allow the connection between end-devices and the base station at a distance that range from few meters to tens of kilometers depending on the deployment environment (urban, sub-urban, rural, etc.). It also turns possible to communicate with devices that could be located in the basement of buildings, behind concrete walls or elevators.

The capability of an IoT network protocol to fulfill the aforementioned requirements needs to be carefully investigated before a massive deployment can be implemented since different IoT applications have different requirements, depending on many factors, such us, the data rate.

Considering the fact that high data rates brings with them large power consumption, with power being a resource highly constrained in IoT devices, it can be concluded that it is worth examining the possibility that for certain applications, lower data rates are not only better, but actually ideal.

Table 2.3 illustrates five IoT applications examples, where different requirements can be seen among the different applications, such as power consumption, coverage, data rate and periodicity.

Category	Use Case	Coverage	Energy	Troughput	Periodicity	Mobility	Real-Time	Security
Infrastructure monitoring	Water/Electric/Gas Metric	Urban Areas	Low	Medium	Tens of minutes	No	Medium	Low
	Agriculture/soil & oil	Open fields	Low	Low	Event driven	No	Low	Medium
Transportation	Traffic congestion monitoring	Urban Areas	Low	High	Tens of minutes	High	Medium	Low
	Public transport management	Urban areas	Low	Medium	Event driven	High	Medium	Medium
Asset tracking	Supply chain monitoring	Urban areas/in-building	Low	Low	Event driven	Medium	Low	Low
	Vehicle tracking	Urban areas/open fields	Low	High	Several minutes	High	Medium	Low
Security	Access control & building security systems	In-building	Low	Low	Event driven	No	High	High
	Natural disasters preparedness	Urban areas/open fields	Low	Low	Event driven	No	High	Medium
Healthcare	Health status monitoring	Urban areas/in-building	Low	Medium	Tens of minutes	Medium	Low	Low
	Medical alert	Urban areas/in-building	Low	Low	Event driven	Medium	High	Low

Table 2.3 – Different IoT applications requirements [15]

The low energy consumption is an extremely important parameter and common for the various IoT applications described in Table 2.3. Reducing consumption is a factor that greatly influences the energy efficiency of the IoT application, and therefore taken into account in any type of wireless network [12].

At the coverage level, each application has a specific type environment where it is more suitable. Applications in the transport sector are usually integrated into an urban type of environment, while applications in the agricultural sector are more geared towards open (rural) environments.

It is also necessary to take into account the periodicity and amount of data that is transmitted by the IoT devices. In the case of the agricultural sector, devices can send little information over a long period of time, unlike vehicle tracking, that the continuous sending of large-data data is very important.

It is expected that the number of connected consumer electronics and M2M devices will exceed the number of human subscribers that use mobile phones, personal computers, tablets and laptops by the year of 2020 (Figure 2.4). This leads to an expected total device connection to be around 26 billion by 2020 [6].

Connectivity is the foundation for IoT, and the type of access required will depend on the nature of the application. Currently, there are many IoT connectivity solutions with different network standards that aims to cover all the examples bellow, and they are described in the next subchapter.

2.5 Solutions for IoT connectivity

Three different main wireless technologies have been designed so far to connect IoT devices which vary in range, throughput and cost.
Not necessarily only one of these approaches will survive, since each one has some strengths and weaknesses when compared to the others. Nevertheless, there is currently a competition between multiple architectures, and that one will prevail and end up providing the bulk of the connectivity to IoT devices. The purposed wireless technologies are presented next.

2.5.1 WSN – Wireless Sensor Networks

WSN (Wireless Sensor Networks) technologies create small networks, typically covering and interconnecting the devices owned by an individual or operating in a house. These standards provide low data rates and short-range communication, in order to focus on efficient battery use. Several low power wireless technologies can be utilized for WSNs, however, most of the references tend to focus mainly on Bluetooth and Zigbee, such as [16] and [17]. A brief of this technologies is presented below.

2.5.1.1 Bluetooth

Bluetooth classic is a WPAN (Wireless Personal Area Network) technology based on IEEE standard 802.15.1. It utilizes the licensed free 2.4 GHz frequency band in the ISM spectrum, with up to 1MHz channel frequency band.

Released in 1999 by Ericsson, Bluetooth v1.0 was initially designed to, wirelessly, replace cables to connect devices typically used together, such as cell phones, laptops, headsets, key-boards, etc., offering a maximum data rate up to 1Mb/s, by adopting FHSS (Frequency Hoping

Spread Spectrum) transmission technique, and a short range of communication, in theory, up to 100 m (at maximum transmission power), realistically, 5–10 m.

After v1.0, Bluetooth SIG (Special Interest Group) has released more 3 Bluetooth classic versions, within multiple updates throughout the time, until BLE (Bluetooth Low Energy) was released [18].

Fully compatible with classic Bluetooth, this extension provides an even more lower-power interface than the classic Bluetooth and is optimized to communicate with very-low power devices, such as wireless sensors.

The Low-Energy extensions were inspired by the need to support sensors in home and office environments, including motion sensors, light detectors, thermostats, pedometers, and heart monitors. The design's power target was to run a wireless sensor for at least one year on a single coin cell (approximately 200 mA) and to communicate with it using a laptop or cell phone at a data rate suited to these applications. In fact, Bluetooth LE is limited to approximately 200 kbps, but is adequate to support common sensor applications that require only a small amount of data to be transmitted periodically, perhaps once per second or minute, depending on the situation [19].

More recently, the Bluetooth SIG has presented the specifications of Bluetooth 5, whose primary purpose is to offer significant enhancements compared to the preceding specification, regarding the range, speed, and broadcasting capacity. In the twisted battle for the control over the IoT communication standards, these new improvements aim to help BLE to prevail and to become the ultimate standard for IoT [20].

2.5.1.2 IEEE 802.15.4/Zigbee

Zigbee is one of the most widely utilized Wireless Sensor Network standards with low power, low data rate, low cost and short time delay characteristics, simple to develop and deploy and provides robust security and high data reliability.

Zigbee is commonly called IEEE 802.15.4, however, they are not the same. ZigBee is a standard based network protocol supported solely by the ZigBee alliance that uses the transport services of the IEEE802.15.4 network specification. ZigBee alliance (software) defines the network, security and application layers. IEEE802.15.4 (hardware) defines the physical and the MAC (Media access control) layers for WSN's [21].

Supporting three unlicensed frequency bands, 868 MHz (Europe), 915 MHz (North America and Australia) and 2.4 GHz (worldwide), Zigbee is capable of offering up to 20kbps, 40kbps and 250kbps data rate respectively [22].

The IEEE 802.15.4 standard employs 64-bit and 16-bit short addresses to support theoretically more than 65,000 nodes per network. ZigBee network can have up to 653356 devices, the distance between ZigBee devices can be 297 up to 50 meters, and each node can relay data to other nodes [21].

Zigbee uses DSSS (Direct Spread Spectrum Sequence) transmission technique, which is able to provide a very significant range (up to 150 meters), and with a very good power consumption (typically around 1 mW). This leads the capability of making a very big network, which covers significant distances, and with less power than Bluetooth, which uses FHSS transmission technique.

A general comparation between Zigbee and the various classes of the Bluetooth technology are presented in the following table:

Feature	**Bluetooth Classic**	**Bluetooth 4.x**	**Bluetooth 5**	**IEEE 802.15.4 - ZigBee**
Radio Frequency (MHz)	2400 to 2483.5	2400 to 2483.5	2400 to 2483.5	868.3, 902 to 928, 2400 to 2483.5
Distance/Range (meters)	Up to 100	Up to 100	Up to 200	Up to 150
Medium Access Technique	Frequency Hopping	Frequency Hopping	Frequency Hopping	CSMA/CA
Nominal Data Rate (Mbps)	1-3	1	2	0.02-0.25
Latency (ms)	<100	<6	<3	<4
Network Topology	Piconet, Scatternet	Star-bus, Mesh	Star-bus, Mesh	Mesh
Multi-hop Solution	Scatternet	Yes	Yes	Yes
Profile Concept	Yes	Yes	Yes	Yes
Nodes/Active Slaves	7	Unlimited	Unlimited	Unlimited
Message Size (bytes)	Up to 358	31	255	100
Certification Body	Bluetooth SIG	Bluetooth SIG	Bluetooth SIG	ZigBee Alliance

Table 2.4 – Comparison of features between Bluetooth and Zigbee [20]

2.5.2 Cellular IoT

WSN technologies identified above are mainly limited by their short range. Although this need of rich coverage has been solved by the existing cellular technologies (usually with low bandwidth), e.g., GSM (Global System for Mobile communications), UMTS (Universal Mobile Terrestrial Service), etc., or satellite connectivity, the increased costs and the high level of power demanded by these systems make them unsuitable for long-term M2M networks composed by a massive number of devices.

Due to the limitations of the WSN technologies and this demanding's by the traditional cellular networks, the 3GPP proposed CIoT (Cellular IoT) standards, which operate in licensed bands and leverage the already existing cellular network coverage to provide internet access to IoT devices: The fact that the infrastructures for the network are already installed is a great benefit and will make deployment time very short.
Currently, three different standards have been proposed: EC-GSM (Extended Coverage GSM), LTE-M (Long Term Evolution for Machines) and NB-IoT (Narrowband-IoT).

EC-GSM is designed to leverage and improve on legacy EDGE (Enhanced Data rates for GSM Evolution) and GPRS (General Packet Radio Service) systems to provide better coverage and range, with limited power requirements.

LTE-M will integrate with LTE to make use of its capacity and performance and bring new power saving options to increase device battery life.

Finally, the new NB-IoT standard will focus on ultra-low-end IoT applications, once again leveraging the existing LTE infrastructures. [14]

Although CIoT might sound a good solution for an IoT network connectivity, these technologies are still in a very early stage of deployment, even though LTE-M being expected to be released soon [11], the usage of licensed frequencies involves operating costs that are not negligible. Moreover, the high data rates that are offered to the connected end-devices leads to significant power consumption, which may become a great issue for battery power devices.

5G networks are also expected to provide connectivity to IoT devices by design, in order to compete even more with the proprietaries and most frequently used IoT technologies in the market, the LPWAN, described in the next subchapter [23].

2.6 LPWAN – Low Power Wide Area Networks

Sensor networks have survived so far with the existing classic solutions described above, but the main point of industrial M2M networks is the huge increase in the number of devices composing them and the notable widening of the covered areas.

According to Analysis Mason in [2], the number of M2M connections will increase to about 1,3 billion by 2025 (Figure 2.2) and this enormous growth requires (i) minimized cost per unit; (ii) optimized edge-nodes energy consumption; (iii) high network scalability; and (iv) wide network coverage, which none of the technologies described before offers.

As a result, another range of protocols and technologies called LPWAN has arisen as one of the most promising IoT enabling technologies and with the promise to complement the existing cellular and short range wireless technologies in addressing diverse requirements of IoT applications.

LPWAN is a generic term for a group of technologies that are characterized by having a wide coverage, with a lower power consumption, when compared to other IoT connectivity solutions. These features are possible due to the sporadically transmission of small packets at low data rates. These group of technologies aims essentially to offer unique sets of features, by prioritizing longer range and low power, over higher bit rates.

Until recently, most M2M and IoT services have largely relied on WSN and traditional cellular networks for their wide area connectivity requirements, however, those are proved to not be the most suitable technology to be used for IoT connectivity, but yes, LPWAN. The conceptual differences between WSN, Cellular-network and LPWAN paradigms are presented in Table 2.5.

WSN	**Cellular Communications**	**LPWAN**
Limited bandwidth	High bandwidth	Limited bandwidth
Sporadic traffic	Continuous traffic	Sporadic traffic
High number of devices	Limited number of devices	High number of devices
Short coverage	Wide coverage	Wide coverage
Reduced network and device costs	Expensive network and device costs	Reduced network and device costs

Table 2.5 – Difference between WSN, Cellular Communications and LPWAN paradigms. Adapted from [24]

LPWANs presents better tradeoffs between range, coverage, data rate, power consumption and cost, when compared to the other IoT connectivity solutions, making them unique candidates for IoT applications. Figure 2.7 highlights these compromises.

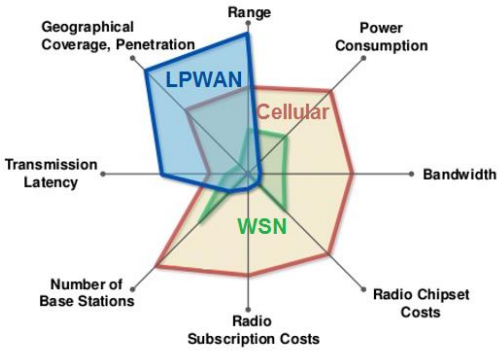

Figure 2.7 – Trade-offs between IoT connectivity technologies [25]

The key objective of LPWA technologies is to achieve a long range with low power consumption and low cost unlike cellular networks, for which achieving higher data rate, lower latency and higher reliability may be more important. Because of that, LPWA have a tremendous market forecast in the sense of becoming the world's most popular solution technology for IoT connectivity.

2.6.1 LPWA Market forecast

The market for LPWA technologies has enormous potential and so there are many sources of research with different opinions. According to Strategy Analytics in [26], more than 1 billion LPWA connections are expected by the end of 2018, which doubles by the end of 2019, and still rise to more than 5 billion by the end of the year 2022. In terms of profit, more than $ 13 billion in revenue from connectivity is expected by operators of these technologies. Figure 2.8 illustrates they're prediction on the number of connections from the LPWA networks in the various business areas.

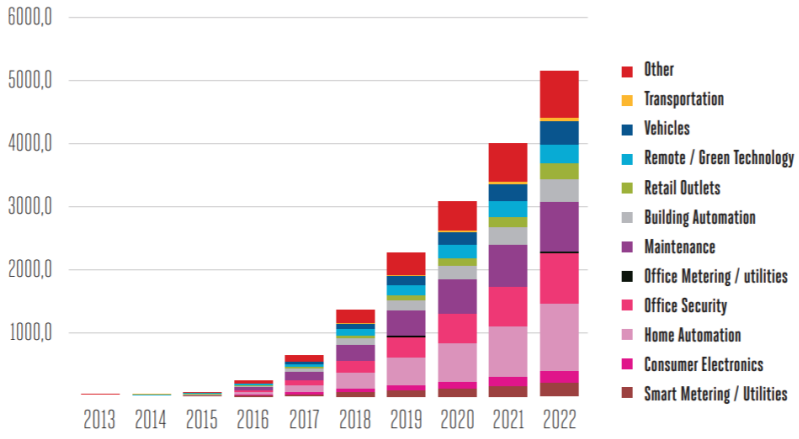

Figure 2.8 – LPWA connections worldwide by the end of 2022 [26]

Analysis Mason, in a more optimist way, expects about 3.5 billion LPWA connections and a revenue of 5 billion dollars for the same period of 2022 [27].

Despite the lack of results between the two sources, it is similar for both that the number of potential applications for this type of networks will be a growing trend and will cover practically all business areas, generating quite acceptable revenues.

2.6.2 Design goals

The success of LPWA technologies lies in their ability to take the most benefits of both traditional cellular and sensor networks, and combine them into one single technology to overcome the main IoT goals, already described in chapter 2.4: Low device cost; Low power consumption and Long Range.

Among these goals, probably the two former ones are the easiest to reach.

Low device cost can be achieved due to the less complexity of it's hardware.

The lifetime of ten years of battery can be achieved by limiting the number of messages sent by each node per day, giving them an extremely low-power communication, although this naturally limits the range of applications [12], [28].

Therefore, the third problem, namely the long range, is the main focus in this thesis, thus described next.

2.6.2.1 Long Range

The main goal in the long range is to achieve a wide area coverage and an excellent signal propagation to hard-to-reach indoor places, such as basements, with a target of a +20 dB gain over legacy cellular systems and also a link budget of 150 ±10 dB that enables a range of a few kilometers and tens of kilometers in urban and rural areas respectively. Sub-GHz band and special modulation schemes are exploited to achieve this goal [12].

- **Sub-GHz band**: Firstly, when compared to the 2.4 GHz band, the lower is the frequency (f_c), the bigger is the wavelength (λ), and consequently less attenuation will be caused mainly by the obstacles present in the connection, allowing a better received power

(P_{RX}), and consequently a good link budget link. Equation 2.1 demonstrates this affirmation:

$$P_{RX} = P_{TX} G_{TX} G_{RX} \left(\frac{\lambda}{4\pi d}\right)^2, \text{ where } \lambda = \frac{c}{f_c} \quad (2.1)$$

Secondly, sub-GHz is less congested than 2.4 GHz, a band used by most-popular wireless technologies e.g. Bluetooth, ZigBee. The resulting higher reliability enables long range and low power communication.

- **Modulation techniques**: Also according to the expression above, the more distance a signal reaches, the more attenuated it gets and therefore, more difficult it gets to be received. LPWA receivers have the particularity of decoding severely attenuated signals correctly, through the modulation scheme they use. The type of modulation, thus the number of $bits/symbol$ it uses (N_b), directly affects the range of the link. Expression 2.2 shows that, the slower is the modulation rate (R_s), more energy can be allocated in each symbol, decreasing the data rate (R_b). This allows to raise the receiver's sensitivity, which in LPWAN technologies is around -130 dBm.

$$R_b = R_s * N_b \; [bit/s] \quad (2.2)$$

Thus, two classes of modulation approaches have been adopted by different LPWAN technologies, namely, Narrowband and Spread Spectrum. A description on both is given bellow:

  - **Narrowband** makes use of narrow RF channels (with bandwidth usually less than 25kHz) to provide higher sensitivity and long range at the expense of limited data rates. A particularity of narrowband modulation is called UNB (Ultra-Narrowband), which uses a bandwidth as short as 100 Hz further reducing the experienced noise and increasing the number of supported end-devices (e.g., SigFox), however also decreasing drastically the data rate, raising the air-time of each transmission, which are limited according to the regulations [11].

  - **Spread Spectrum** technique consists in the spread of a narrowband signal over a wider frequency band (typically with a bandwidth in the order of 50kHz, 125kHz, or 500kHz), but with the same power density. This allows to lodge multiple users in one single channel, as long as they use orthogonal codes.

There is no definition of ideal modulation technique in IoT. Each of the techniques described above have their vantages and advantages, as described. It all depends on the LPWA technology to decide which modulation to use. A spectrum comparation between these techniques are illustrated in Figure 2.9.

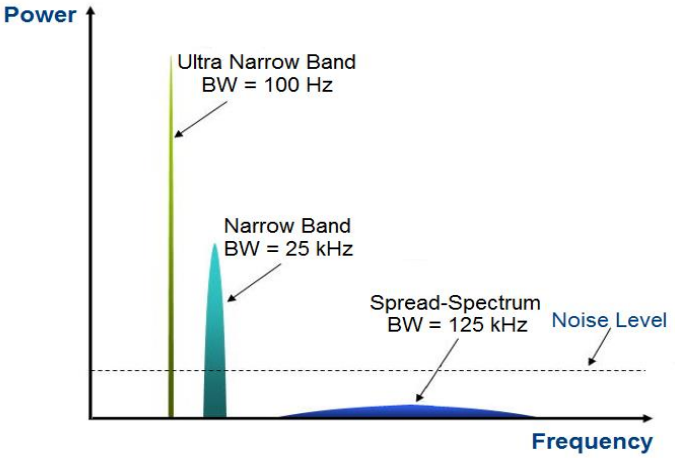

Figure 2.9 – Spectrum comparation between Narrow Band, Ultra Narrow Band and Spread Spectrum signals [30]

In the next subchapter LPWA proprietary technologies will be further described, but Sigfox and Weightless-N are a few examples of LPWA technologies that use UNB modulation, whereas spread spectrum can have two different variants: CSS (Chirp Spread Spectrum) and DSS (Direct Sequence Spread Spectrum), used by LoRa and RPMA respectively.

2.6.3 Technologies

Recently, a number of different platforms following the LPWAN paradigm have arisen, each of them with their own particularities and individual features that makes them more suitable for different types of IoT applications. However, all of them aiming to achieve the goals mentioned before. With an exception of a few, most of these technologies use the sub-GHz unlicensed ISM frequency band, which offers robust and reliable communication at low power budgets.

In the following section it is presented an overview of some of the most prominent LPWAN platforms so far [31]. Many of these proposals are still in an early development stage and others

have already begun their architecture deployment. SigFox, Weightless, Ingenu and LoRa are currently the platforms with the greatest momentum and they have been reviewed in recent works [19], [11]. To this last one is given a special focus in the next section, since it is the adopted technology in this dissertation.

SIGFOX [32] was the first LPWAN technology proposed in the IoT market has been growing very fast since then. Funded in 2009 in France, this proprietary standard offers an end-to-end LPWAN solution based on its patented technology to serve low throughput M2M and IoT applications. The current access to the Sigfox network includes coverage over more than 50 countries.

Sigfox employs a proprietary UNB (100 Hz) modulation DBPSK (Differential Binary Phase Shift Keying) in the sub-GHz ISM band carrier. By using UNB, Sigfox promotes bandwidth efficiency and experiences very low noise levels. This results in a high receiver sensitivity and a very low power consumption. However, this benefit comes at a price, with Sigfox only achieving a maximum data rate of 100 bps and by transmitting messages with a maximum payload length of 12 bytes in uplink and 8 bytes in uplink, with a maximum of 140 messages that an end-device can send and only 48 messages allowed for the gateway to send.

Meanwhile, using this low bitrate permits large ranges of 10 km and beyond with very low transmission power, which allows saving energy at edge-nodes. Sigfox's technical sheets claim a typical stand-by time of 20 years with a 2500 mA battery [31].

Sigfox also claims that each gateway can handle up to a million connected objects, with a coverage area of 30–50 km in rural areas and 3–10 km in urban areas [33].

Weightless [34] is both the name of a group, the Weightless Special Interest Group (WSIG), and the technology. Weightless technology delivers wireless connectivity for LPWANs specifically designed for the Internet of Things. The Weightless SIG proposed three standards (Weightless-W, Weightless-N, Weightless-P) each providing different features, range and power consumption while still operating in the sub-GHz band.

Weightless-W standard relies on a system with a star topology which makes use of the TV whitespace spectrum. It provides several modulation schemes, spreading factors and packet sizes. Weightless-W claims data rates from 1kbps to 10Mbps with very low overhead. Furthermore, communication ranges can be established along 5 kilometers. The shared access of the

TV white spaces is permitted only in few regions, therefore WSIG defines the other two standards in ISM band, which is globally available for shared access.

Weightless-N, likewise Sigfox, supports a star network architecture for unidirectionality only communications with a connectivity up to 100 bps through the adaptation of a UNB modulation with a significant energy efficiency and ranges of several kilometers, even in challenging urban environments. This is possible due to the simplicity of this solution.

Weightless-P puts together the most appropriate attributes of the previous standards and claims to be essentially focused on the industrial sector, aiming to offer performance along with network reliability and security characteristics. It uses a narrowband modulation scheme GMSK (Gaussian Minimum Shift Keying), and OQPSK (Offset Quadrature Phase Shift Keying) with channels of 12.5kHz in both ISM and licensed spectrum and with an adaptive data rate in the range between 200 bps and 100 kbps.

In order to provide the reliability demanded by some industrial applications, Weightless-P presents valued features such as acknowledged transmissions, auto-retransmission, frequency and time synchronization, channel coding, among others. [31]

Table 2.6 summarizes the key priorities of each Weightless standard described above.

Standard	**Weightless - W**	**Weightless - N**	**Weightless - P**
Modulation	16-QAM, BPSK, QPSK, DBPSK	UNB DBPSK	GMSK, offset-QPSK
Band	TV white spaces 470-790 MHz	ISM Sub-GHZ EU (868 MHz), US (915 MHz)	Sub-GHz ISM or licensed
Data rate	1 kbps-10 Mbps	30kbps-100kbps	200bps-100kbps
Range	5km (Urban)	3km (Urban)	2km (Urban)
Nrº of channels	16 or 24 channels (UL)	Multiple 200 Hz channels	Multiple 12,5 kHz channels
Topology	star	star	star
Packet Size	>10 bytes	<20bytes	>10bytes
Authentication and Encryption	AES 128b	AES 128b	AES 128/256b

Table 2.6 – Weightless standards specifications [12], [31]

Ingenu, formerly known as On-Ramp Wireless, has been pioneering the standardization of the physical layer specifications under IEEE 802.15.4k standard. The company developed and

owns the rights of the patented technology called RPMA (Random Phase Multiple Access) which is deployed in different networks. Unlike most other LPWAN technologies, it does not propagate in the sub-GHz band. Instead, Ingenu's RPMA operates in 2.4 GHz ISM band due to more relaxed spectrum regulations on radio duty cycle and maximum transmission power in this band across multiple regions. RPMA is reported to achieve a receiver sensitivity of about -142 dBm and 168 dB link budget [35]

LoRa is a physical layer technology that modulates the signals in SUB-GHZ ISM band using a proprietary spread spectrum technique which was initially developed by Semtech [36], and now is under the control of the LoRa Alliance [37]. Unlike the LPWAN technologies described above, LoRa is based on CSS modulation, which spreads a narrow band input signal over a wider channel bandwidth. The resulting signal has noise like properties, making it harder to detect or jam, thus distant receivers can decode a severely attenuated signal several dBs below the noise floor. Very long range of communication can be achieved with LoRa thanks to the sub-GHz radio bands and very low data rates, ranging from 300 bps to 37.5 kbits/s depending on the channel BW (Bandwidth) which are 125, 250 or 500 kHz and the SF (Spreading Factor), which is the number of chirps per symbol.

LoRa supports multiple spreading factors (between 7-12) to decide the trade-off between range and data rate. Higher spreading factors delivers long range at an expense of lower data rates and vice versa. Moreover, the spreading factor for a LoRa link may be varied depending on the communication distance and desired on-air time. Since the spreading codes for different SFs are orthogonal, the simultaneous transmission in the same frequency channel using different SFs is possible [13]. LoRa also combines FEC (Forward Error Correction) with the spread spectrum technique to further increase the receiver sensitivity.

3

LoRa technology

3.1 Introduction

This chapter presents an overview of the LoRa technology, namely the LoRa and the LoRaWAN specifications

Section 3.2 describes the physical layer, LoRa, with the description of each parameter (SF, BW, CR). It also describes the packet structure, and the Time-On-Air calculations.

Section 3.3 presents an architecture of the LoRaWAN system, where each individual contributor is detailed, including the end-nodes classes. Finally, the end-devices setup and the spectrum regulations are also reflected.

3.2 Long Range (LoRa)

LoRa technology, which stands for “Long Range”, was initially proposed by Semtech [36] and is currently developed by the LoRa Alliance [37]. Having energy consumption as a major priority, the system aims at being usable in battery-powered devices that require a long lifetime.

LoRa can commonly be associated to two distinct layers: a physical layer (PHY) that uses a proprietary radio modulation owned and patented by Semtech, the CSS (Chirp Spread Spectrum) and forward error correction techniques to make the communication robust against noise and interference and also increasing the receivers sensitivity; and a MAC layer protocol developed by the LoRa Alliance and defined as LoRaWAN, which enables many end-devices to communicate with a single gateway using the LoRa modulation [38].

3.2.1 Physical Layer

LoRa physical layer uses CSS modulation, a proprietary technique initially developed and patented by Cycleo, a French company acquired by Semtech [36], to modulate the signals in the sub-GHz ISM.

The idea behind CSS modulation is that a sinusoidal narrowband signal of linearly varying frequency and fixed duration, called chirp, can be employed to "spread" information over a wider spectrum than it would normally need to occupy, conferring higher resilient to the signal as a result.

The transmitter starts by generating chirp signals by varying their frequency over time while ensuring the phase remains constant between adjacent chirp symbols. These chirps are often referred to as up-chirps, if they are continuously increasing in frequency, or down-chirps if they are continuously decreasing in frequency.

The resulting signal is noise alike, which is resistant to multipath fading and doppler shifts, robust to interferences and jamming attacks and difficult to decode by hackers, allowing LoRa devices to be reachable in movement, as it concluded in the studies from the authors in [39], [40]. Moreover, it enables LoRa systems to demodulate signals that are 20dB below the noise floor when the demodulation is combined with FEC (Forward Error Correction) to further increase the receiver sensitivity [41].

LoRa technology allows to adjust several parameters in the physical layer, namely, the TP (Transmission Power), CF (Carrier Frequency), BW (Bandwidth), SF (Spreading Factor) and CR (Coding Rate). The combination of these parameters provides different energy consumption, transmission range and resilience to noise. A description of these parameters is given next:

- **Carrier Frequency ($\boldsymbol{CF}$)**. LoRa makes use of the sub-GHz band as described already in this dissertation. Common LoRa modules, such as the Semtech SX1272 [42] supports communication in the frequency range [860–1020] MHz. Eight channels separated by 0.3 MHz can be used to communicate in the European 868 MHz ISM band.

- **Transmission Power ($\boldsymbol{TP}$).** Similar to almost all LPWA technologies, LoRa transceivers also allow for adjusting the transmission power, affecting drastically the energy re-

quired to transmit a packet. By increasing the transmission power, the power consumption also increases, but maximizes the range of the communication link. Transmission power is, however limited via Hardware trough the legal regulations, depending on the frequency band LoRa operates. For instance, the maximum transmission power of LoRa modules in the Europe region (868 MHz band) is +14 dBm.

- **Bandwidth ($\boldsymbol{BW}$):** BW represents the range of frequencies in the transmission band. LoRa provides three scalable BW settings of 125 kHz, 250 kHz and 500 kHz.
  The higher is the bandwidth, the shorter is the air time of a packet, but consequently, the lower is the sensitivity of the receiver, and vice versa. Lora transmitters sends the data at a chip rate equal to the system bandwidth in chips per-second, meaning that LoRa's Chip-Rate (R_c) is computed as:

$$R_c = BW\ [chips/s] \tag{3.1}$$

- **Spreading Factor ($\boldsymbol{SF}$)**: CSS modulation is performed by representing each bit of payload information by multiple chips of information. The ratio between the chip rate (R_c) and the rate at which the information is spread (symbol rate (R_s)), expresses the spreading factor, and it represents the number of symbols sent per bit of information. In LoRa, each symbol is spread by a spreading code of length 2^{SF} chips. The length of the spreading code can be from 6 to 12, although the use of spreading factor 6 is currently not enabled by Semtech [36], resulting in a range from 2^7 to 2^{12} chips/symbol and a symbol rate (R_s) that can be computed as:

$$R_S = \frac{R_c}{2^{SF}} = \frac{BW}{2^{SF}}\ [symbols/s] \tag{3.2}$$

From Equation 3.2, the duration of a LoRa symbol (T_S) can be determined. That is given by:

$$T_S = \frac{1}{R_S} = \frac{2^{SF}}{BW}\ [s] \tag{3.3}$$

It is important to highlight that the usage of different SF's leads to tradeoffs between throughput, coverage area, link robustness or energy consumption.

Higher SF's increases the SNR (Signal-to-noise Ratio), as well as lower sensitivity and higher range, but also increases the total duration of the packet, and consequently implies a slower data-rate.

Table 3.1 relates the available SF's and the chip length in LoRa:

Spreading Factor (SF)	Chip length - 2^{SF}(chips/symbol)
7	128
8	256
9	512
10	1024
11	2048
12	4096

Table 3.1 – Relation between Spreading Factor and the Chip length

It can be noted from Table 3.1 that each increment in the SF halves the transmission rate and therefore doubles the time-on-air, increasing the energy consumption of a LoRa device.

- **Coding Rate (CR):**

In order to enhance the robustness of the communication link, such its reliability in the presence of interference, LoRa supports FEC techniques with a variable number of n redundant bits, ranging from 1 to 4. CR is given by the following expression:

$$CR = \frac{4}{4+n} \tag{3.4}$$

The more interference bursts are expected, the higher the coding rate that should be used to maximize the probability of successful packet reception. Although higher CR value gives extra protection, it also increases the ToA (Time on Air).

By taking into account the parameters previously described, Equation 3.5 allows to compute the nominal bit rate (R_b) of a LoRa transmission:

$$R_b = SF * \frac{BW}{2^{SF}} * CR \ [bps] \tag{3.5}$$

Through the expression above, it can be concluded that, for a fixed coding rate, the symbol rate and the bit rate at a given spreading factor are proportional to the frequency bandwidth, so a doubling of the bandwidth will effectively double the transmission rate.

For instance, a setting with BW = 125 kHz, SF = 7, CR = 4/5 gives a bit rate of $R_b = 5.5\ kHz$, while the same settings but with a bandwith of 250 kHz gives a bit rate of $R_b = 11\ kHz$.

Figures 3.1 a), b) and c) illustrate the relation between these three parameters, whereas one of those remains fixed, varying the other two.

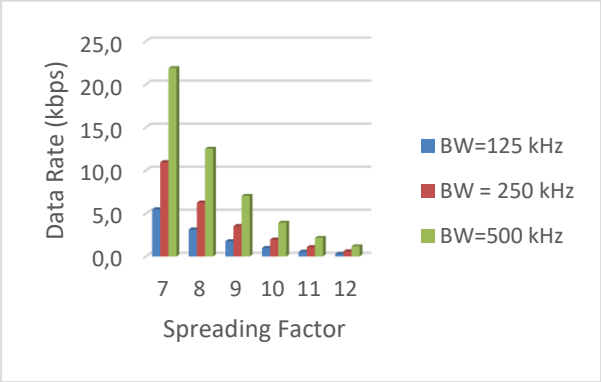

Figure 3.1 a) – Data Rates offered in LoRa with different spreading factor and bandwidth values (CR = 1)

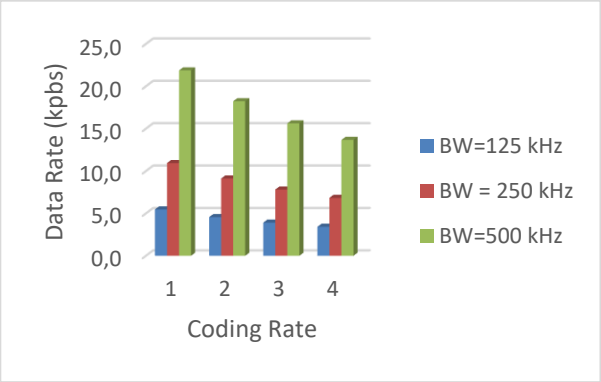

Figure 3.1 b) – Data Rates offered in LoRa with different coding rate and bandwidth values (SF = 7)

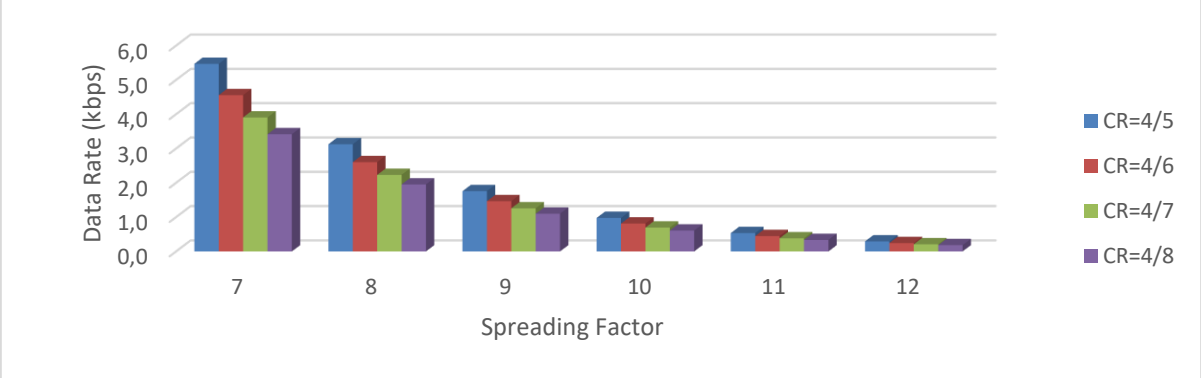

Figure 3.1 c) – Data Rates offered in LoRa with different spreading factor and Coding Rate values (BW = 125 kHz)

3.2.1.1 Packet structure

Semtech's transmitters and receivers implement a specified physical frame format for information exchange. LoRa's packet structure is consisted of a Preamble, an Header and a Payload, and the bandwidth and spreading factor are constant for each frame. Lora's physical frame is shown in Figure 3.2.

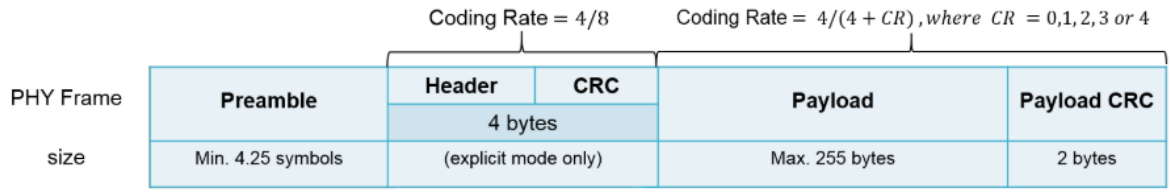

Figure 3.2 – LoRa packet structure [16]

Preamble is used to sync the receiver with the transmitter at the beginning of a transmission. The preamble starts with a sequence of constant up-chirps that cover the whole frequency band. The last two up-chirps encode a sync word, which is a one-byte value that is used to differentiate LoRa networks that use the same frequency bands. Accordingly to [43], the sync word for EU863-870MHz ISM band is defined as 0x34, meaning that a device configured with this sync word will stop listening to a transmission if the decoded sync word does not match its configuration.

The sync word is then followed by two and a quarter downchirps, for a duration of 4.25 symbols. In the band mentioned above, 8 programmed symbols follow the min. length, meaning the total preamble length can be configured between 12.25 and 65,539.25 symbols.

Header is an optional parameter that carries the information about the LoRa configuration and the size of the payload. The optionality of the header is used to allow disabling it in situations where it is not necessary, for instance when the payload length, coding rate and CRC (Cyclic Redundancy Check) presence are known in advance. Depending upon the chosen mode of operation two types of header are available: explicit header mode and implicit header mode.

In explicit mode, the number of bytes in the header field specifies FEC code rate, payload length and presence of CRC in the frame.

The implicit mode is used when the payload and coding rate are fixed, allowing to remove this field from the packet. The implicit header is always encoded with the FEC of the highest code rate of 4/8.

Payload is a variable-length field with a maximum of 255 bytes that contains either LoRaWAN MAC layer control packets or the actual data coded at the error rate either as specified in the header in explicit mode or in the register settings in implicit mode. Optionally, it can be followed by the payload CRC field that contains 2 bytes for error protection.

3.2.1.2 Time on Air

For a given combination of SF, CR and BW, the total transmission time (often called Time on air) of a Lora packet (T_{packet}) is the sum of the duration of the preamble ($T_{preamble}$) and the transmitted payload ($T_{payload}$), given by Equation 3.6:

$$T_{packet} = T_{preamble} + T_{payload} \tag{3.6}$$

The preamble length ($T_{preamble}$) is calculated as follows:

$$T_{preamble} = \left(n_{preamble} + 4{,}25\right).T_S \tag{3.7}$$

Where $n_{preamble}$ is the programmed preamble length, which can vary between regions, but in Europe, the LoRa protocol uses 8 symbols.

The payload duration ($T_{payload}$) depends upon the header mode that is enabled. Equation 3.8 gives the number of payload symbols, recurring to equation 2.5.

$$T_{payload} = n_{payload} * T_S \tag{3.8}$$

The computation of $n_{payload}$ is however, more complicated, since it depends on many different parameters, such as:

- **PLoad** – Number of bytes of the payload;
- **SF** – Spreading factor;
- **IH** – Implicit Header (IH= 1, when implicit header mode is enabled; IH = 0 when explicit header mode is used);
- **DE** – Data Rate Optimization (DE=1 indicates the use of the low data rate optimization and DE=0 when disabled);
- **CRC** – Cyclic Redundancy Check on the payload. (CRC = 1, when CRC is used; CRC=0 when it's not);
- **CR** – Coding Rate, ranging from 1 to 4.

Given the above parameters, the number of payload symbols results in:

$$n_{payload} = 8 + \max\left(ceil\left[\frac{(8PLoad - 4SF + 44 - 20IH)}{4(SF - 2DE)}\right] * (CR + 4), 0\right)^{1} \quad (3.9)$$

The total packet duration can be simplified using Equations 3.7 and 3.8, and is described as:

$$T_{packet} = T_S(n_{preamble} + n_{payload} + 4{,}25) \quad (3.10)$$

From the above expression, three different analysis were performed to conclude does the payload variation affect the total air time for a LoRa packet, by varying the SF, CR and BW. For this analysis, different payload sizes were defined, 10, 50, 100, 150, 200 and 250 bytes.

The results obtained are illustrated in Figures 3.3 a), b) and c).

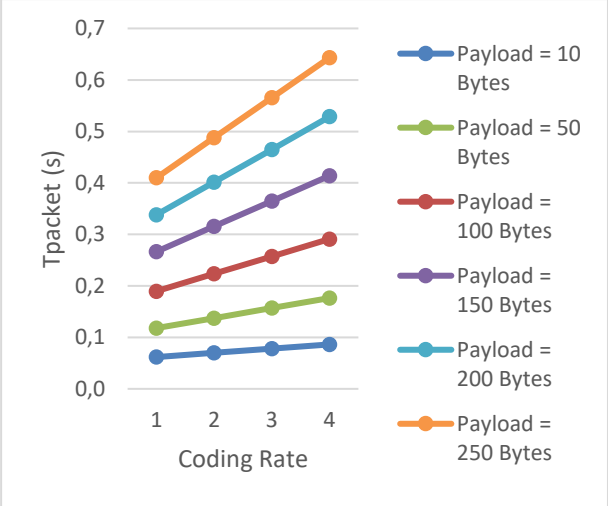

Figure 3.3 a) – LoRa packet time variation with Coding Rate (BW=125 kHz and SF=7)

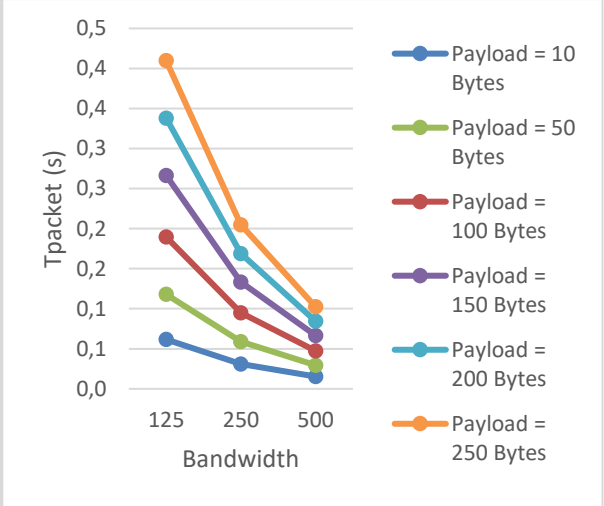

Figure 3.3 b) – LoRa packet time variation with Bandwidth (CR=4/5 and SF=7)

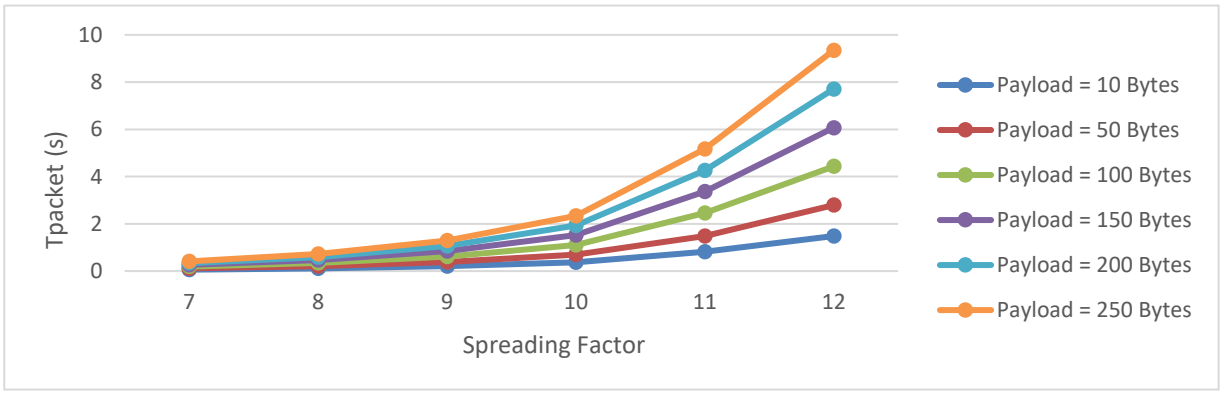

Figure 3.3 c) – LoRa packet time variation with Spreading Factor (BW=125 kHz and CR=4/5)

[1] *ceil* function indicates that the portion of the equation in square brackets should be rounded up to the next integer value. The *max*function compares the evaluated *ceil* function result and returns 0 or the result - whichever is higher

It can be concluded that Spreading Factor and Coding Rate has a direct influence on the time on air of the LoRa packet, regardless the Payload length, since time on air increases with the increase in size of the payload and with both CR and SF values (Figure 3.3 a) and Figure 3.3 c). Figure 3.3 b) demonstrates that bandwidth also influence the time on air of a packet. The higher is the bandwidth, the lower is the time on air.

3.2.2 MAC Layer – LoRaWAN

As described in Section 2.6.1, LoRa is a proprietary physical layer for LPWA connectivity. Promoted by the LoRa Alliance [37], LoRaWAN defines the communication protocol and system architecture for the LoRa PHY layer. This protocol and network architecture have the most influence in determining the battery lifetime of a node, the network capacity, the quality of service, the security, and the variety of applications served by the network.

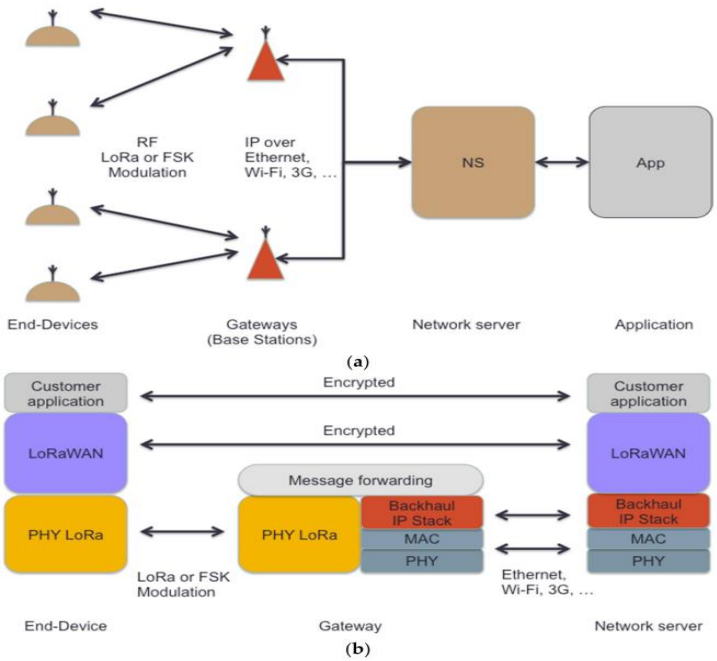

Figure 3.4 – LoRaWAN system a) and protocol architecture b) [44]

A LoRaWAN network architecture is based on a star-of-stars topology composed of three elements: end-devices, gateways and a central network server (Figure 3.4 a).

End-Devices are low-power sensors/actuators that communicate with the network server through the connection via LoRa radio interface to one or more gateways;

Gateways act as concentrators that forward packets coming from end-devices to a network server through an IP backhaul interface, which provides a higher throughput, such as 3G or ethernet (Figure 3.4 b). It is possible that multiple gateways coexist in the same LoRa deployment, which could lead that different gateways receive the same packet, while the network server sends messages to end-devices through a specific gateway;

Network Server is the entity that responsible for the management of the overall network. For instance, it filters the duplicated packets from different gateways, does security check, send ACKs (Acknowledgements) to the gateways.

The architecture is essentially composed of dedicated gateways serving as transparent bridges between end-nodes and the network server, where the data is stored and made available to the subscriber.

The nodes in a LoRaWAN network are asynchronous and communicate following a simple ALOHA scheme, meaning that the nodes transmit information whenever they want to transmit. Since LoRaWAN permits the usage of different channels and/or orthogonal spreading factor codes, it is possible for multiple devices to communicate at the same time, and the network is still able to decode their information correctly [45].

LoRa network allows the end-devices to individually use any of the possible data rates and Tx power. This feature resides in the network server and is used by the LoRaWAN to adapt and optimize the data rate and Tx power of static end-devices. This is referred to as ADR (Adaptive Data Rate) and when this is enabled, the network will be optimized to use the fastest data rate possible.

In many IoT applications described in Table 2.3, the end-devices are static most of the time, meaning that is possible for them to request the network server to optimize the data rate under those circumstances. However, when those end-devices are subject to any kind of mobility, it can cause significant temporarily variations for the radio channel characteristics (Doppler Effect) [40]. In this situation, when the Network Server is unable to control the data rate of a device, the device's application layer should control it by using a fixed data rate.

LoRaWAN also considers security issues, so a cryptographic suite based on AES encryption is included by default in order to secure the transmitted data at different OSI levels. [24]

3.2.2.1 Devices classes

Due to the energy-related constraints of end-nodes, LPWAN technologies present a highly limited downlink (transmissions from the gateway down to end-nodes), hence LoRaWAN contemplates the use of three different types of end-devices according to their energy limitations and application needs. For that, the MAC layer defines three options for scheduling the receive window slots for downlink communication, which are named as classes A, B, and C. The end device must have a support for class A, but support for classes B and C is optional.

All of the classes support bi-directional communication, but with different downlink latency and power requirements. A more detailed definition is described next.

Class A, bidirectional (for all devices): Class A devices allow for bi-directional communications whereby each end-device's uplink transmission is followed by two short Downlink receive windows. The transmission slot scheduled by the end-device (uplink transmission) is based on its own communication needs with a small variation based on a random time basis (ALOHA-type protocol).
Downlink transmission from the server at any other time has to wait until the next uplink transmission occurs. Class A devices have the lowest power consumption, thus achieves the longest battery lifetime, but also offers less flexibility on downlink transmissions (Figure 3.5 a).

Class B, bi-directional with scheduled receive slots (for beacon): Class B end-devices can schedule downlink receptions, by opening extra receive windows at defined time intervals. Thus, only at these certain times, applications can send control messages to the end-devices. A synchronized beacon from the gateway is therefore required, so that the network server can synchronize all in end devices in the network. When an end device receives this beacon, it can open a short reception window called "ping slot" predictably during a periodic time slot (Figure 3.5 b)

Class C, bi-directional with maximal receive slots (for continuous listening): Class C end-devices have almost continuous receive windows (Figure 3.5 c). This class has a major impact over the devices energy consumption, thus, it is defined for end-devices that do not have energy consumption restrictions

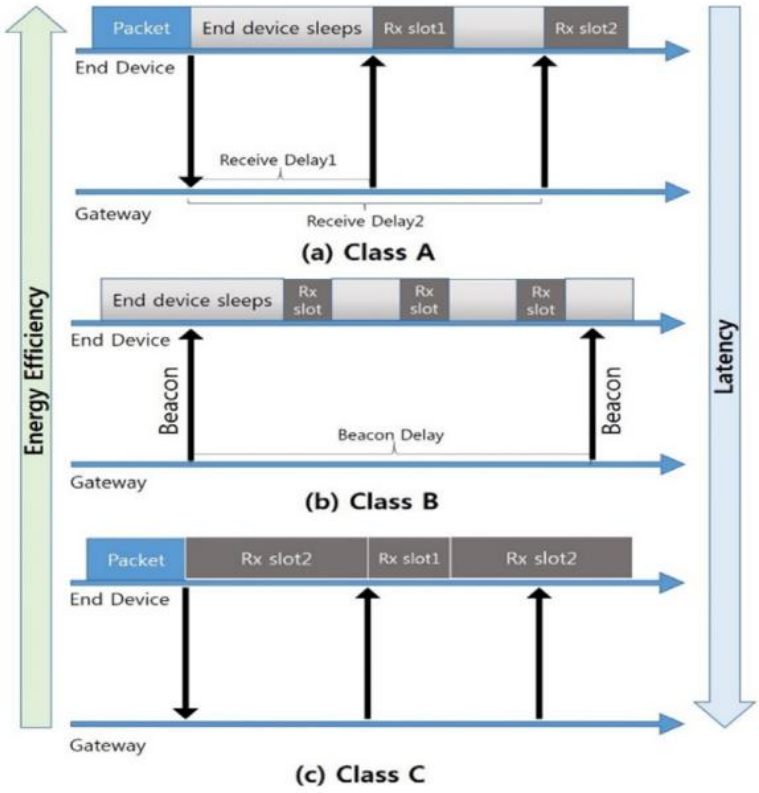

Figure 3.5 a); b) and c) – LoRaWAN device classes receive slot timing [46]

3.2.2.2 Packet Structure

LoRaWAN provides a full stack network protocol, having features of datalink, network and transport layer, and natively supporting encryption, authentication and reliable communication trough packet retransmission

LoRaWAN's MAC packet structure are contained within the radio physical payload (PHYPayload) of the LoRa protocol (Figure 3.2)

The structure of a LoRaWAN **PHYPayload** contains three main fields: **MHDR** (MAC Header), MAC Payload and a **MIC** (Message Integrity Check) and is illustrated next.

Size (bytes)	1	7…N	4
PHY Payload	MAC Header	MAC Payload	MIC

Figure 3.6 – LoRa physical payload structured as a LoRaWAN message [47]

MHDR (MAC header) specifies the Message type and the version of the LoRaWAN, with a maximum length of 3 and 1 bits respectively. **MHDR** frame is shown next.

Bit#	7…5	4…2	1…0
Fields	Message Type	RFU	Major Version

Figure 3.7 – LoRaWAN MAC Header [47]

- **MType** (Message Type): The MAC header specifies the **MType** (Message Type) and according to which major version the frame has been encoded. It distinguishes between 8 different MAC message types, described in the Table 3.2.

MType	Description
000	Join-Request
001	Join-accept
010	Unconfirmed Data Up
011	Unconfirmed Data Down
100	Confirmed Data Up
101	Confirmed Data Down
110	Rejoin-request
111	Proprietary

Table 3.2 – LoRaWAN MAC message types [47]

MAC Payload contains a frame header (**FHDR**) followed by an optional port field (**FPort**) and an optional frame payload field (**FRMPayload**). The length of the MAC Payload is variable since it depends on which data rate is in use.

Size (bytes)	7 … 22	0 … 1	0 … M
MAC Payload	Frame Header	Frame Port	Frame Payload

Figure 3.8 – LoRaWAN MAC Payload [47]

- **FHDR** contains the short device address of the end-device (**DevAddr**), a frame control octet (**FCtrl**) to set up ADR (Adaptive Data Rate), a 2-octets frame counter (**FCnt**), and up to 15 octets of frame options (**FOpts**) used to transport MAC commands.

Size (bytes)	4	1	2	0 ... 15
Frame Header	Device Addr	Frame Control	Frame Counter	Frame Options

Figure 3.9 – LoRaWAN Frame Header [47]

- Frame Port (**FPort**) and Frame Payload (**FRMPayload**) by default LoRaWAN encrypts every Frame Payload by means of the Application Session Key.
  If the Frame Payload carries a MAC command, then the Frame Port is set to 0 and it is encrypted with Network Session Key. If encryption is done above the LoRaWAN layer is possible to disable this features through a MAC command, but it is allowed only if the frame payload does not carry a MAC command itself.

MIC (Message Integrity Code) authenticates each message to the LoRaWAN Network Server with a maximum of 4 bytes. MIC is calculated over all the fields in the message.

$$msg = MHDR \mid FHDR \mid FPort \mid FRMPayload \tag{3.11}$$

In resume, LoRaWAN message format is detailed in Figure 3.10:

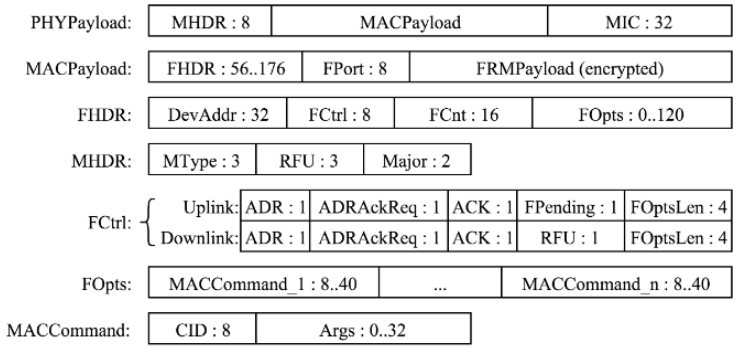

Figure 3.10 – LoRaWAN frame format. The sizes of the fields are in bits [33]

3.2.2.3 End-Devices Setup

In order to participate in a LoRaWAN network, an end-device must be activated. LoRaWAN provided two ways to activate an end-device: OTAA (Over-The-Air Activation), in which each end-device must perform a *join* procedure involving the exchange of some messages with the server infrastructure and ABP (Activation by Personalization), in which the end-devices already know the address and the keys, so they can bypass the join procedure.

In both activation methods, the following information should be passed to an end-device:

- **End-device address (DevAddr):** A 32-bit identifier of the end-device. Seven bits are used as the network identifier, and 25 bits are used as the network address of the end-device.
- **Application identifier (AppEUI):** A global application ID in the IEEE EUI64 address space that uniquely identifies the owner of the end-device.
- **Network session key (NwkSKey):** A 128 bit AES key used for authentication by the network server and the end-device to calculate and verify the message integrity code of all data messages to ensure data integrity.
- **Application session key (AppSKey):** A 128 bit AES key used by the network server and end-device to encrypt and decrypt the payload field of data messages.

While the ABP may be trivially implemented by just load on all end-devices the addresses and the session keys identified above, the OTAA *join* procedure requires both a protocol to get the information form the server, and an algorithm to generate the session keys.

The join procedure consists of two messages:

1. *Join Request*, sent by the end-device to the server and containing AppEUI, DevEUI and DevNonce;
2. *Join Accept*, sent by the server to the end-device and containing DevAddress, NetID and AppNonce, all encrypted with a shared long-term AppKey.

If this procedure successfully completes, both the end-device and the server can run the key generation algorithm to compute the session key as described in [48] .

3.2.2.4 MAC commands

For network administration, a set of MAC commands may be exchanged exclusively between the Network Server and the MAC layer on an end-device [33].

LoRaWAN defines many MAC commands that allow customizing end-device parameters. One of them, *LinkCheckReq*, can be sent by an end-device to test its connectivity. All of the others are sent by the network server. These commands can control the data rate and output power used by the device, as well as the number of times each unconfirmed packet should be sent (*LinkADRReq*), the global duty cycle of the device (*DutyCycleReq*), changing parameters

of the receive windows (*RXTimingSetupReq*, *RXParamSetupReq*) and changing the channels used by the device (*NewChannelReq*). Also, commands to query the battery level and reception quality of a device (*DevStatusReq*) can be sent.

Figure 3.11 contains the list of MAC commands defined in the LoRaWAN 1.1 specification [47].

CID	Command	TX by ED	TX by GW	Description
0x02	LinkCheckReq	x		Used by an end-device to validate its connectivity to a network.
0x02	LinkCheckAns		x	Answer to LinkCheckReq command. Contains the received signal power estimation indicating to the end-device the quality of reception (link margin).
0x03	LinkADRReq		x	Requests the end-device to change data rate, transmit power, repetition rate or channel.
0x03	LinkADRAns	x		Acknowledges the LinkRateReq.
0x04	DutyCycleReq		x	Sets the maximum aggregated transmit duty-cycle of a device
0x04	DutyCycleAns	x		Acknowledges a DutyCycleReq command
0x05	RXParamSetupReq		x	Sets the reception slots parameters
0x05	RXParamSetupAns	x		Acknowledges a RXSetupReq command

CID	Command	Transmitted by ED	Transmitted by GW	Description
0x06	DevStatusReq		x	Requests the status of the end-device
0x06	DevStatusAns	x		Returns the status of the end-device, namely its battery level and its demodulation margin
0x07	NewChannelReq		x	Creates or modifies the definition of a radio channel
0x07	NewChannelAns	x		Acknowledges a NewChannelReq command
0x08	RXTimingSetupReq		x	Sets the timing of the of the reception slots
0x08	RXTimingSetupAns	x		Acknowledge RXTimingSetupReq command
0x80 to 0xFF	Proprietary	x	x	Reserved for proprietary network command extensions

Figure 3.11 – LoRaWAN MAC message types [47]

3.2.2.5 LoRaWAN regulations

In Europe, LPWANs technologies mainly use the 863-870 MHz ISM (so-called SDR860). This band must perform according the regulations present in ETSI (European Telecommunications Standards Institute) EN300-220-1[29]. It specifies the various requirements for SRD (Short Range Device) devices, such as the constraints for the duty cycled transmissions.

The LoRaWAN specification states that LoRaWAN networks should make use of the unlicensed ISM frequency bands, where in Europe it is 863 – 868 MHz. In order to limit the rate at which the LoRaWAN end devices can actually generate messages, these bands were subject to regulations regarding the maximum transmission power and the duty cycle of the end-devices.

There are essentially three levels at which different organizations handle spectrum allocation and limit its use:

1. At the *national level*, the frequency spectrum is managed by National Administrations,

which:

- Compile a table of spectrum allocations.
- Define a framework for use of these bands.
- Assign each band to different users, possibly via licenses.

2. At the *European level*, there are three organisms that cooperate to regulate spectrum usage:

- The European Commission (EC)
- CEPT's Electronic Communications Committee (ECC)
- The European Telecommunications Standard Institute (ETSI)

3. At the *worldwide level*, the International Telecommunication Union (ITU) coordinates regional and national organisms.

In this dissertation, only the ETSI and ECC regulations will be followed.
To evaluate the limitations of the transmission power in this band, ETSI uses the ERP (Effective Radiated Power) metric in their test devices. The ERP is measured using a half-wave dipole instead of an isotropic antenna, as in the EIRP. Since the gain of a half-wave dipole is at most 2.15 dBi (dB relative to an isotropic radiator), the following holds:

$$ERP = EIRP - 2.15 \tag{3.12}$$

LoraWAN is also limited in the maximum time on air. For that, end-nodes are required to either adopt a LBT (Listen-Before-Talk) policy or to duty cycled their transmissions. Duty cycle is defined as the ratio of the maximum transmitter "on" time over one hour, relative to a one hour period, expressed as a percentage.
Since LoRaWAN has defined no LBT mechanism as of now, the latter policy is adopted in the vast majority of the cases. Table 3.3 illustrates the limitations described above.

Edge Freq.-	Edge Freq.+	Field/Power	Spect. Access	Bandwidth
865 MHz	868 MHz	+6.2dBm/100 KHz	1% or LBT AFA	3 MHz
865 MHz	870 MHz	−0.8dBm/100 KHz	0.1% or LBT AFA	5 MHz
868 MHz	868.6 MHz	14 dBm	1% or LBT AFA	600 KHz
868.7 MHz	869.2 MHz	14 dBm	0.1% or LBT AFA	500 KHz
869.4 MHz	869.65 MHz	27 dBm	10 % or LBT AFA	250 KHz
869.7 MHz	870 MHz	7 dBm	No Requirement	300 KHz
869.7 MHz	870 MHz	14 dBm	1% or LBT AFA	300 KHz

Table 3.3 – Channel lineup for LoRa according to ETSI regulations.

As can be seen in Table 3.3, the max duty cycle requirements for spectrum access are very stringent and can vary greatly between bands.

According to LoRaWAN specifications [47], all end-devices must implement three channels of 125 kHz at 868.1 MHz; 868.3 MHz and 868.5 MHz. Also, all of these channels are limited to a duty cycle of 1%, which means that they are only able to stay “on air” for a maximum time of 36 sec in a period of 1 hour, and all share the same limitation on the output power, +14 dBm ERP. Duty cycle regulations is a truly limitation to all the IoT applications that are required to have nodes transmitting more data than the usual.

4

IoT Network Planning

4.1 Introduction

This chapter presents all the mechanisms and calculations proposed to achieve an efficient IoT network planning in terms of coverage, using the LoRa technology. For that, a real life scenario is considered, which is the city of Aveiro.

Section 4.2 describes the defined planning area in the city of Aveiro and its estimation in terms of area, and inhabitants.

Section 4.3 presents a generic IoT network planning, more precisely for the LPWA technologies.

Section 4.4 proposes a Link Budget with some adaptations to the generic coverage. In this dissertation, only the LoRa technology is considered for evaluation. For that, all the link budget calculations, namely the maximum propagation attenuation, are carried out, taking into account the data obtained from the LoRa study of Chapter 3.

Section 4.5 presents the cell radius and the number of sites needed to cover the area in study. For this, the propagation model used to carry out the entire network performance estimation was the *Okumura-Hata*.

4.2 Planning Scenario

The city chosen to perform the IoT network planning was the municipality of Aveiro, capital of the district of Aveiro, a Portuguese city located in the centre-region of Portugal.

Aveiro municipality accounts approximately 78 450 inhabitants accordingly to the latest CENSOS in 2011 [49] and 197,58 km^2 of area, across 10 parishes. It is considered to be an important urban, port, railway, university and touristic centre.

Among the 10 possible parishes in the municipality of Aveiro, only the parishes "Glória" and "Vera Cruz" are considered for the planning of the network and for the next chapters of this dissertation, since their union, Glória e Vera Cruz is consider to be the centre of Aveiro district, and consequently, with the most inhabitants, approximately 18 756 and 45,32 km^2 of area, where Glória contemplates 6,85 km^2 and Vera Cruz 38,47, leading to a density of 413 inhabitants/km^2 [50]. However, most of the area of Vera Cruz is constituted of open land fields, and therefore not interesting to study. With this in mind, the total consideration area for "Gloria e Vera Cruz" is 8,5 km^2 and it is delimited in Figure 4.1.

Figure 4.1 – Footage of "Glória e Vera Cruz" in Google Earth

4.2.1 Environment classification

The usage of models with an empirical component requires the classification of different types of environments. There are several types of classification, generally associated to distinct propagation models, that considers (among others) some parameters such as: ripple of the terrain, density of vegetation, density and height of buildings, existence of open areas and existence of aquatic surfaces [51].

Accordingly to [52], it's usual to distinguish areas among three main categories:

Urban areas, Built-up city or large town with large buildings and houses with two or more stories or large villages with close houses and tall, thickly grown trees;

Suburban areas, Village or highway scattered with trees and houses, some obstacles near the receiving antenna but not very congested;

Rural areas, Open space, no tall trees or buildings in propagation path, plot of land cleared for 300-400 m ahead, e.g. farmland, rice fields and open fields.

According to the description given above, the municipality of Aveiro is considered to be an Urban environment. Therefore, it is expected that the buildings will provoke the existence of numerous reflected rays (which causes fading), and of shadow zones (where the attenuation is vast). Due to these characteristics, the task of measuring a propagation model based on actual measurements is not precise, so there is always significant deviations between signal prediction and reality later implementation.

4.3 General IoT coverage planning

For a real IoT network deployment, an understanding of the radio channel characteristics is essential, regardless the technology in use. The radio channel of a wireless technology describes the behaviour of the signal since it is transmitted, until it reaches the receiver, no matter if it initiated by the sensor or the gateway. The electromagnetic wave that is generated by the transmitter, suffers attenuation (reduction in power density) before reaching the receiver, and that is called path loss. Path loss is a major component in the analysis and design of the link budget of network, since it allows to predict the coverage area, and also to quantify how reliable is the radio link for the city in study.

The link budget of a wireless system is a measure of all the gains and losses from the transmitter, through the propagation channel, to the target receiver. Since IoT devices have bidirectional communication, there is correspondingly an Uplink Path Loss from Sensor to Gateway, and a Downlink Path Loss from Gateway to Sensor (although the majority is Uplink), and consequently both needs to be considered in the link budget calculations.

As other wireless technologies, the link budget in an IoT network contemplates several factors, such as emission power values, various equipment losses (gateway, sensors, cables, connectors, etc.), antenna gains and propagation effects. For this last one, the signal in the propagation medium, which is air, is subject to attenuation, such as fading (multipath or Doppler),

shadowing (interference caused by obstacles), interference and noise, further described in this dissertation. Friis formula relates all of these factors and is expressed in Equation 4.1:

$$P_{RX} = P_{TX} + G_{TX} + G_{RX} - Att - L_p \quad (4.1)$$

Where:

- P_{RX}, is the received power $[dBm]$
- P_{TX}, is the transmission power $[dBm]$
- G_{TX}, is the transmission antenna gain $[dBi]$
- G_{RX}, is the reception antenna gain $[dBi]$
- Att, is the cables; connectors and jumpers attenuation $[dB]$
- L_p, is the propagation loss $[dB]$

The resulting calculations with the combination of an appropriate propagation model, allows to determine the cell radius, meaning the range a single gateway can cover, the distance between gateways and the number of gateways required to cover the entire area of study defined in subchapter 4.2. A description of propagation models is described next.

4.3.1 Propagation Models

The propagation signal of IoT devices are affected by the atmospheric conditions, the topography and the morphology of the terrain, which forces the choice of a suitable propagation model for the area under study. Through the propagation model and based on the calculated maximum attenuation, the cell radius can be determined, that is, the maximum range of a radio link, the distance between the sites and the number of sites needed to cover the planning area.

The models of propagation fall into two main categories:

- **Empirical** - Based on measurements and leading to simple relationships between attenuation and distance. Empirical models lead to curves and equations that best fit the measurements and have the advantage of accounting for all factors that affect propagation. Since every environment differs from each other, this propagation model implies validation of the various factors that affects the propagation loss; An example of empirical models includes *Hata* model, *Okumura-Hata* model and *COST-231* model.

- **Theoretical** – Requires essentially the usage of topographic databases. Theoretical models do not account for all the factors and do not consider the environment in which question. They allow easy changeover to other parameter values and truly depends on the geographic databases.

There is also semi-empirical models, models which contemplate both empirical and theoretical perspectives, like *Cost-231 Walfisch-Ikegami*. The advantage of semi-empirical models is that they have some flexibility, can be gauged with actual measurements carried out in the specific propagation environments where they will be used. In this way, the error between the estimation of the signal predicted by the propagation model and the subsequent reality when the physical implementation of the gateway is minimized.

It is important to point out that there is no general method or algorithm that is universally accepted as the best propagation model for an IoT network planning. Each model can be useful for some specific environment and the accuracy of any particular technique or algorithm depends on the fit between the parameters available for the area concerned and the parameters required by the model [51].

4.3.1.1 Free-Space Path Loss model

FSPL (Free-space path loss) is the loss in signal strength of an electromagnetic wave that would result from a line-of-sight path through free space (usually air), with no obstacles nearby to cause reflection or diffraction. FSPL is proportional to the square of the distance between the transmitter and receiver, and also proportional to the square of the frequency of the radio signal, as given in Equation 4.2:

$$\mathrm{F}SPL = \left(\frac{4\pi d f_c}{c}\right)^2 \tag{4.2}$$

Where:

- f_c, is the signal frequency $[Hz]$;
- d, is the distance from the transmitter [meters];
- c, is the speed of light in vacuum, approximately $3 * 10^8\ m/s$

Equation 4.2 is given in the logarithmic domain as follows:

$$FSPL = 20\log_{10}\left(\mathrm{f}_{\mathrm{c}_{[\mathrm{MHz}]}}\right) + 20\log_{10}\left(\mathrm{d}_{[\mathrm{km}]}\right) + 32{,}45 \tag{4.3}$$

4.3.1.2 *Okumura-Hata* model

Okumura-Hata is an empirical formulation of the model proposed by *Okumura* based on measurements in the [150, 2000] MHz band. *Okumura* presented the results in the form of curves, *Hata* established expressions that approached some of these curves. It is a standard model in the calculation of free space propagation attenuation for the various types of environments already mentioned.

This model applies to a distance between the gateway and the sensor of 1 to 20 km, height of the gateway between 30 and 200 m and an height of the sensors between 1 and 10 m. The propagation attenuation according to this model is given by:

$$L_{p_{50\%}} = A + B * \log\left(d_{máx_{[km]}}\right) + C \tag{4.4}$$

Where *A*, *B* and *C* are factors that depend on frequency and antenna height:

$$A = 69{,}55 + 26{,}16\log\left(f_{c_{[MHz]}}\right) - 13{,}82\log\left(h_{Gateway_{[m]}}\right) - \alpha(h_{Sensor}) \tag{4.5}$$

$$B = 44{,}9 - 6{,}55\log\left(h_{Gateway_{[m]}}\right) \tag{4.6}$$

Where:

- $L_{P_{50\%}}$, is the median path loss for 50% of coverage $[dB]$
- f_c, is the frequency of the link $[MHz]$
- $h_{Gateway}$, is the height of the gateway $[meters]$
- h_{Sensor}, is the height of the sensor $[meters]$
- $d_{máx}$, is the maximum distance between the sensor and the gateway $[km]$
- $\alpha(h_{Sensor})$, is the correction factor for the sensor height $[dB]$

The function $\alpha(h_{Sensor})$ and the factor *C* depends on the type of environment:

- **Urban environment:**

Small and Medium size cities:

$$\alpha(h_{Sensor}) = \left[1{,}10\log\left(f_{c[MHz]}\right) - 0{,}70\right] h_{Sensor} - \left[1{,}56\log(f_{c[MHz]}\right) - 0{,}80] \qquad (4.7)$$
$$C = 0$$

Large size cities:

$$\alpha(h_{Sensor}) = \begin{cases} 8{,}29\log(1{,}54h_{Sensor})^2 - 1{,}10, & f \leq 300\ MHz \\ 3.2\log(11.75h_{Sensor})^2 - 4{,}97, & f > 300\ MHz \end{cases} \qquad (4.8)$$
$$C = 0$$

- **Suburban environment:**

$$C_{[dB]} = -2\left[\log\left(\frac{f_{c[MHz]}}{28}\right)\right]^2 - 5{,}4 \qquad (4.9)$$

- **Rural environment:**

$$C_{[dB]} = -4{,}78\log^2\left(f_{c[MHz]}\right) + 18{,}33\log\left(f_{c[MHz]}\right) - 40{,}98 \qquad (4.10)$$

The function $\alpha(h_{sens})$ in suburban and rural areas is the same as for urban (small and medium-sized cities) areas.

By simplifying equation 4.4, it is possible to estimate the total distance between the gateway and the sensor, meaning the maximum coverage the gateway can achieve for 50% of coverage. This results in Equation 4.11:

$$d_{máx[km]} = \frac{\left(10^{Lp_{50\%}} - A - C\right)}{B} \qquad (4.11)$$

4.3.1.3 Generic propagation model

A generic propagation model is usually considered when field measurements are further derived (which is the case in this dissertation). Here, the mean path loss ($\overline{PL}$), as a function of distance, d, between the sensor and gateway is proportional to a path loss decay (n) and relative to a reference distance, d_0:

$$\overline{PL}(d) = \propto \left(\frac{\mathrm{d}}{\mathrm{d}_0}\right)^n \tag{4.12}$$

$\overline{PL}\ (d)$ is often stated in decibels, as shown below:

$$\overline{PL}(d)\ _{[dB]} = \overline{PL}(d_0) + 10nlog\left(\frac{d}{d_0}\right) \tag{4.13}$$

Where:

- $\overline{PL}(d_0)$, is the mean path loss at a reference distance d_0, typically found through field measurements or is calculated using the free-space path loss given by Equation 4.3 [dB].

From Equation 4.13, a statistical output for all possible values of the path loss for a given distance (d) is obtained. The reference distance (d_0) is usally considered to be 1 km for macro-cellular planning, and between 1 m and 100m for micro-cellular environments. Linear regression for a MMSE (*Minimum Mean-Squared Estimate*) of $\overline{PL}$ vs. d in a logarithmic scale (for distances greater than d_0) yields a straight line with a slope equal to $10n$ dB/decade. n, the decay coefficient depends entirely on the environment in study. In free-space, $n = 2$ is considered, but for urban environments, $n = 3$ is usually defined [53]. Many measurement campaigns have also been conducted and reported in the literature to define the decay coefficient (n) for different locations, some of which are summarized in Table 4.1.

Source	City	Decay coefficient ($\boldsymbol{n}$)
[54]	Outdoor, Hamburg, Germany	2,5
	Indoor, Frankfurt	3,8
[28]	Car Oulu, Finland	2,32
	Boat, Oulu, Finland	1,76

Table 4.1 – Decay Coefficient results based on real location measurements

As demonstrated in Table 4.1, $n = 3$ is a reasonable approximation to take in consideration for an IoT network planning in an urban city like Aveiro. The more obstructed the environment is, the higher the decay coefficient is. Taking as an example the 2nd and 4th entry of Table 4.1, the measurements of the indoor environment in the city of Frankfurt have conducted to a much more higher n than the tests conducted in the Boat in Oulu, which is by definition a much more wider and open environment.

4.3.2 Margins

Propagation models only calculate propagation losses for a coverage probability of 50% (Figure 4.2). This means that at the edge of the gateway's coverage area, only 50% of the spots are covered with signal levels above the minimum sensitivity, which in a real-life scenario is not suitable.

In order to appropriately design the IoT network in terms of the coverage probability of the whole cell, typically a value between 90% and 99% is considered. Therefore, a value of 95% is aimed in this IoT planning. Increasing the probability of coverage is achieved by adding a coverage margin to the link budget calculations.

This margin is considered according to the reliability required from the system to provide reliable communications over the entire cell coverage area and also guarantees a coverage planning with a greater precision and less susceptible to failures in a practical deployment.

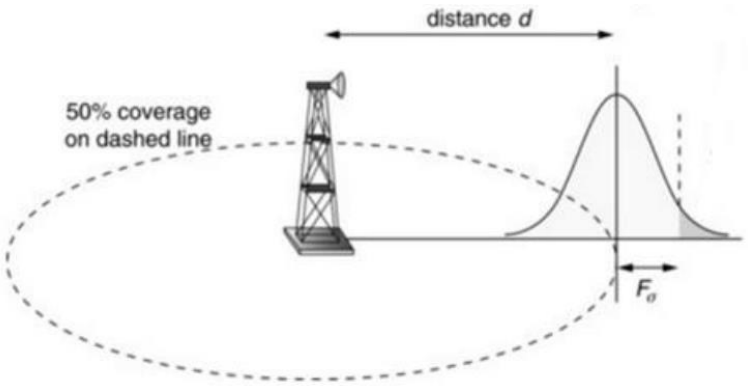

Figure 4.2 – Example of a cell covering only 50% of the locations at the cell border

The coverage margin to be added attempts to compensate for some factors that are not considered in the propagation models and that influence the level of the signal that arrives at the sensors/gateways. In a connection of this type, where there are many variable characteristics at

the time, it is natural that the received signal power varies over time, even though the power of the emitted signal remains constant. This phenomenon is known as fading and it's detailed next.

4.3.2.1 Fading

Fading is a significant part of any wireless communication design and is important to model and predict accurately. There are two very different types of fading: large scale fading (often called slow fading or shadowing) and small-scale fading.

Large scale fading is caused mainly by the shadowing effect, where a large obstacle such as hill, forest or large building obscures the main signal path over large distances. These obstacles also reflect the transmitted signal and generate other paths of transmission, often called as multipath. This causes deep fades within small distances between the transmitter and the receiver and is referred as small-scale fading. Usually, fading is often handled in a wireless system with diversity schemes [55].

Figure 4.3 illustrates the effect of both fading types in a telecommunication system. In an ideal scenario, path loss (PL) decreases linearly with the logarithm of the distance, as shown in Equation 4.13, thus $\frac{P_{Rx}}{P_{Tx}}$ has a constant value for the same value of (d), regardless of the environment the transmitter and receiver are placed at. However, in the presence of shadowing and/or multipath, the environment conditions are considered, thus different values of PL are expected for the same d.

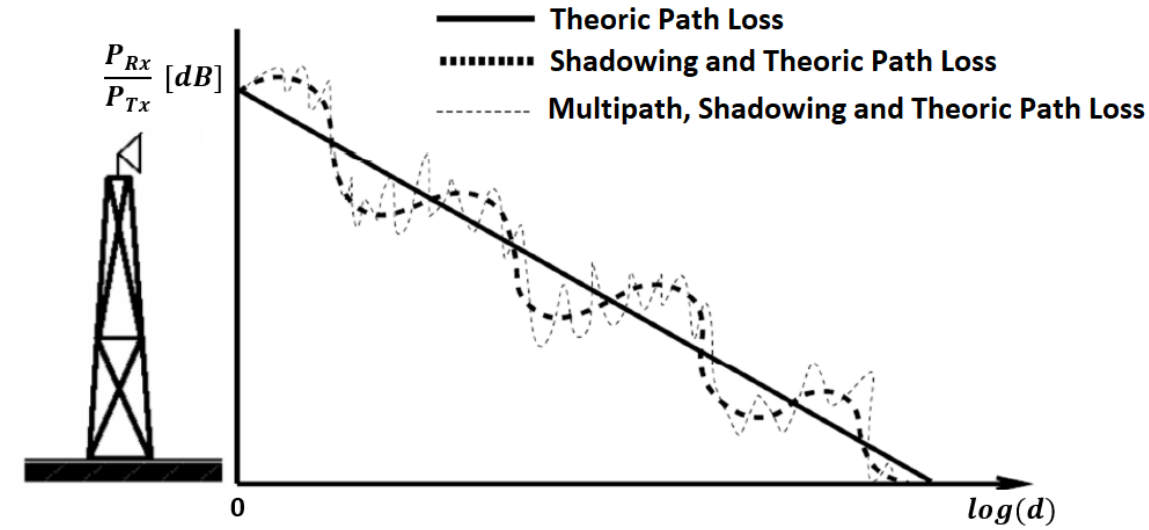

Figure 4.3 – $\frac{P_{Rx}}{P_{Tx}}$ variation with the increase of $\log(d)$ in the presence of shadowing and multipath fading

4.3.2.1.1 Large-Scale Fading

If we consider a Smart City environment, the IoT devices will usually be placed outdoors, and therefore subjected to day-to-day and seasonal variations over long periods time, such as hours, days, months or even years. Those variations are usually caused by slow changes in the atmosphere and the propagation medium, namely, temperature, rainfall, ducts, cloudiness, and due to the presence of large obstacles such as hills or large buildings. Therefore, long-term variations in the signal level, which translates into discrepancies in the mean path loss, are expected and must be considered for the overall link design.

The signal strength value computed by propagation models is considered as a mean value of the signal strength in a small area, meaning that 50% of the locations (for example at the cell borders) can be considered to have a signal strength that exceeds the predicted value.

In order to plan for more than 50% probability of signal strength above the threshold, a log-normal fading margin, LNF_{Marg}, has to be considered during the design process. In order to determine this LNF_{Marg}, two common reliability methods are considered: cell edge and area reliability.

- **Cell Edge Reliabilty**:

Studies have demonstrated that shadowing variations follows a log-normal distribution [54], [56], [57]; which means that, when shadowing power levels are measured in dB, they follow a Normal or Gaussian distribution. Shadowing can be modelled as a log-normal process with a mean (μ), that is the average path loss, and a standard deviation σ. For this reason, a Gaussian random variable (X_σ) with $\mu = 0$ (dB) and standard deviation σ (dB) is considered. This can be mathematically translated as $X_\sigma \sim N\ (0, \sigma)$.

The standard deviation σ is chosen according to the type of environment, since the signal strength for unobstructed free space propagation decreases accordingly to the value of n between the emitter and the receiver, but with obstacles this exponent increase, which means it eases faster (Table 4.1). As in any given environment there are always obstacles, and Aveiro city is not an exception whether buildings or trees, the signal intensity begins to decrease with an increasing exponent depending on the number of obstacles. Common σ values depending on the type of environment are presented in Table 4.2 accordingly to [56].

Type of environment	$\sigma[dB]$
Dense Urban	10
Urban	8
Rural	6

Table 4.2 – Standard deviation values accordingly to the type of environment [56]

Since Aveiro city is characterized as being an Urban environment, let us assume a value for $\sigma = 8$.

Equation 4.13 is an average of the Path Loss, which doesn't take in consideration the shadowing effect, and therefore not adequate to describe any particular signal path. It is necessary to provide for variations about the mean since the environment locations may be quite different for similar sensor-gateway distances. With this in mind, the new Path Loss (PL) can be described on Equation 4.14:

$$PL\ (d)\ _{[dB]} = \overline{PL}(d_0)_{[dB]} + 10nlog\left(\frac{d}{d_0}\right) + X_{\sigma_{[dB]}} \tag{4.14}$$

Moreover, by taken Friis Formula in consideration and assuming an uplink scenario with unitary gain antennas at both sensor and gateway, and without attenuation caused by jumpers; connectors $(A_{tt} = 0)$ and feeders, it can be seen that the distance dependent received power from the gateway (P_{RX}) depends also on the sensor radiated power (P_{TX}). This can be traduced as:

$$P_{RX}\ (d)_{[dBm]} = P_{TX_{[dBm]}} - PL(d)_{[dB]} \tag{4.15}$$

Since $PL\ (d)$ is a random variable that follows a normal distribution, Equation 4.15 shows that $P_{RX}(d)$ also follows the same path. $P_{RX}(d)$ can also be described as:

$$P_{RX}\ (d)_{[dBm]} = P_{TX_{[dBm]}} - \left[\overline{PL}(d_0)_{[dB]} + 10nlog\left(\frac{d}{d_0}\right) + X_{\sigma_{[dB]}}\right] \tag{4.16}$$

The PDF (probability density function) of a normal distribution with a mean value (μ) and a standard deviation (σ) is defined as:

$$p(x) = \frac{1}{\sigma\sqrt{2\pi}} e^{-\frac{(x-\mu)^2}{2\sigma^2}} \tag{4.17}$$

Where x is the random variable (here the slow fading signal), μ is the mean value of x and σ is the standard deviation of x.

If we consider that on the cell boundary, the probability that the received power ($P_{RX}(d)$) exceeds a certain threshold γ, then:

$$[Prob(P_{RX}(d) > \gamma)] = \int_{\gamma}^{\infty} \frac{1}{\sigma\sqrt{2\pi}} e^{\frac{-(\gamma-\overline{P_{RX}(d)})^2}{2\sigma^2}} \partial P_{RX}(d) \quad (4.18)$$

By integrating the probability density function from γ to ∞, with the $erf(x)$ function, the edge reliability results in:

$$Prob(P_{RX}(d) > \gamma) = \frac{1}{2} + \frac{1}{2}\text{erf}\left(\frac{(\overline{P_{RX}(d)}-\gamma)}{\sigma\sqrt{2}}\right) \quad (4.19)$$

With this expression, the additional margin that considers shadowing in the link budget, meaning, the margin that assures that the signal strength $P_{RX}(d)$ is $Prob(P_{RX}(d) > \gamma)$ % of the time above a threshold γ is given by: $LNF_{Marg} = \overline{P_{RX}(d)} - \gamma$.

Alternative representations of that formula sometime make use of the *Q* function:

$$Prob(P_{RX}(d) > \gamma) = Q\left(-\frac{(\overline{P_{RX}(d)}-\gamma)}{\sigma}\right) \quad (4.20)$$

Figure 4.4 illustrates the relation between LNF_{Marg} and $Prob(P_{RX}(d) > \gamma)$ using Eq. 4.19. This figure can be used to calculate the required LNF_{Marg} for any IoT Link Budget in a dense-urban; urban and rural environment, which have a typical σ associated, accordingly to Table 4.2.

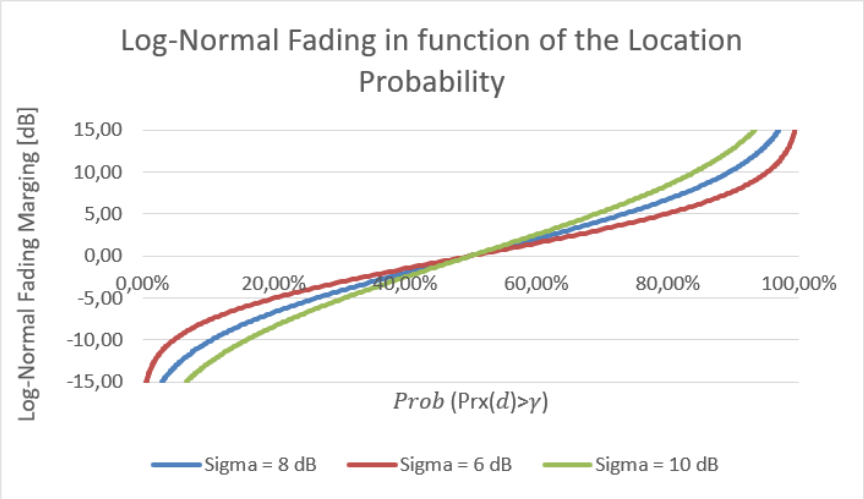

Figure 4.4 – LNF_{Marg} in function of the cell border coverage percentage for the various σ

From Figure 4.4 it can be concluded that LNF_{Marg}:

- Is negative if $Prob(P_{RX}(d) > \gamma)$ is below 50%;
- Grows towards infinity when $Prob(P_{RX}(d) > \gamma)$ grows close to 100%;
- Is 0 dB if $Prob(P_{RX}(d) > \gamma)$ is 50%;
- For the same value of $Prob(P_{RX}(d) > \gamma)$, it increases with the increase of σ, meaning that in order to maintain the same $Prob(P_{RX}(d) > \gamma)$ in a dense-urban environment as in a rural environment, a bigger LNF_{Marg} is required.

It is also important to note that, if $Prob(P_{RX}(d) > \gamma)$ increases from 50% to the coverage percentage, which is 95%, then slow fading margin increases from 0 dB to 13.16 dB (considering an urban environment where $\sigma = 8\ dB$), and therefore the cell range gets shorter.

The previous expressions only considers a reliability of an IoT connection in the border of the cell. Instead of an edge reliability, the reliability in the entire cell area is often more useful to be considered since the signal level usually becomes stronger closer to the transmitter.

- **<u>Area Reliability</u>:**

Due to shadowing effects in a real-life scenario, any cell coverage follows a non-linear pattern (Figure 4.5).

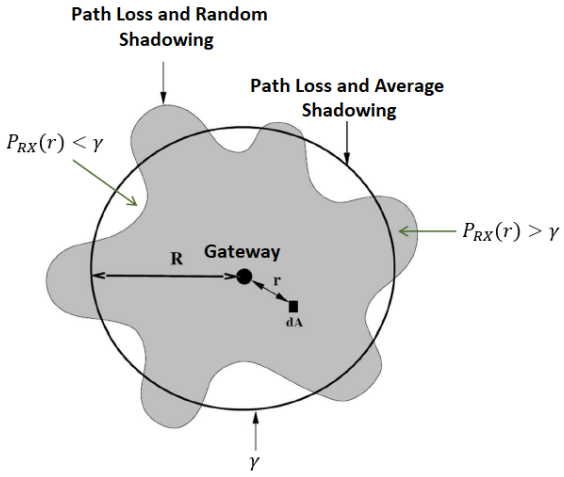

Figure 4.5 – Real-Life cell coverage pattern

For the sake of simplicity, let us assume a circular coverage area with radius R, centred on an IoT gateway, with some desired received signal threshold, γ and d representing the radial distance from the gateway, varying from $0 \leq d \leq r$.

$U\ (\gamma)$ defines the useful service area within a circle of radius R where the signal level received by the mobile station exceeds a given threshold γ at a distance $d = r$.

If $Prob(P_{RX}(r) > \gamma)$ is the probability that the received signal, $P_{RX}(r)$, exceeds γ in an area dA, then the useful area can be calculated as the integration of the probability function over the area, as shown below:

$$U\ (\gamma) = \frac{1}{\pi R^2} \int [Prob(P_{RX}(r) > \gamma)]\ \partial A =$$

$$U\ (\gamma) = \frac{1}{\pi R^2} = \int_0^{2\pi} \int_0^R [Prob(P_{RX}(r) > \gamma)]\, r\ \partial r\ \partial \theta \tag{4.21}$$

From Equation 4.20, $Prob(P_{RX}(r) > \gamma)$ is expressed as:

$$Prob(P_{RX}(r) > \gamma) = Q\left(-\frac{\overline{(P_{RX}(r)} - \gamma)}{\sigma}\right) \tag{4.20}$$

Where $\overline{P_{RX}(r)}$ is the distance dependent received signal mean power, given by Equation 4.22:

$$\overline{P_{RX}(r)}_{[dBm]} = P_{TX} - \overline{PL}(r) \tag{4.22}$$

In order to determine the path loss as referenced to the cell boundary ($r = R$), if a simple radial path loss dependence $\left(\frac{1}{r^n}\right)$ is assumed, then:

$$\overline{PL}(r) = PL(R) + 10nlog\left(\frac{r}{R}\right) =$$

$$\overline{PL}(r) = \overline{PL}(d_0) + 10nlog\left(\frac{R}{d_0}\right) + 10nlog\left(\frac{r}{R}\right) \tag{4.23}$$

Replacing Eq. 4.22 and Eq. 4.23, in Eq. 4.20, $Prob(P_{RX}(r) > \gamma)$ can be expressed as:

$$Prob(P_{RX}(r) > \gamma) = Q\left(-\frac{\left[P_{TX} - \left(10nlog\left(\frac{R}{d_0}\right) + 10nlog\left(\frac{r}{R}\right) + \overline{PL}(d_0)\right)\right] - \gamma)}{\sigma}\right) \tag{4.24}$$

Or using the erf function:

$$Prob(P_{RX}(r) > \gamma) = \frac{1}{2} - \frac{1}{2}\text{erf}\left(\frac{\gamma - \left[P_{TX} - \left(10nlog\left(\frac{R}{d_0}\right) + 10nlog\left(\frac{r}{R}\right) + \overline{PL}(d_0)\right)\right]}{\sigma\sqrt{2}}\right) \tag{4.25}$$

If we consider the following substitutions:

$$a = \frac{\gamma - P_{TX} + \overline{PL}(d_0) + 10nlog\left(\frac{R}{d_0}\right)}{\sigma\sqrt{2}} \tag{4.26}$$

$$b = \frac{10nlog_{10}e}{\sigma\sqrt{2}} \tag{4.27}$$

Then, $U(\gamma)$ is given by:

$$U(\gamma) = \frac{1}{2}(1 - \text{erf}(a) + e^{\left(\frac{1-2ab}{b^2}\right)}\left[1 - \text{erf}\left(\frac{1-ab}{b}\right)\right] \tag{4.28}$$

The relation between Eq. 4.28 and Eq. 4.25 is illustrated in Figure 4.6 and it is often called Jake's curves. This curves allows an efficient extraction of the LNF_{Marg} in terms of area coverage, for a relation of σ/n.

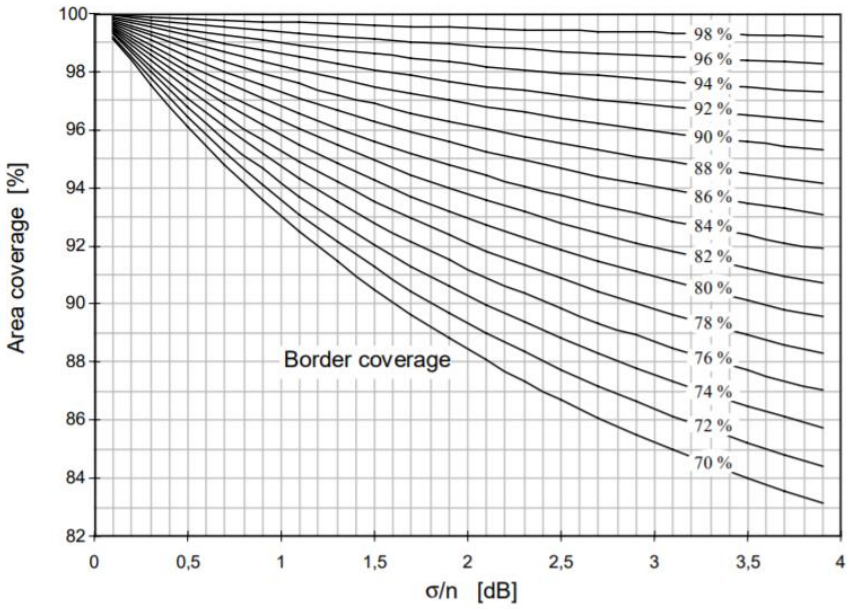

Figure 4.6 – Family of curves relating fraction of total area with signal above threshold, $U(\gamma)$ as a function of probability of signal above threshold on the cell boundary $Prob(P_{RX}(r) > \gamma)$ [58]

After choosing an Area Coverage percentage for a given σ/n, the percentage of coverage on the cell boundary is extracted. With the CDF (Cumulative Density Function) illustrated in Figure 4.7, the margin in dB (LNF_{Marg}) to go from the original 50% coverage at the cell border to the given border percentage is given by:

$$LNF_{Marg} = x * \sigma \tag{4.29}$$

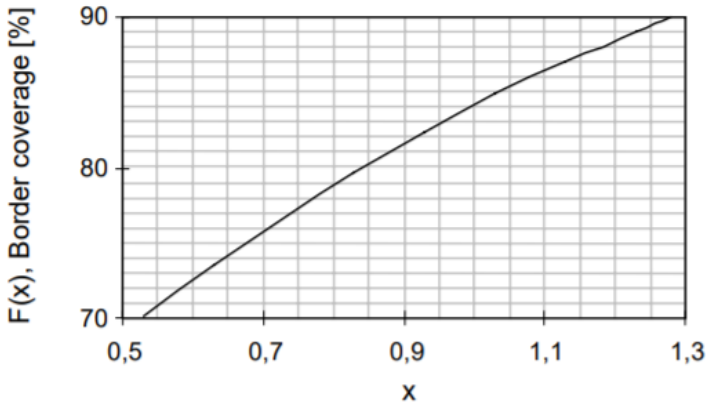

Figure 4.7 – CDF of the coverage in the cell border [58]

In Figure 4.7 x is the variable in the cumulative normal function F(x), when F(x) has the value of the border percentage given by Jakes formulas in Figure 4.6

With this, if we consider an area reliability of $Prob(P_{RX}(r) > \gamma) = 95\%$, a decay coefficient $n = 3$ and a standard deviation $\sigma = 8$ for the city of Aveiro, then the Log-Normal fading margin is given by:

$$LNF_{Marg} = 1{,}15 * 8 = 9{,}2\ [dB]$$

4.3.2.1.2 Small-Scale Fading

Small-scale fading refers to the dramatic changes in signal amplitude and phase that can be experienced as a result of small changes (as small as a half-wavelength) in the spatial separation between a sensor and a gateway.

In an IoT network system, a signal can travel from the transmitter to the receiver over multiple reflective paths; This phenomenon is defined as multipath, and occurs mainly in urban and suburban environments, where there is a high probability that the sensors are not in line of sigh with the gateways. Since this effect causes fluctuations in the received signal's amplitude, phase, and angle of arrival, it rises the terminology of multipath fading. Multipath mechanisms include reflection from objects such as buildings, mountains, large bodies of water, atmospheric ducting, ionospheric reflection and refraction. It should be noted that these mechanisms can give rise to both constructive and destructive interference.

In addition to that, another different cause of fading is that of small frequency variations such as Doppler effect. When there is movement from the sensors (i.e when they are placed in a car or being used in any application that requires movement), abrupt changes in the received signal strength are expected due to the phase changes of the components of the received signal, causing fading.

Small-scale fading is also described as Rayleigh fading since the multiple reflective paths are large in number, and there is no line-of-sight signal component, the envelope[2] of the received signal is statistically described by a Rayleigh PDF. When there is a dominant nonfading signal component present, such as a line-of-sight propagation path, the small-scale fading envelope is described by a Rician PDF [56].

Depending on the application, most of the IoT sensors will be placed in a fixed location, without line-of-sight from the gateways, and without motion. In that case, they'll not be subject to Doppler Effect and fading will entirely be due to multipath conditions, and it can be described

2 The envelope of an oscillating signal is a smooth curve outlining its extremes.

as a Rayleigh distribution. A Rayleigh fading distribution is plotted in [59]. From that figure, it can be seen that the median 50 percentile is exceeded by about 1 dB 5% of the time, and 90% of the time the signal does not drop more than 2 dB below the median value.

The difference between these values is the Rayleigh Fading margin (RF_{Marg}) that needs to be considered for this planning, and it is given as:

$$RF_{Marg} = 1 - (-2) = 3\ [dB]$$

However, if we consider the possibility that the sensors are placed in an outdoor environment and subject to mobility due to their application, then Doppler Effect must be considered in any IoT network planning.

In order to evaluate the time varying channel behaviour in a small-scale region, the channel can either be evaluated on the frequency domain, on in the time domain, described by the Doppler spread (B_D) and the coherence time (T_c), respectively.

Doppler spread (B_D) is a measure of the spectral broadening caused by the time rate of change of the devices radio channel and is defined as the range of frequencies over which the received Doppler spectrum is essentially non-zero. It essentially describes how fast the transmitter, receiver, and scatters in-between are moving; the faster they are moving, the faster the radio channel changes, and the more doppler shifts (f_d) will be present. f_d is a function of the relative velocity of the end-node (v), the wavelength (λ) and the angle θ between the direction of motion of the end-node and direction of arrival of the scattered waves, as shown in equation 4.30 [60].

$$f_d = \frac{v}{\lambda}\cos(\theta)\ [Hz] \tag{4.30}$$

Doppler shift distribution varies, but an approximation of the maximum doppler shift (f_m) is simply given by:

$$f_m = \frac{v}{\lambda} = \frac{v * f_c}{c}\ [Hz] \tag{4.31}$$

And the maximum Doppler spread (B_D) is given by:

$$B_D = 2 * f_m\ [Hz] \tag{4.32}$$

Coherence time (T_c) is the time duration over which the channel impulse response is essentially invariant, and is inversely proportional to Doppler maximum spread as shown in Equation 4.33:

$$T_c = \frac{1}{f_m}\ [s] \tag{4.33}$$

T_c can also be defined as the time duration over which the channel's response to a sinusoid has a correlation of at least 0.5, and is given as:

$$T_c = \frac{9}{16\pi f_m}\ [s] \tag{4.34}$$

In practice, Equation 4.33 suggests a time duration which a Rayleigh fading signal may fluctuate wildly, and Equation 4.34 is a little more restrictive. A popular "rule of thumb" is to define T_c as the geometric mean of both expressions. This results in:

$$T_c = \frac{0.423}{f_m}\ [s] \tag{4.35}$$

In resume, the channel characteristics varies accordingly to the mobility of the end-nodes. When compared to the transmitted symbol (T_S) or the signal bandwidth (B_S), the wireless channel can be classified as fast fading or slow fading.

Fast fading will occur when:

- $T_S > T_C$, if the channel is analysed in the time domain.
- $B_S < B_D$, if the channel is analysed in the frequency domain.

Slow fading will occur when:

- $T_S < T_C$, if the channel is analysed in the time domain.
- $B_S > B_D$, if the channel is analysed in the frequency domain.

4.3.2.2 Interference

The sensitivity of an IoT receiver depends essentially on the SNR of the connection to which it is subject. In an IoT radio link, the power of the received carrier must be large enough to overcome both the noise and the interference generated by other carriers in the same frequency band. This is defined as co-channel interference.

Most of the LPWAN technologies seen in Chapter 2 makes use of unlicensed ISM frequency band in EU (868 MHz), meaning that they can be largely interfered by other technologies that operate in a closer band, such as GSM 900.

In LoRa's case, *Semtech* claims that the interference can be as much as 20 dB larger than the transmitted signal that the receiver will still be able to decode it successfully [61], however, in a real-life scenario this is not always true and depends on the technology chosen.

Therefore, in order to obtain a more accurate coverage forecast, an interference margin (IF_{Marg}) must be added to consider this possible interference. None of the reviewed literature seems to suggest a precise value, so consequently a value of 2 dB is suggested. Note that this value is only considering few devices within a network. In case an huge amount of IoT devices are transmitting data at the same time, the interference will be higher, and therefore this value might not be considerable good.

$$IF_{Marg} = 2\ [dB]$$

4.3.2.3 Building Penetration and Vehicle Penetration Loss

The *Okumura-Hata* formulas assume signals will pass through clutter that is typical of a small city and that the signals are received by a device placed outside. To plan an IoT network for signals being usable indoors, the link budget needs to incorporate an additional Building Loss (BPL_{Marg}), which is the amount by which a signal will be attenuated on passing from outdoors into the building.

The overall building penetration loss is the sum of the following three contributions [10]:

1. Losses caused by the external walls of buildings;
2. Losses caused by the internal walls of buildings;
3. Gain in received power thanks to the fact that a IoT device is above the first floor.

Whether indoors or outdoors, each end-device must receive signals above the minimum sensitivity level. In order to ensure a good coverage for devices placed indoors, the work in [62] recommends the usage of a margin of 18 dB for an urban environment; 15 dB for a suburban environment and 10 dB for a rural environment. It must be noted that if the aim is to have very good coverage in lower floors, the planning threshold must be higher than when compared to cases where the important floors are higher.

In case the IoT devices are placed inside a vehicle, instead of BPL_{Marg}, a Car Penetration Loss margin CPL_{Marg} has to be considered. This margin is needed to compensate the loss due to the body of a car, which is mainly constituted of metal, and therefore RF signals struggle to penetrate. CPL_{Marg} typically vary between 5 to 15 dB accordingly to [62].

4.3.2.4 Body Loss

The margins defined above contemplates the losses that will exist in most of the IoT applications defined in Chapter 2. In addition to that, some applications will require the IoT sensors to be placed next to the human body, and since it absorbs energy from electromagnetic waves, it will cause some degradation in the signal. Therefore, in order to consider the losses introduced by the human body, a Body Loss Margin (BL_{Marg}) of 5 dB is recommend by ETSI for 900 MHz [63]. Since LPWAN's operate in a nearby frequency (868 MHz), it is also a suitable value to be considered.

4.3.3 Required Signal Strength

To the sensitivity level of an IoT sensor/gateway ($SS_{Sensor/Gateway}$), margins have to be added to compensate for Rayleigh fading, interference and body loss, described above. The obtained signal strength(SS_{Req}) is what is required to a real-life situation for an IoT device to receive some data regardless the environment it is placed at. Equation 4.36 presents the calculation on the Uplink, and Equation 4.37 on the Downlink [64].

$$SS_{Req_{UL_{[dBm]}}} = SS_{Sensor_{[dBm]}} + RF_{Marg_{[dB]}} + IF_{Marg_{[dB]}} + BL_{Marg_{[dB]}} \quad (4.36)$$

$$SS_{Req_{DL_{[dBm]}}} = SS_{Gateway_{[dBm]}} + RF_{Marg_{[dB]}} + IF_{Marg_{[dB]}} + BL_{Marg_{[dB]}} \quad (4.37)$$

4.3.4 Design Signal Strength

Extra margins have to be added to SS_{Req} to handle the Log-Normal fading as well as different types of penetration losses. These margins depend on the environment and on the desired area coverage. The obtained signal strength is what should be used when planning the system and it will be referred to as the design level, SS_{Design}. This signal strength is the value that should be obtained on the border of the cell. Different SS_{Design} considerations are proposed next, depending on the type of the environment that needs to be considered [64].

$$SS_{Design_{UL_{outdoor}[dBm]}} = SS_{Req_{[dBm]}} + LNF_{Marg_{[dB]}} \quad (4.38)$$

$$SS_{Design_{UL_{indoor}[dBm]}} = SS_{Req_{[dBm]}} + LNF_{Marg_{[dB]}} + BPL_{Marg_{[dB]}} \quad (4.39)$$

$$SS_{Design_{UL_{in-car}[dBm]}} = SS_{Req_{[dBm]}} + LNF_{Marg_{[dB]}} + CPL_{Marg_{[dB]}} \quad (4.40)$$

4.4 LoRa's Link Budget

Subchapter 4.3 presented all the aspects that needs to be considered in order to perform a coverage planning for a general IoT technology. However, each LPWA has their own specifications, and therefore the link budget will be restrictive to the technology chosen. Therefore, a detailed link budget considering LoRa technology is presented next.

4.4.1 LoRa's Sensitivity

As stated already in Chapter 3, LoRa is a technology that uses CSS as modulation, using a scalable bandwidth (B) of $125kHz$, $250kHz$ or $500kHz$, and a variable spreading factor (SF). Due to these specifications, it is possible to play with the trade-off between data rate and range, in order to plan/optimize a LoRa network depending on the application (e.g some IoT applications might require the devices to have a better throughput but less range to the gateway and vice versa). The range that is achieved in a LoRa communication, is directly related to the sensitivity of the LoRa module built-in the device (either sensor or gateway). As Equation 3.5 demonstrates, for a fixed BW and CR, increasing the SF to the maximum (12) results in a lower bit rate (R_b) when compared to the lowest SF (7), however higher SF's, allows LoRa to achieve

a much higher processing gain which results in significant improvements in the SNR which is the ratio between the received power signal and the noise floor power level, in other words, the minimum ratio of wanted signal power to noise that can be decoded correctly. The lower is the SNR, the more sensitive a receiver will be. Besides that, other factors influence the sensitivity of a LoRa device. Semtech in [61] expresses the following formula for the sensitivity calculation at room temperature:

$$SS_{LoRa_{[dBm]}} = 10\log_{10}(k * T * 1000)_{[dBm]} + 10\log_{10}(BW)_{[dB]} + NF_{[dB]} + SNR_{[dB]} \quad (4.41)$$

Where:

- k, is the Boltzmann's constant ($1.38 * 10^{-23}$)
- T, is the room temperature ($293ºK$)
- BW, is the receiver's bandwidth (Hz)
- NF, is the receiver noise figure, entirely dependent on the hardware $[dB]$

From Equation 4.41, the first term is due to thermal noise in 1 Hz of bandwidth and can only be influenced by changing the temperature of the receiver. It is typically simplified to -174 dBm.

Finally, SNR represents the signal to noise ratio required by the underling modulation scheme. Also in [61], Semtech reinforces the idea that LoRa is capable of demodulating 20 dB below noise level, significantly improving immunity to the interference when combined with integrated forward error correction, but they don't specify any kind of expression for it.

When data is transmitted over a LoRa link, there is a possibility of errors being introduced into the system. If errors are introduced into the data, then the integrity of the system may be compromised. As a result, it is necessary to assess the performance of the system, and bit error rate, BER, provides an ideal way in which this can be achieved.

The problem with these pre-defined values of SNR, is that they don't take in consideration how is the BER (Bit Error Rate) in a LoRa system. For that, authors of [65] estimates an analytical expression for computing the BER in a CSS modulation, which is given by:

$$BER_{CSS} = Q\left(\frac{\log_{12}(SF)}{\sqrt{2}}\frac{E_b}{N_0}\right) \quad (4.42)$$

Where $Q(z)$ is the Q-function, that is related to $erf(z)$ function defined in Equation 4.43:

$$Q(z) = \frac{1}{2}\left[1 - \text{erf}\left(\frac{z}{\sqrt{2}}\right)\right] \quad (4.43)$$

and E_b/N_0 is the energy per bit to noise power spectral density ratio. Equation 4.42 can then be rewritten as:

$$BER_{CSS} = \frac{1}{2}\left[1 - \text{erf}\left(\frac{log_{12}(SF)}{2}\frac{E_b}{N_0}\right)\right] \quad (4.44)$$

This equation shows that for higher SF's, the BER is more acute and it can be related to E_b/N_0 as shown in Figure 4.8:

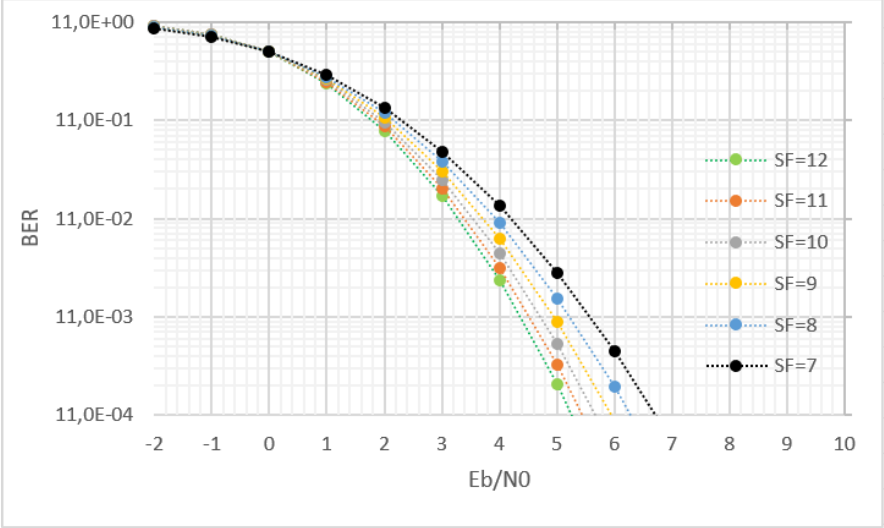

Figure 4.8 – Relation between BER and E_b/N_0

The problem of this expression is that it uses E_b/N_0 which in practise does not reflect the perfect case, because in CSS modulation the energy is spread over a large band and depends on several parameters that vary from one system to another, but it stills give a good approximation for the calculation of the SNR. From the study carried by [66], it is possible to establish a relation between E_b/N_0 and SNR for a LoRa system that is translated by expression 4.45:

$$SNR_{[dB]} = E_b/N_0 + 10\log_{10}(R_S) + 10\log_{10}(SF) + 10\log_{10}(CR) - 10\log_{10}(BW_n) \quad (4.45)$$

Where BW_n is the Noise Bandwidth (Hz).

For this, we have to consider that $BW_n = BW$. Equation 4.45 then translates the real sensitivity of a LoRa device, depending on the chosen Spreading Factor, Coding Rate and Bandwidth. Note that this equation is either valid for an end-node acting as a sensor, and for a gateway.

The resulting SS_{LoRa} can then be applied in Equation 4.36 and 4.37, in order to extract the values from SS_{Req} and SS_{Desgin}.

4.4.2 Doppler Effect resistance

Semtech in [61] claims that the chirp pulse of a LoRa packet is relatively broadband and thus LoRa offers immunity to multipath and fading, making it ideal for use in urban and suburban environments, where both mechanisms dominate, however this is not always true [40]. The robustness to these small-scale effects is totally dependent on the type of modulation of the physical layer of the technology in usage, which in LoRa's case is CSS modulation. The main reason why CSS performs well against doppler shifts is because it uses a large chirp rate (which is equal to the Bandwidth as defined in Eq. 3.1, and therefore it assures a better synchronization between the transmitter and the receiver.

However, as already mentioned in the previous chapters, LoRa provides long-range communication with a trade-off with Data-Rate (Equation 3.5 demonstrates this relation), which inevitably affects the chirp-rate, and therefore Doppler shifts are expected.

If we combine Equations 4.31 and 4.35, the new coherence time (T_C) results in:

$$T_C = \frac{0.423c}{v f_c} \; [s] \tag{4.46}$$

We have stated before that fast fading occurs when $T_S > T_C$, where T_S is the symbol time of a LoRa packet, given in Equation 3.3. With this, we can estimate the maximum velocity of a LoRa device until signal distortions start to appear. For that, Figure 4.9 illustrates the variation of both T_S and T_C with the velocity of the end-node. T_S does not depend on the velocity, and therefore is a constant value. T_C decreases exponentially with the increase of velocity. We can consider that when this two equations cross graphically, we are in the limit of the presence of fast fading ($T_s = T_C$), and therefore the maximum velocity at that point can be extracted. For illustrations purposes, if we assume for example three distinct combinations, for instance: $SF = 12/BW = 125\ kHz$; $SF = 10/BW = 125\ kHz$ and $SF = 9/BW = 250\ kHz$, then it can be

expected that for the first mode, a velocity bigger than 16 km/h would start being a limitation in terms of reception of packets; for the second configuration, the end-node would be able to move without any distortions up to a velocity of 64 km/h, and for the last one, since T_S is much smaller, then until a value of 256 km/h no fast fading would be expected.

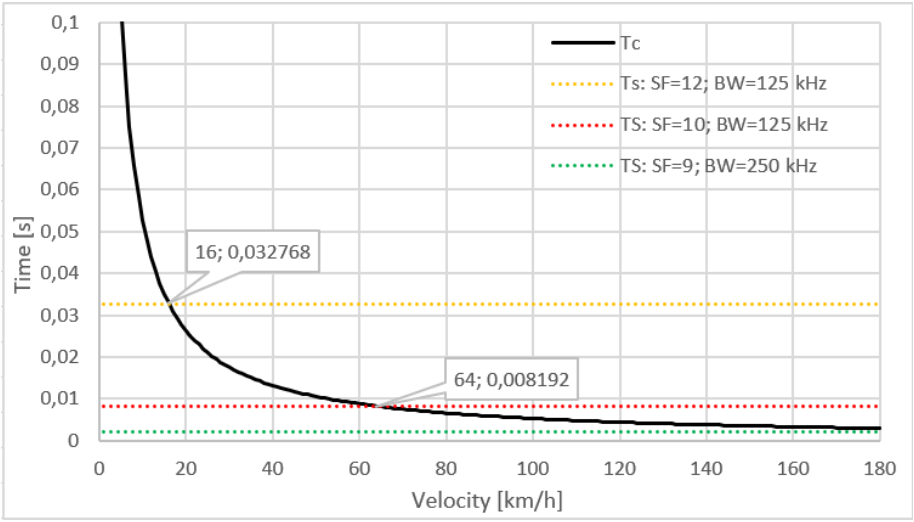

Figure 4.9 – Comparison of the coherence time and symbol times for LoRa signals with different spreading factors and bandwidths

This analysis is very important for any network planning that requires a drive-testing in the field afterwards.

4.4.3 Equipment characteristics

As demonstrated in subchapter 4.3, the link budget estimation for an IoT network has some similarities with Radio technologies, such as GSM 900 especially due to the fact of both technologies operating in a very close frequency band. In order to estimate the Link Budget for the city of Aveiro with LoRa technology, some real equipment's have to be assumed and its characteristics have to be considered.

4.4.3.1 Gateway and End-device

In a real LoRa network deployment, the gateways form the bridge between the end-nodes and the NS (network server) as described in Figure 3.4. The end-nodes are connected to the Gateways through LoRa and LoRaWAN, while the Gateway uses high bandwidth networks like WiFi, Ethernet or Cellular to connect to the network server, which is typically the TTN

(*The Things Network*). As stated already in subchapter 3.2.2, all gateways within reach of an end-node will receive the device's messages in an uplink transmission and forward them to the NS, which will deduplicate the messages and select the best gateway to forward any messages queued for downlink. A single gateway can serve thousands of devices, but a single device can be served by only one gateway. There are mainly two modes of function of a LoRaWAN Gateway:

MSG (Multiple-Channel Gateways) are able to scan 8 channels and properly detect and decode correctly up to 8 packets at the same time, even using different combinations of Spreading Factors and Data Rates. (e.g Kerlink IoT Station, The Things Gateway)[67];

SCG (Single-Channel Gateways) can only receive LoRa packets on one channel and one spreading factor at the same time. The major problem of this gateways is that they are not LoRaWAN compliant. Nevertheless, since they are much cheaper compared to the multiple-channel gateways, they are an excellent alternative for beginners in LoRa technology.

In both of the gateway types, they are essentially constituted of 3 elements: A LoRa concentrator board to receive LoRaWAN packets, an antenna, to receive and transmit the signals; and a processor, to process incoming and outcoming LoRaWAN packets, and to exchange them back and forth with the concentrator board. MCG are usually built in using a SX1301 or SX1257 module (i.e Kerlink Gateway), contrarily to SCG that uses SX1272 or SX1271, illustrated in Figures 4.10 a) and b), respectively.

Figure 4.10 a) – MCG (Kerlink IoT Station with SX1301 embutted)

Figure 4.10 b) – SCG (RN2483 module with SX1272 embutted)

In order to plan a more realistic IoT network with LoRa technology, meaning for the maximum capacity, scalability in the network is required, and therefore MCG are mandatory to be used. However, for the sake of simplicity and since the objective of this dissertation is focused on the evaluation of the physical layer only (LoRa technology), the gateways are considered to implement a single-channel functionality, meaning that they will receive only packets from the end-nodes that share the same configuration (same channel frequency, bandwidth and spreading factor).

As for the end-devices, since they also transmit data in a pre-defined channel and don't need to scan multiple channels at the same time, the same LoRa module can be used to define both end-nodes and gateway. For that reason, SX1272 module is taken in consideration for this planning. From [42], the following specifications are extracted:

- $Tranmission\ Power\ \left(P_{TX_{i_{[dBm]}}}\right) = +14\ dBm$, where $i = Gateway\ or\ Sensor$
- $Sensivity\ \left(SS_{LoRa_{[dBm]}}\right) = -137\ dBm\ (Using\ SF = 12\ and\ BW = 125\ kHz, variable\ acording\ to\ the\ desired\ configuration\ according\ Eq.\ 4.45)$

4.4.3.2 Antennas

The antennas in both Gateway and end-devices are needed in order to distribute the RF signals. In general, two types of antennas are usually considered in a wireless telecommunications system according to their radiation characteristics: Directional and Omnidirectional. Directional antennas are more suitable in other kinds of applications, such as Cellular Networks, whereas in an IoT network, Omnidirectional antennas are the best choice.

Omnidirectional antennas are characterized essentially for having an isotropic pattern in a given plane (the azimuth plane), and a directional pattern in an orthogonal plane (the elevation plane). This type of antennas are adequate for an IoT network since there is no specific knowledge of the end-devices locations, and therefore they provide coverage in all directions (horizontally).

The frequency of radiation is one of the most important parameters of the antennas since it has a direct influence on the attenuation. Larger frequencies introduce larger path losses.

With this, two antennas respectively for the gateway and for the end-device were considered (Figure 4.11 a) and b). Their technical specifications are extracted from the manufacturer datasheet, resulting in the following :

- $Frequency\ (f_c) = 868\ MHz$
- $Gains$:
  - $Sensor\ Antenna\ Gain\ (G_{Sensor}) = 0\ dBi$
  - $Gateway\ Antenna\ Gain\ (G_{Gateway}) = 6\ dBi$

Figure 4.11 a) – Omnidirectional antenna for the gateway

Figure 4.11 b) – Omnidirectional antenna for the end-node

4.4.3.3 Cables and Connectors

When LoRaWAN is used, the gateway must have a connection to the internet in order to forward the packets to the Network Server. Most of the commercial LoRa gateways supports WiFi, Cellular and Ethernet connections for this purpose. Although LoRaWAN is not taken in consideration for this deployment, a connection to the Internet through a CAT5 Ethernet cable is recommended for future purposes.

Besides this, the gateway needs a connection to the antenna in order to transmit the packets to the end-nodes. This is normally done by a LDF ½'' or LDF 7/8'' coaxial cable with two connectors attached on each side. On the uplink scenario, cables loss are usually despicable, and therefore not considered.

The following coaxial cables specifications are a viable consideration for a LoRa network planning:

Type	$L\ [dB/100m]$	$L\ [dB/10m]$	$Quantity\ [m]$	$L_{Total_{[dB]}}$
LDF 1/2’’	6,85	-	0	0
LDF 7/8’’	3,87	-	5	0,1935
CAT5		3,3	1	0,33
			Total:	0,5235

Table 4.3 – Cables characteristics

From this table, the attenuation caused from the feeds (L_{Feeds}) can be defined as:

$$L_{Feeds_{[dB]}} = L_{7/8''_{[dB]}} + L_{CAT5} = 0{,}1935 + 0{,}33 = 0{,}5235\ dB \tag{4.47}$$

LDF 1/2 "cables are characterized by being the ones with the higher insertion losses every 100 meters. In contrast, these cables are the thinnest, which can sometimes be useful, for Indoor applications, where the cable in addition to having a better visual impact, is also handier. For Outdoor applications, both LDF 1/2 "and LDF 7/8" cables, presented in Figure 4.12 a) and b) respectively, are commonly used.

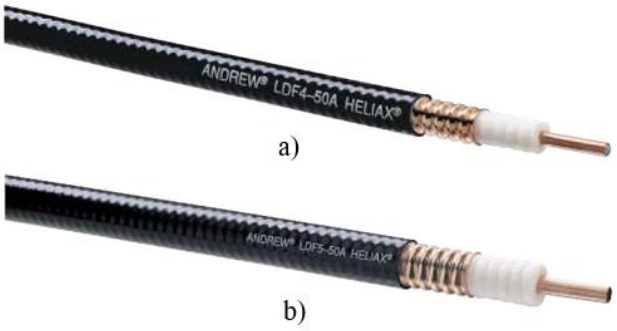

Figure 4.12 – LDF 1/2’’ feeder (a); LDF 7/8’’ feeder (b)

Besides the cables, also the connectors need to be considered. Four connectors on the gate-way side, and two connectors on the end-device are necessary:

Type	$L\ [dB]$	$L\ [dB]$	$Quantity$	$L_{Total_{[dB]}}$
SMA	0,1	-	6	0,6
			Total:	0,6

Table 4.4 – Connectors characteristics

The attenuation caused from the connectors ($L_{Connectors}$) can be defined as:

$$L_{Connectors_{[dB]}} = 0{,}6\ dB$$

4.4.4 Path Loss estimation

From all the definitions specified in subchapter 4.4.1, and with the equipment's specifications defined, the path loss can be estimated for a LoRa communication in both directions for any consideration area, which in this dissertation is the city of Aveiro.

Aveiro city is considered to be an urban environment, and therefore only this type of environment is considered for the link budget calculations. The LoRa end-nodes can be placed indoor and outdoor, thus both scenarios have to be considered, since the path loss will differ between them. Also, it was already demonstrated that the sensitivity of a LoRa device varies accordingly to Eq. 4.45, so different path losses value are also expected depending on the mode in usage. In order to estimate this, four modes of operation are defined for evaluation: worst case (lower spreading factor and higher bandwidth); best case (higher Spreading Factor and lower bandwidth), and two other combinations varying between the best and the worst case. For all the combinations, it is considered that $CR = 4/5$.

In order to estimate the path loss for a LoRa communication, both UL (Uplink) and DL (Downlink) scenarios have to be considered. However, if both end-devices and gateway share the same characteristics, then the link budget in theory is exactly the same. In practise this is not completely true, since the uplink is usually much weaker compared to the downlink. In both cases, all the gains, losses and margins must be considered, as illustrated in Figure 4.13.

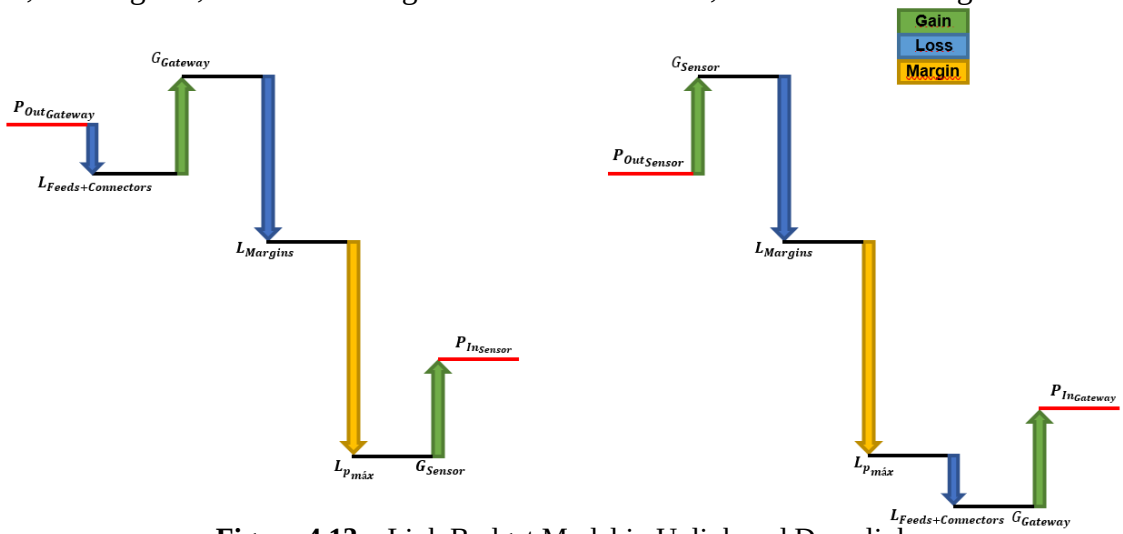

Figure 4.13 – Link Budget Model in Uplink and Downlink

With this is consideration, and by adapting Equation 4.1, the path loss that accounts for 95% of coverage is given by:

$$L_{p_{95\%}} = P_{TX_i} + G_{Sensor} + G_{Gateway} - L_{Connectors} - L_{Feeds} - SS_{Design} \quad (4.48)$$

Where i, is referred to the Sensor or de Gateway, depending if the link budget is considered in the uplink or downlink, respectively.

SS_{Design} is given by 4.38, 4.39 and 4.40, depending on the location (outdoor, indoor or in-car) conditions and this is the key for the path loss calculations, since it is the parameter that takes in consideration the different combinations of a LoRa device and all the margins related to the environment in study.

With this in consideration, Table 4.5 presents the link budget calculations for the defined LoRa operational modes, considering an outdoor and indoor environment.

	SF=12 BW=125 kHz		**SF=10 BW=125 kHz**		**SF=9 BW=250 kHz**		**SF=7 BW=500 kHz**	
	Outdoor	Indoor	Outdoor	Indoor	Outdoor	Indoor	Outdoor	Indoor
$P_{TX_i}[dBm]$	14		14		14		14	
$G_{Gateway}[dBi]$	6		6		6		6	
$L_{Feeds}[dB]$	0,5		0,5		0,5		0,5	
$L_{Connectors}\ [dB]$	0,6		0,6		0,6		0,6	
$SS_{LoRa}\ [dBm]$	-137,4		-132,1		-126,6		-118,6	
$RF_{Marg}[dB]$	3		3		3		3	
$IF_{Marg}\ [dB]$	2		2		2		2	
$SS_{Req}\ [dBm]$	-132,4		-127,1		-121,6		-113,6	
$LNF_{Marg}[dB]$	9,2		9,2		9,2		9,2	
$BPL_{Marg}[dB]$	-	15	-	15	-	15	-	15
$SS_{Design}\ [dBm]$	-123,2	-108,2	-117,9	-102,9	-112,4	-97,4	-104,4	-89,4
$L_{p_{95\%}}\ [dB]$	142	127	136,8	121,8	131,2	116,2	123,3	108,3

Table 4.5 – Link Budget estimation for outdoor and indoor environment, and for four types of LoRa configuration

In Table 4.5, SS_{LoRa} is the result of Eq. 4.45. The obtained results for the various combinations are very similar to the theoretical values defined by the authors in [33], and also by the LoRa module datasheet in [42]. The slightly difference among those is because we've considered a BER of 10^{-4} for the SNR accordingly to equation 4.44, while in the documents mentioned, there is no reference to the BER.

Taking in consideration the urban environment-related parameters and all the necessary margins, SS_{Design} can be extracted, which leads to the maximum path loss for 95% of coverage. It's notorious that when BPL_{Marg} is considered (when sensors are placed inside walls), the path loss reduces drastically (15 dB). This will take even more impact on a dense urban environment, where the recommended margin is 18 dB [62]. For the sake of simplicity, in-car penetration loss was not considered.

Semtech claims that the LoRa module defined for the gateway/end-nodes can receive packets up to a maximum of 157 dB of path loss when configuring the module to achieve the highest range possible [42]. In Table 4.5, it can be concluded that a maximum path loss of 142 dB is achieved for the same kind of configurations, which is fairly similar to the theoretical values defined, especially when the results obtained in Table 4.5 considers a 95% of reliability in the area of service, whereas *Semtech* only classifies this for 50% of coverage.

With the estimation of the path loss for the various modes of LoRa, the coverage area can then be projected using a propagation model defined in subchapter 4.3.1. Accordingly to the study carried by [68][24], *Okumura-Hata* seems to be a good approach for a LoRa planning considering the characteristics of the LoRa technology already presented in Chapter 3.

In order to estimate the coverage range with *Okumura-Hata* model, the effective height for the end-nodes (h_{Sensor}) and the gateways ($h_{Gateway}$) have to be considered. For that, $h_{Gateway}$ was defined with a realistic height for the buildings in the city of Aveiro. As for the sensors, since they can have a variety of applications, and sometimes be placed in the floor or in a top of a building, it is considered a mean height, similar to what is considered in mobile network planning, thus the following associations can be expressed:

- $Frequency\ (f_{c_{[MHz]}}) = 868\ MHz$
- $Gateway\ Height\ \left(h_{Gateway_{[m]}}\right) = 30\ m$
- $Sensor\ Height\ \left(h_{Sensor_{[m]}}\right) = 1{,}5\ m$

From Equations 4.7 and 4.11, the maximum distance between the gateway and the sensor can be extracted, and that is present in Table 4.6. The equations used are related to a medium city.

	SF=12 BW=125 kHz		**SF=10 BW=125 kHz**		**SF=9 BW=250kHz**		**SF=7 BW=500kHz**	
	Outdoor	Indoor	Outdoor	Indoor	Outdoor	Indoor	Outdoor	Indoor
$\boldsymbol{\alpha(h_{Sensor})}$ $[\boldsymbol{dB}]$	0,5	0,029	0,3	-0,119	0,1	-0,277	-0,1	-0,503
$\boldsymbol{d_{máx}}$ $[\boldsymbol{km}]$	2,9	1,070	2,0	0,760	1,4	0,528	0,8	0,314

Table 4.6 – Estimation of the maximum distance between the sensor and the gateway, for outdoor and indoor environment, and for four types of LoRa configuration

The results presented in Table 4.6 shows that a maximum range of 2,9 km is expected in an outdoor urban environment like the city of Aveiro, when using the Okumura-Hat model. This result is just an approximation since we've demonstrated that several factors impact the path loss, and the propagation model translates a significant importance to this estimation.

Nevertheless, Indoor coverage seems to be a pretty challenge for LoRa, since it's maximum range is less than the double of the outdoor $d_{máx}$ for all configuration modes.

For other types of environments (dense-urban and rural), different ranges are expected, being rural the environment that would represent the best improvement, since it has much less attenuation when compared to urban or dense-urban environment.

4.5 Coverage Area

After determining the cell radius, meaning the maximum distance between the end-nodes and the gateway, it is necessary to define a geometric shape that characterizes the coverage area of each cell. Ideally the area would follow a circular geometry, but as shown in Figure 4.5, due to different propagation effects, the coverage of the cells follows a non-regular pattern, and therefore this is not the best approach. Instead, hexagons are proved to be a good approximation to estimate the coverage of the area in study [69].

The advantage of using the hexagonal pattern to represent the cell's format is because it allows to use the symmetry properties of this polygon. Each hexagon then represents the coverage area of a gateway.

The gateways are placed on a regular grid, with fixed inter-site distances and positioned using a non-orthogonal 60º cartesian pair of axis (u, v). Each gateway will consider a service

area limited by a cell radius, R, which is this case is equivalent to $d_{máx}$, as shown in Figure 4.14.

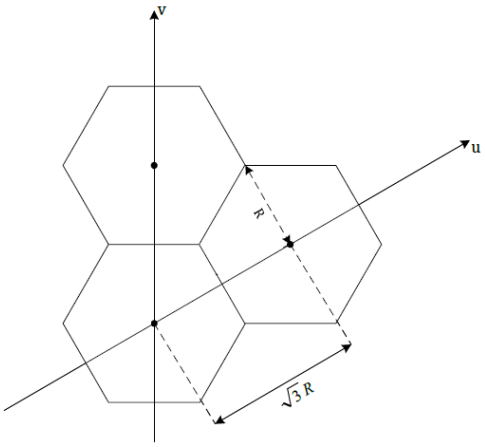

Figure 4.14 – Coordinate system to determine the distance between gateways [53]

The distance between two adjacent gateways (d_{GW-GW}) and the area of coverage for each of them ($A_{Gateway}$) is given by equations 4.49 and 4.50 respectively:

$$d_{GW-GW} = \sqrt{3R} \tag{4.49}$$

$$A_{Gateway} = 3 * \frac{\sqrt{3}}{2} * R^2 \tag{4.50}$$

After choosing an appropriate place for the position of the 1st Gateway, the remaining's can be placed within a distance of $\sqrt{3R}$ from each others, respecting the pattern illustrated in Figure 4.14.

It's important to highlight that for this planning, the LoRa gateways are considered to transmit always in the same channel, therefore the concept of frequency reuse (often used in radio planning [70]), is not considered here. This will indeed cause interference between adjacent cells, but for this reason, the interference margin has to be considered in the link budget calculations.

Finally, the number of needed gateways to cover the area in study can be estimated by:

$$N_{Gateways} = \frac{A_{Total}}{A_{Gateway}} \tag{4.51}$$

For this planning, it was already defined in subchapter 4.2 that the total area of Aveiro municipality (A_{Total}) is 8,5 km^2, therefore the number of gateways necessary to cover the area in study can be expressed in Table 4.7 for the various LoRa modes of configuration.

	SF=12 BW=125 kHz		**SF=10 BW=125 kHz**		**SF=9 BW=250kHz**		**SF=7 BW=500kHz**	
	Outdoor	Indoor	Outdoor	Indoor	Outdoor	Indoor	Outdoor	Indoor
A_{Total} $[km^2]$	8,5		8,5		8,5		8,5	
d_{GW-GW} $[km]$	4,939	1,853	3,509	1,316	2,439	0,915	1,452	0,545
$A_{Gateway}$ $[km^2]$	21,127	2,973	10,665	1,501	5,153	0,725	1,825	0,257
$N_{Gateways}$	1	3	1	6	2	12	5	34

Table 4.7 – Estimation of the Number of Gateways, for outdoor and indoor environment, and for four types of LoRa configuration

It's notorious that the Number of gateways increases with the decrease of spreading factor and also with the increase of bandwidth, for both Outdoor and Indoor applications. This is explained due to the fact that Higher SF's and Lower BW's increases the sensitivity of a LoRa device, and therefore a bigger distance between the gateway and end-node is achieved. The bigger is the link range ($d_{máx}$), the less is the number of number of gateways.

In order to cover all the outdoor city of Aveiro with SF=12, one gateway would be enough, as for SF=7, at least 5 gateways would be needed.

Note that these results don't take in consideration any possible "blind spots" that might appear in the real environment, as this is just an estimation of coverage. Depending on those, some other gateways might be required in order to achieve the desired % of coverage in the area. Also, these results might be different if the capacity of the network is evaluated, which is not the case in this dissertation.

5

Simulation of a LoRa Network

5.1 Introduction

This chapter is focused in validating the theoretical calculations of the LoRa network from the previous chapter, through a set of simulations, using a RF Propagation *Software*.

Section 5.2 compares several *Software's* available in the market and highlights the one chosen for this dissertation, *CloudRF*.

Section 5.3 provides the coverage results observed in the Simulator tool for various scenarios, such as different modes of transmission and different propagation models. For that, a detailed analysis of the city of Aveiro, where using *Google Earth*, the best places for the placement of the gateways are chosen. For that, several factors are taken into account, such as the terrain morphology and height of the buildings, in order to achieve not the best coverage area, but also to reduce the number of sites required determined in the calculations.

Section 5.4 compares the calculated results described in chapter 3, with the simulation results obtained in section 5.3.

5.2 Software Simulator

RF wave propagation simulation software that are used to predict the behaviour of a radio system allows the testing of the network that was planned from theoretical calculations based on mathematical formulas, analysis techniques and programming algorithms. This increases the efficiency of planning and reduces the costs that would have to be spent on tests with real equipment to guarantee the coverage, while also minimizing the number of sites needed to cover

the entire target area, which translates into cost savings, which is an important factor in engineering.

These simulators, based on prediction tools, allows to adjust locations, heights (either sites, sensors and even buildings), parameters of emission and reception of sites and sensors, propagation models and other parameters to make the simulation as close as possible of the reality. There are many RF Planning simulators available online. Some of them requires a purchase license for a simple usage, while others, such as Radio Mobile and *CloudRF*, can be used for free, however, with some usage limitations.

All of these simulators have different features among each other's, but essentially, all of them would be viable for a generic cellular network planning only.

In order to perform the simulations of the planned network described in the previous chapter, an IoT network planning simulator, preferable with LoRa technology, would be the most viable option. However, with an exception of ATDI simulator [71], that requires a purchased license of 500€/month, there isn't any dedicated IoT or LoRa Simulator available for free in the market.

For that reason, the challenge in this dissertation was to find a generic, but appropriate RF Planning Software Simulator, and through the manipulation of some parameters in the software, adapt it to the planned IoT network of chapter 3.

After some deep research in the finding of the most suitable software, *CloudRF* [72], detailed descripted bellow, was the chosen Simulator to perform all the simulations. A more

5.2.1 *CloudRF*

The *Software* used for the simulations of the planned LoRa network was *CloudRF*, which is a *Software* that allows the modifications of several important parameters and that assures a precise network planning. The version of *CloudRF* employed in this thesis was the freeware version, although it offers three types of monthly-paid plans: Standard, Expert and Enterprise, thus Enterprise the plan without limitations, however with a cost of 100€/month.

Regardless the type of license used, the freeware version of *CloudRF* allows the customization of very important parameters detailed next.

5.2.1.1 Terrain Data

Uses a variety of open DEMs (Digital Elevation Models) with global coverage and accuracy ranging from 90 to 2 meters, depending on the location. Most of the coverage is provided by SRTM (Shuttle Radar Topography Mission), version 3, where the data is provided by NASA (National Aeronautics and Space Administration) and offers a resolution of 90 meters. Most of the world's territory (99%) is covered between -60 and +60 degrees by default, so it perfectly covers the region of Aveiro, as can be seen in Figure 5.1.

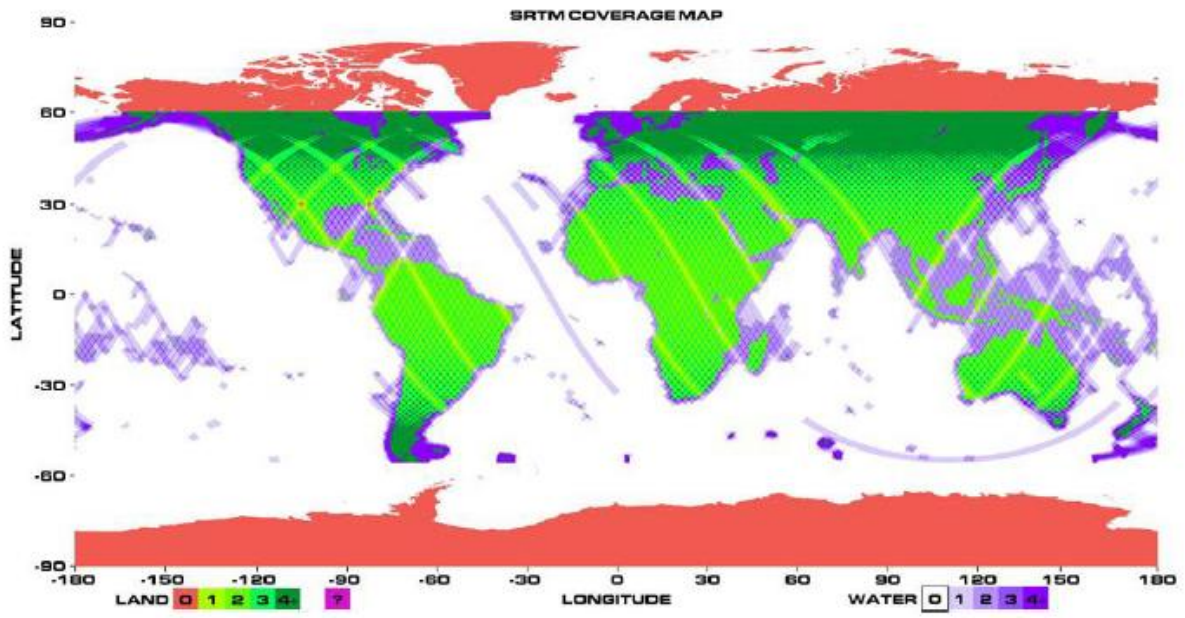

Figure 5.1 – SRTM Coverage [73]

In addition to DEM models, *CloudRF* also offers the possibility of including data obtained from LIDAR (Light Detection and Ranging) technology, which are more accurate data and increases the resolution of the terrain to 2 meters, however, this is only possible in certain locations of the globe, i.e United Kingdom, and for purchased licenses.

5.2.1.2 Propagation Models

It allows the selection of a variety of propagation models for different purposes, all of which are open source so that anyone can examine the algorithms used. For the execution speed to be maximum, the models are all written in C ++ language. Telecommunications professionals and

those who develop algorithms of this type are encouraged to give feedback to update and optimize models wherever possible. Among the various models available in the paid versions, the following models can be used in the freeware version:

- **ITM (Irregular Terrain Model)** – Also known as the Longley-Rice model, it is a general-purpose model that can be applied to a wide variety of engineering problems in the range of frequencies between 20 MHz and 20 GHz. It is based on the electromagnetic theory and on statistical analyses of both ground characteristics and radio measurements. It predicts the average attenuation of a radio signal as a function of distance and signal variability in time and space.
- ***Okumura-Hata*** – An empirical model operating in the range of [150, 2000] MHz. This is the propagation model used in network planning and already presented in the previous chapter.

5.2.1.3 Antenna Patterns

It has a large database of antenna models and allows the adjust of the antenna radiation diagram (azimuth and elevation) for all user subscriptions. Using a pattern greatly enhances the accuracy of the planning, since it simulates the radiation capacity with the characteristics of the actual antennas that are intended to be used. It also allows to load the real antenna pattern that can be obtained from a hardware vendor like *Telewave* [74] or *Kathrein* [75]

5.2.1.4 Ground Clutter

Ground Clutter

Landcover data or clutter is essential for accuracy in RF planning. It describes obstacles above the earth such as trees, buildings or vegetation which are not normally reflected in digital terrain due to the way the terrain is created. *CloudRF* supports three different types of ground clutter: Random, Point and Landcover.

- ***Random clutter*** is the simplest type of clutter, which is defined as a height in the interface. This height is then applied to the digital terrain to enhance the height evenly around the transmitter. This is easy to implement for broadcasting predictions but lacks accuracy and is not able to differentiate between an urban area or a block of trees for example.

- ***Point clutter*** allows to improve accuracy by adding precision clutter above ground level to simulate buildings, tree lines and other features not represented by the SRTM data. When an item of clutter is added at a point, it causes the ground height to be increased by the height of the obstacle. It's also possible to create custom obstacles within Google Earth (or any other KML (Keyhole Markup Language) mapping tool) to make points on the map, by using either the placemark, polygon or line tools.

- ***Landcover clutter*** data is available in the system with an accuracy of 0.004 degrees which equates to between 200m and 400m per point dependent on latitude. The MODIS Landcover data has been published for public use by the University of Maryland and is Copyright University of Maryland, Department of Geography and NASA. MODIS data has 17 bands which equate to different types of landcover. *CloudRF* translates these bands into obstacle heights according to the ITU-R P.452-11[76] standard that are presented in Table 5.1

Class	Terrain	*CloudR*F height
0	Water	0m
1	Evergreen Needleleaf forest	20m
2	Evergreen Broadleaf forest	20m
3	Deciduous Needleleaf forest	15m
4	Deciduous Broadleaf forest	15m
5	Mixed forest	15m
6	Closed shrublands	4m
7	Open shrublands	2m
8	Woody savannas	4m
9	Savannas	2m
10	Grasslands	2m
11	Permanent wetlands	0m
12	Croplands	2m
13	Urban and built-up	20m
14	Cropland/Natural vegetation mosaic	2m
15	Snow and ice	0m
16	Barren or sparsely vegetated	0m

Table 5.1 – SRTM Coverage [73]

In addition to the features presented, it is a user-friendly and practical software whose interface is shown in Figure 5.2.

Figure 5.2 – GUI interface of *CloudRF*

5.3 Simulation results

In order to confirm and validate the network planning proposed in chapter 3, various simulations using *CloudRF* were performed. The software only allows to perform simulations in the Downlink, which doesn't interfere with the conclusions taken on Chapter 3, since we've assumed that the Downlink path loss would be equal to the Uplink.

As stated in 5.2, the freeware version of *CloudRF* allows the user to choose between two types of propagation models: *Okumura-Hata* and ITM. Although Chapter 3 have only proposed a network planning using *Okumura-Hata*, it would be interesting to compare both propagation models trough simulations, therefore both are presented in this sub-chapter.

For both propagation models, two simulations approach are presented: firstly, only one gateway is considered, regardless the mode of operation for the LoRa nodes; then, a secondary approach where all the gateways needed to offer a proper coverage to the area in study are presented.

In both cases, a previous analysis of the area in study was done with Google Earth, where the terrain, elevation, buildings etc… were analysed before deciding the more suitable locations to place the gateways accordingly to the mode of configuration of the LoRa end-nodes.

This led to the environment classification in *CloudRF* as defined in Figure 5.3

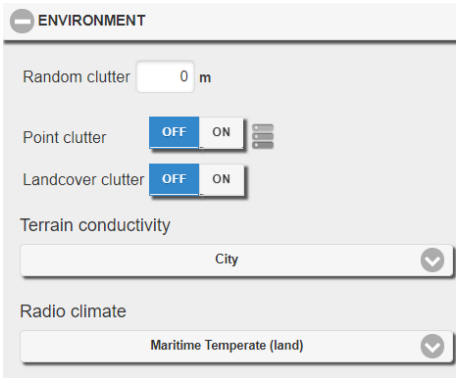

Figure 5.3 – Environment conditions in *CloudRF*

5.3.1 *Okumura-Hata*

As mentioned before, in order to validate the proposed planning with the *Okumura-Hata* model, two simulation approaches were performed for each of the four LoRa configuration modes. As seen in Table 4.10, when using a SF lower than 10, more than 1 gateway is required to be placed, and therefore the distance between the gateways (d_{GW-GW}) given by Equation 4.49 must be respected. However, sometimes this cannot be fully followed, since this is just a theoretical value, and when analysing the real geographical area, d_{GW-GW} results in locations that are not suitable to place the gateway. Therefore, some approximations have to be taken forward.

With this in consideration, all the gateway and sensor parameters mentioned in Friis formula given by Equation 4.1 were placed in the simulator GUI (Figure 5.2). In this case, since only Downlink is considered, the gateway is the TX and the end-node is the RX. For the propagation model, all the parameters given in Equation 4.4 were respected, and "Knife Edge Diffraction" option was activated in order to consider the diffractions caused by the edge of the buildings.

Finally, the simulation results with *Okumura-Hata* model are illustrated in Figure 5.4 to Figure 5.9. Each figure represents a single LoRa configuration mode, with the theoretical sensitivity of the end-device calculated in Table 4.5 being the only difference among them on the configuration of *CloudRF*.

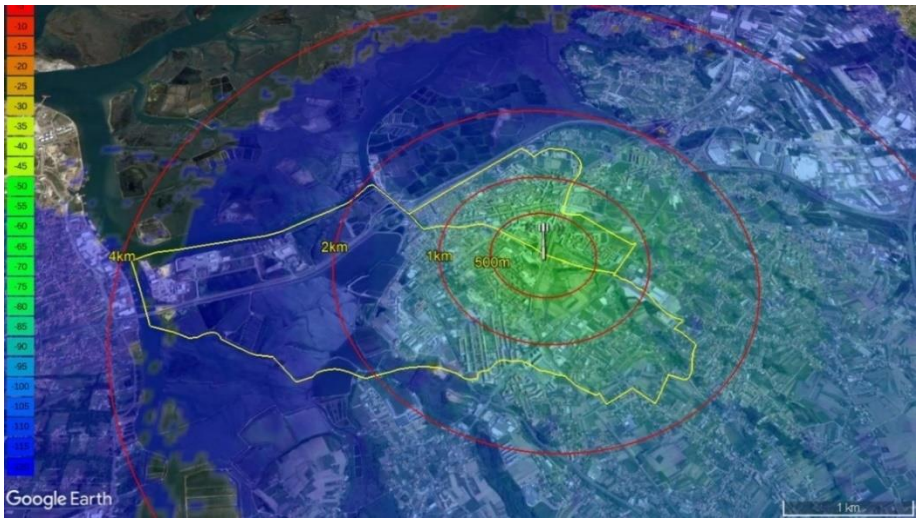

Figure 5.4 – Simulation with 1 Gateway for SF=12/BW=125 kHz, using *Okumura-Hata*

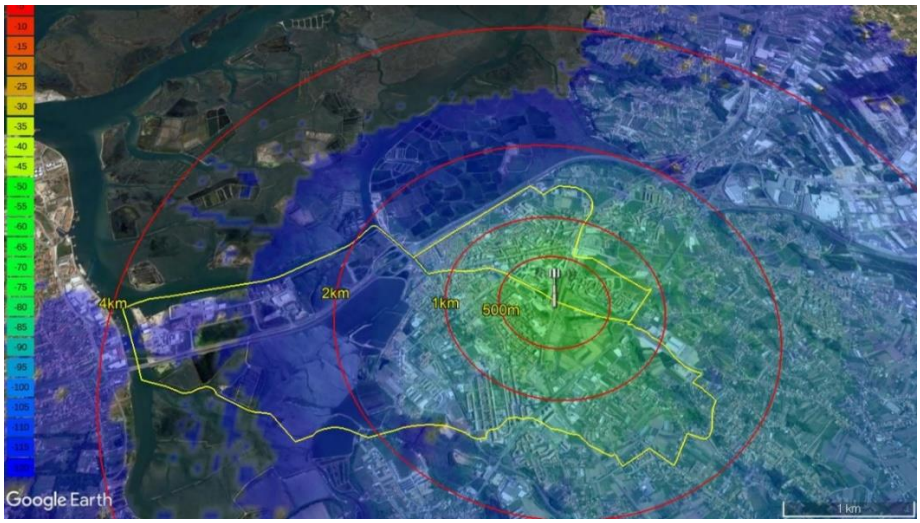

Figure 5.5 – Simulation with 1 Gateway for SF=10/BW=125 kHz, using *Okumura-Hata*

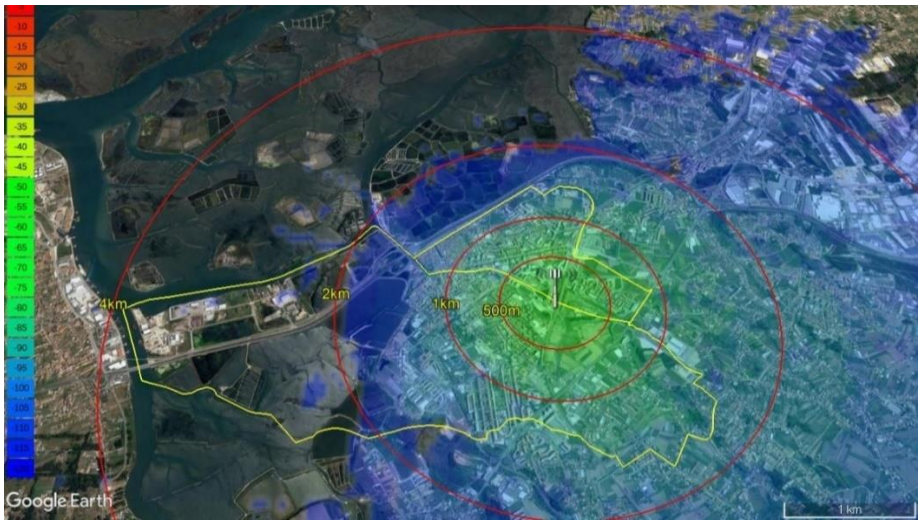

Figure 5.6 – Simulation with 1 Gateway for SF=9/BW=250 kHz, using *Okumura-Hata*

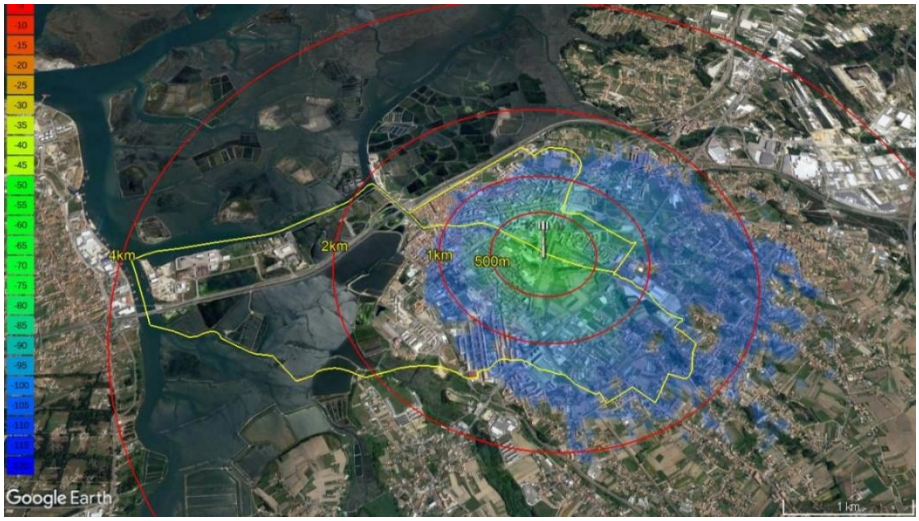

Figure 5.7 – Simulation with 1 Gateway for SF=7/BW=500 kHz, using *Okumura-Hata*

Figure 5.4 and Figure 5.5 proved that LoRa has quite a long range, covering all the area in study with only gateway, as it was predicted in subchapter 4.5. It's notorious that the coverage is more extensible to the southbound side, although it also reaches some areas in the west side, which makes sense since it a much more wide and open area of the district of Aveiro (however not interesting for this evaluation). Although they present similar results in terms of coverage range, to cover the municipality of Aveiro delighting in all the Figures above in yellow line, the configuration of $SF = 10/BW = 125\ kHz$, would be more suitable, since it would provide the same coverage, but with an higher bit rate, as demonstrated in Equation 3.5 (Figure 5.5).

When using $SF = 9/BW = 250\ kHz$, not all the area in study is covered with only one gateway, and therefore another gateway has to be placed (Figure 5.6). Similar to this, also Figure 5.7 shows that one gateway is not enough and for that reason, others have to be added. In both cases, d_{GW-GW} was respected, and it was concluded that two gateways would cover the city with $SF = 9/BW = 250\ kHz$, as shown in Figure 5.8.

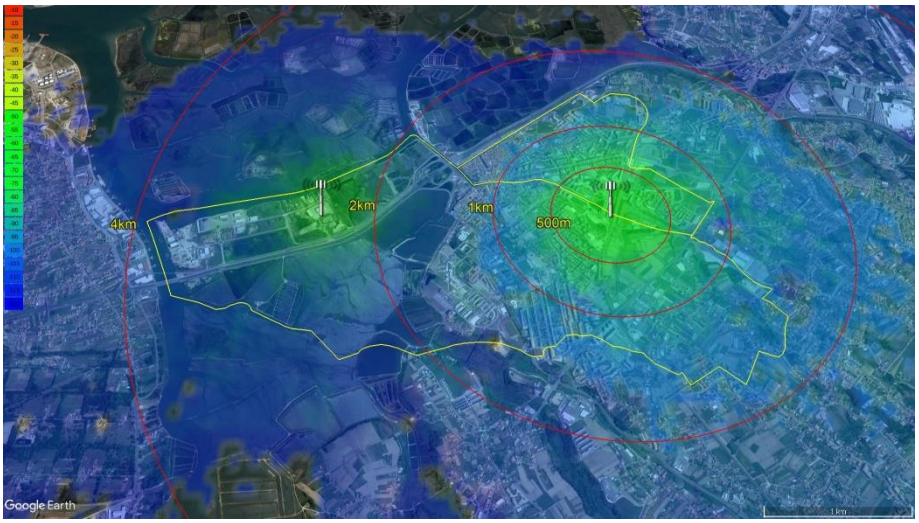

Figure 5.8 – Simulation with 2 Gateways for SF=9/BW=250 kHz, using *Okumura-Hata*

With $SF = 7/BW = 500\ kHz$ not all the locations are still reached with 5 gateways implemented in the network. In order to maximize it, another gateway at least shall be placed. However, the locations that are not covered are mainly in the west side river, and therefore not critical and justifiable to increase the number of gateways and cost of the network.

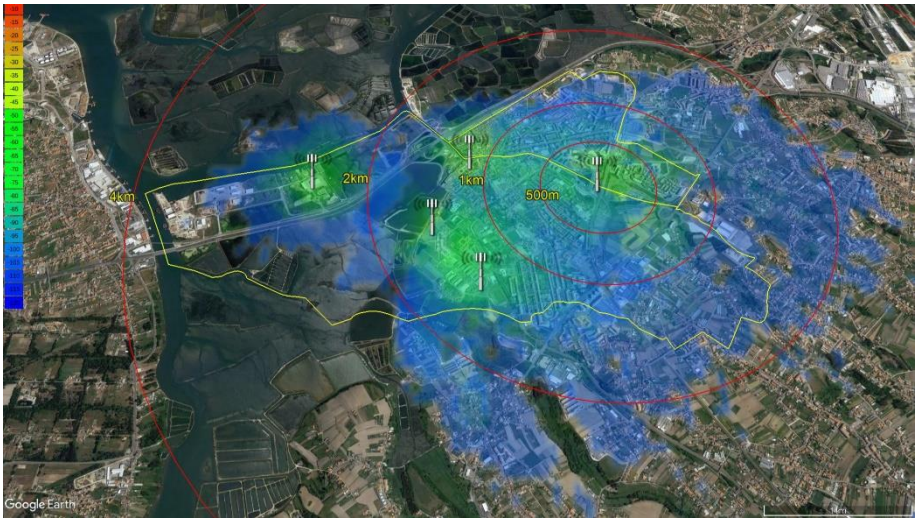

Figure 5.9 – Simulation with 5 Gateways for SF=7/BW=500 kHz, using *Okumura-Hata*

5.3.2 ITM

In the study carried by the authors in [77], ITM model was proven to be a conservative and a more realistic model when compared to others. Because of that, it imposes greater attenuations and/or more attenuations to the propagation signal, as such, the signal levels throughout each cell will be inferior to those of the model of *Hata* and, consequently, it forces to the use of more sites to cover the same area. On one hand, the planning is safer in terms of coverage, on the other hand it implies higher costs compared to the *Okumura-Hata* model. Figures 5.10 – 5.13 presents the same simulations as Figures 5.4 – 5.9, but using the ITM model instead.

Figure 5.10 – Simulation with 1 Gateway for SF=12/BW=125 kHz, using ITM

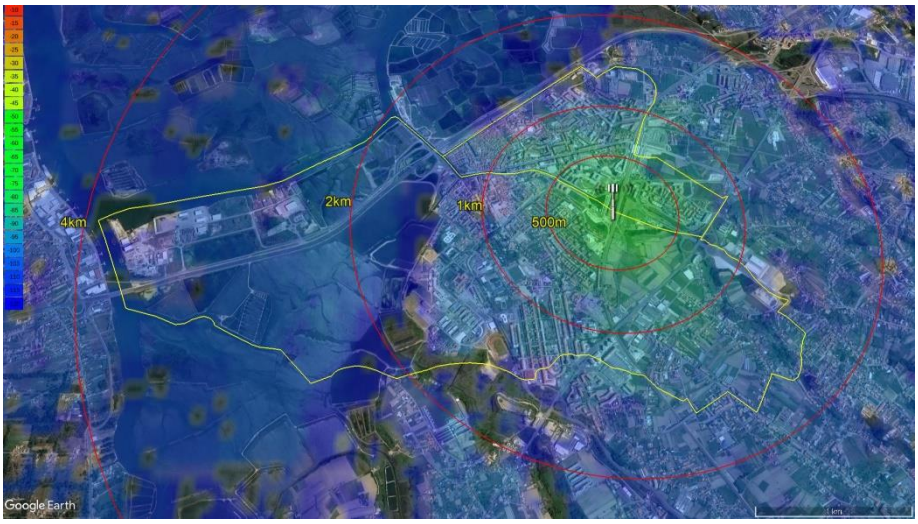

Figure 5.11 – Simulation with 1 Gateway for SF=10/BW=125 kHz, using ITM

Figure 5.12 – Simulation 1 Gateway for SF=9/BW=250 kHz, using ITM

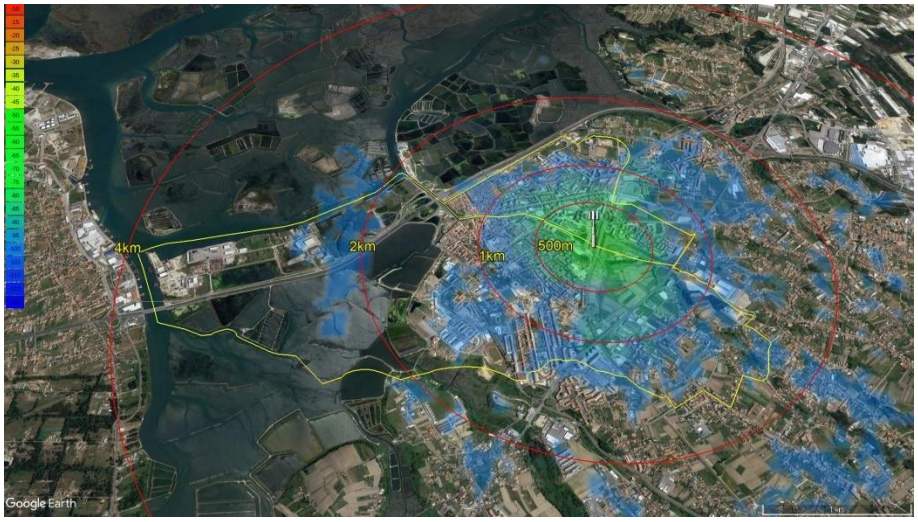

Figure 5.13 – Simulation with 1 Gateway for SF=7/BW=500 kHz, using ITM

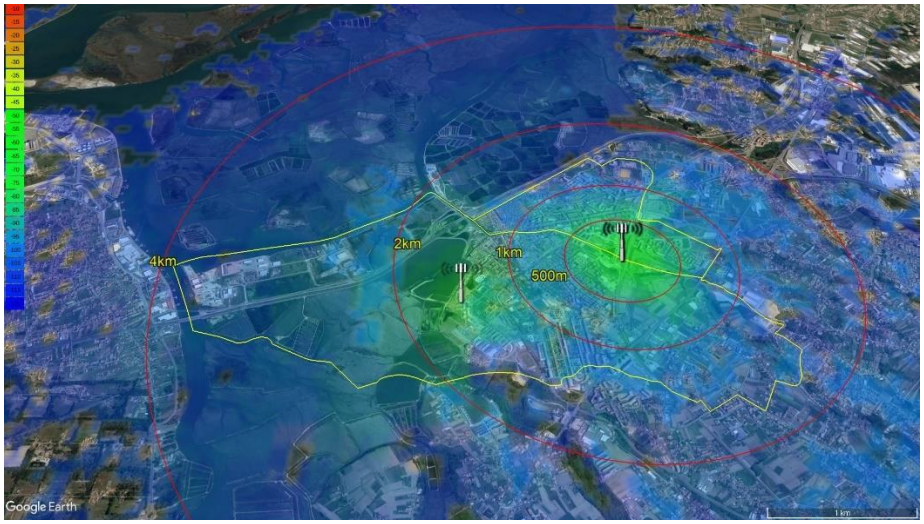

Figure 5.14 – Simulation with 2 Gateways for SF=9/BW=250 kHz, using ITM

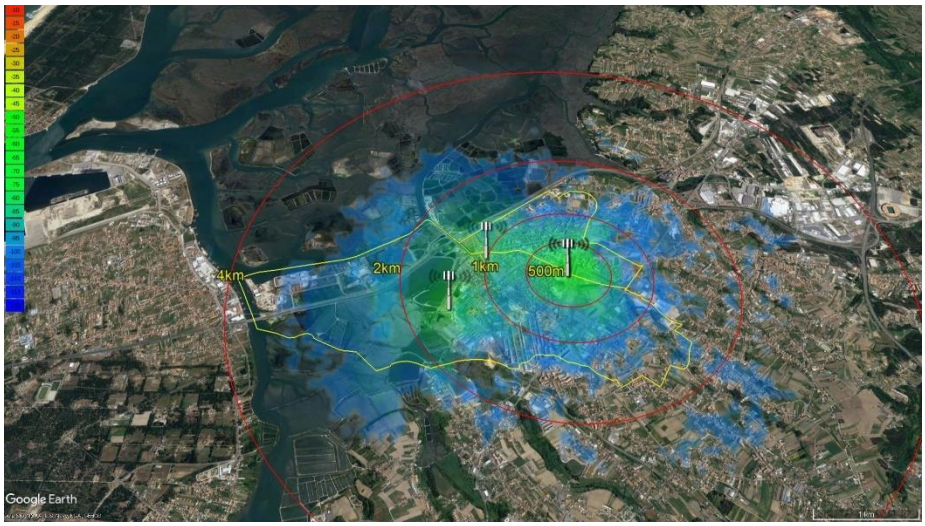

Figure 5.15 – Simulation with 3 Gateways for SF=9/BW=250 kHz, using ITM

5.4 Comparison of results

For all of the simulation results presented in the previous subchapter, the goal was to present a coverage for the city of Aveiro with the minimum gateways possible, in order to reduce the cost of a possible implementation. The coverage for the city of Aveiro was always assured within a range between -50 and the minimum receiver sensitivity accordingly to the mode of operation, which in this case varies between -104 and -123 dBm.

For all the configuration modes, the simulation results with *Okumura-Hata* demonstrated that OH is a very consistent model for all the regions of the city, while ITM is a more conservative model in zones where the density of buildings is higher, such as the city centre, and less conservative in open areas (West and South side of the city of Aveiro). In the case of the first two modes, one gateway was enough to cover all the entire city pretty well with the OH model. ITM also offers a pretty decent coverage, however with some blind spots next to the coverage of 2 km. For the remaining two modes, only one gateway will present indecent coverage, and therefore others have to be added using OH (Figures 5.8 and 5.9), and also for the ITM model (Figures 5.14 and 5.15).

Table 5.2 gives a comparation between the expected results and obtained results in terms of coverage between the theoretical results and the coverage obtained for both of the propagation models among the four modes.

		Expected	Obtained w/ OH	Obtained w/ ITM
SF=12/BW=125kHz	$A_{Gateway}$ $[km^2]$	21,127	181,04	155,46
	$N_{Gateways}$	1	1	1
SF=10/BW=125kHz	$A_{Gateway}$ $[km^2]$	10,665	143,79	131,16
	$N_{Gateways}$	1	1	1
SF=9/BW=250kHz	$A_{Gateway}$ $[km^2]$	5,153	81,31	86,22
	$N_{Gateways}$	2	2	2
SF=7/BW=500kHz	$A_{Gateway}$ $[km^2]$	1,825	2,65	6,5
	$N_{Gateways}$	5	5	3

Table 5.2 – Comparation of the results between the theoretical coverage area, OH model and ITM model

As expected, the simulations results in a much wider coverage when compared to the theoretical results. This is due to the fact that in the propagation model calculations, a single type of environment is defined (i.e urban), and the coverage area is estimated based on that. In the simulation results, since the software considers a much more detailed environment type, zones without buildings, wider and open areas or with LOS, it will translate in a much better quality signal at the reception. Apart from this, the ITM model although being more conservative, it presented better results for the low-range modes, being able to cover the entire city with only 3 gateways, when from OH at least 5 gateways were needed (Figure 5.15). In the next chapter different analysis will me made in order to compare the theoretical and simulation results with the real measurements taken in the city of Aveiro.

6

Implementation and Evaluation

6.1 Introduction

This chapter describes the tests that have been performed with the LoRa technology, to validate the proposed planning, as long as the obtained results, its range and quality in distinct scenarios.

Section 6.2 describes the Hardware setup for both the LoRa devices that were used to perform the measurements.

Section 6.3 presents the results obtained in a reliability and availability analysis for the different locations.

6.2 Hardware Setup

In order to validate the proposed planning and simulations, some real tests were necessary to be done in the city of Aveiro. For that, a gateway and a end-device were required. IT (Instituto de Telecomunicações) of Aveiro, has developed a solution containing a Single Channel Gateway already placed in in the city and ready for usage. The advantage of this solution resides in the fact that it's a much cheaper and simple solution when compared to commercial gateways, which are very expensive (i.e 1500€ for the Kerlink IoT Station) and sometimes non-open source or difficult to customize.

Each device has a core element which is a Raspberry Pi 3 board with the following characteristics:

Processor	**1.2GHz 64-bit quad-core ARMv8 CPU**
Memory	1 GB
WiFi Networking	2.4GHz 802.11n Wireless LAN
Operating System	64-bit Raspbian GNU

Table 6.1 – Raspberry Pi 3 Model B specifications

To implement the proposed solution, IT have used the SX1272 LoRa modules manufactured by Libelium. Libelium's LoRa module works in both 868 and 900 MHz ISM bands. Those frequency bands are lower than the popular 2.4 GHz band, so path loss attenuation is better in LoRa. In addition to that, 868 and 900 MHz are bands with much fewer interference than the highly populated 2.4 GHz band. Besides, these low frequencies provide great penetration in possible materials (brick walls, trees, concrete), so these bands get less loss in the presence of obstacles than higher bands.

Figures 6.1 a) and 6.1 b) present the module alone and a Raspberry Pi with the shield of the module.

Figure 6.1 a) – SX1272 Module

Figure 6.1 b) – Raspberry Pi 3 with Multiprotocol Radio Shield and SX1272 Module

The SX1272 LoRa module counts with a C++ library that provides the management of the SX1272 LoRa module in a simple way. This Application Programming Interface (API) offers a simple-to-use open source system. Some of the main functions are listed in Table 6.2.

Functions	Description
ON()	Opens the SPI and switches the SX1272 module ON.
OFF()	Closes the SPI and switches the SX1272 module OFF.
setLORA()	Sets the module in LoRaTM transmission mode.
setMode()	Sets the BW, CR and SF of the LoRaTM modulation.
setHeaderON()	Sets the module in explicit header mode (header is sent).
setHeaderOFF()	Sets the module in implicit header mode (header is not sent).
setCRC_ON()	Sets the module with CRC on.
setCRC_OFF()	Sets the module with CRC off.
setChannel()	Sets the indicated frequency channel in the module.
setPower()	Sets the signal power indicated in the module.
setNodeAddress()	Sets the node address in the module.
getSNR()	Gets the SNR value in LoRaTM mode.
getRSSI()	Gets the current value of RSSI from the channel.
getRSSIpacket()	Gets the RSSI of the last packet received in LoRaTM mode.
sendPacketTimeoutACK()	Sends a packet to a destination before a timeout and wait for an ACK response
receivePacketTimeout()	Receives information before a timeout expires.
receivePacketMAXTi-meout()	Same as previous function with maximum timeout

Table 6.2 – Example of functions of the SX1272 module [78]

There are ten predefined modes in the API, including the largest distance mode, the fastest mode, and eight other intermediate modes. All of them can be modified or deleted, and also it is possible to attach new modes in the appropriate function. The predefined modes and its properties are shown in the next table.

Mode	BW (Hz)	CR	SF	Sensitivity	Comments
1	125	4/5	12	-134	Max range, slow data rate
2	250	4/5	12	-131	
3	125	4/5	10	-129	
4	500	4/5	12	-128	
5	250	4/5	10	-126	
6	500	4/5	11	-125,5	
7	250	4/5	9	-123	
8	500	4/5	9	-120	
9	500	4/5	8	-117	
10	500	4/5	7	-114	Min range, fast data rate

Table 6.3 – Functional mode characteristics of SX1272 module [78]

The proposed solution implementation was developed by IT (Instituto de Telecomunicações), using Python 3.5 programming language. The API developed has a defined packet structure that is shown in Table 6.4

dst	src	packnum	length	data	retry
1 byte	1 byte	1 byte	1 byte	variable	1 byte

Table 6.4 – Packet structure of a LoRa packet with IT API

This structure has many fields to be filled by the user or the application, such as:

dst - Destination node address: this parameter is indicated as an input in the function used by the user;
src - Source node address: this parameter is filled by the application with the module's address (previously set by the user);
packnum - Packet number: this parameter indicates the packet number and is filled by the application. It is a byte field, so it starts in 0 and reaches 255 before restarting. If the packet is trying to be retransmitted, the packet number is not incremented;
length - Packet length: this parameter indicates the total packet length and is filled by the application;
data [MAX PAYLOAD] - Data to send in the packet: It is used to store the data to send to other nodes. All the data to send must be stored in this field. Its maximum size is defined by MAX PAYLOAD. The maximum payload size is 250 bytes;
retry - Retry counter: this parameter is filled by the application. It is usually equal to 0. Only when the retries feature is used, this value is incremented from 0 to the maximum number of retries stored in the global variable maxRetries which value is 3 by default. If the packet is sent successfully, or if the maximum number of retries is reached without success, the retry counter is set to 0.

6.3 LoRa Range Evaluation

To evaluate the capabilities of LoRa in terms of its communication range and quality, several tests have been performed in different conditions of the urban city of Aveiro.

Firstly, analysis is undertaken to determine the reliability of LoRa packet transmissions to various fixed locations. Afterwards a second analysis is performed, where the LoRa sensor is placed in a movement car to demonstrate its availability by analysing the RSSI, and determine its maximum coverage range for different places in the municipality of Aveiro, and also to evaluate its robustness against Doppler shifts, since LoRa is often described in the literature as being immune to Doppler's effect [39], [40].

For both analysis, three LoRa modes were tested, a short range mode, a middle-long range mode and a long range mode. Mode 1 was taken out of scope for this tests because it implies a very high time-on-air, and besides that, it wouldn't be suitable for the availability analysis (since at a speed of 16 km/h most of the packets would be loss, as shown in figure 4.9). Therefore, the specifications for the other three modes presented throughout this dissertation are presented in Table 6.5.

Mode	**BW** $[MHz]$	**CR**	**SF**	**Sensitivity** $[dB]$
3	125	4/5	10	-129
7	250	4/5	9	-123
10	500	4/5	7	-114

Table 6.5 – LoRa modes used for tests

In both scenarios, the LoRa gateway is equipped with a Libelium SX1272 transceiver and fixed on the top of a building in 30m of height, at "Fábrica da Cerâmica" (Figure 6.2), with an omnidirectional antenna providing 6 dBi gain over the 868 MHz band.

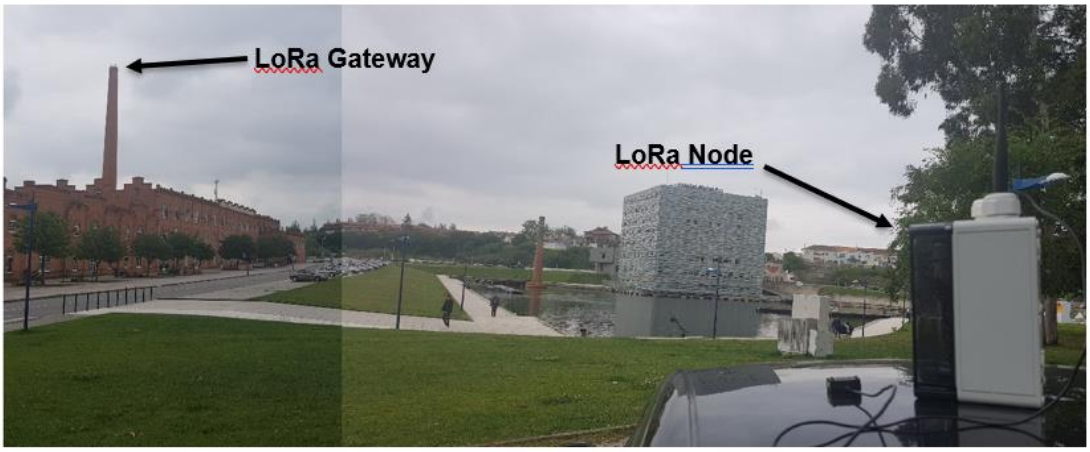

Figure 6.2 – LoRa Gateway (left), at an height of 30m and LoRa Node placed in a car (right), at an height of 1.5m from the ground

The LoRa end-node is powered by a 5V battery and built upon Raspberry Pi 3 development board, with Libelium multiprotocol shield and Libelium LoRa SX1272 communication module, communicating with a 868MHz omni-directional antenna with 4.5 dBi gain and attached to the roof-rack of the car and with approximately at 1,5 m height of the ground (Figure 6.2).

Table 6.6 lists the complete parameters used for both nodes in the availability and reliability analysis.

Characteristics	Gateway	Node
Processor	Raspberry Pi 3	Raspberry Pi 3
LoRa Module	Libelium SX1272	Libelium SX1272
Modulation	LoRa	LoRa
Antenna Gain [$\boldsymbol{dBi}$]	6 dBi	6 dBi
Transmit Power [$\boldsymbol{dBm}$]	+14 dBm	+14 dBm
Frequency [$\boldsymbol{MHz}$]	865.2	865.2

Table 6.6 – LoRa Gateway and Node configuration parameters

During the measurements, the LoRa end-node was periodically sending an uplink packet to the gateway including a sequence number, Global Positioning System (GPS) information (velocity and location), which were used to estimate the packet loss rate and the position of the node respectively. Upon decoding it, the gateway would determine the value of the SNR and RSSI, which was used to provide an estimation of the coverage based on the position of the end-node. A specie of delivery mechanism was used to let the end-device know that the packet was successfully received by gateway: a downlink "ACK" packet of 1 byte would be transmitted back to the end-device. The downlink link budget was expected to be estimated from this method, however after some measures it was concluded to be not reliable, and therefore not considered for this analysis. The period of the packets was defined in order to assure that it was bigger than LoRa's maximum TOA given by Eq. 3.10. In both ends, a *.log* file would be generated containing all of the information described above, as shown in Figure 6.3.

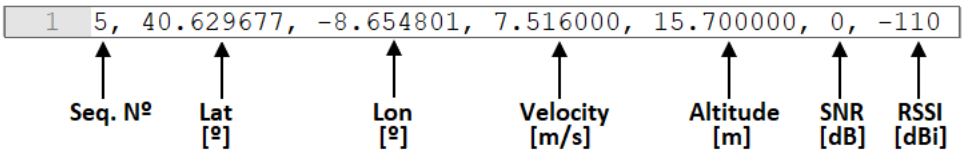

Figure 6.3 – Example of a file extracted from the gateway

6.3.1 Reliability analysis

The reliability tests in any application consists typically in setting up strategically IoT device installation points. For most of the IoT applications, the devices will be placed in a indoor environment, inside buildings and houses. However, it has already been demonstrated that walls and any kinds of construction materials introduces several attenuations to the propagation signal, thus, since this analysis is done with only one gateway, there would be a high change that the results wouldn't be the best for evaluation. To avoid that, twelve strategical places were defined in an outdoor environment only, where ten are part of the city centre of Aveiro, considered to be an urban environment, and two are outside of the city centre, similar to rural environment characteristics. The reason for the definition of this two last points is to verify the maximum range in an open area. Figures 6.4 illustrates all the locations in study. Figure 6.4 a) gives a top-view of the general map, and Figure 6.4 b) illustrates each individual location from a real-footage taken in every point.

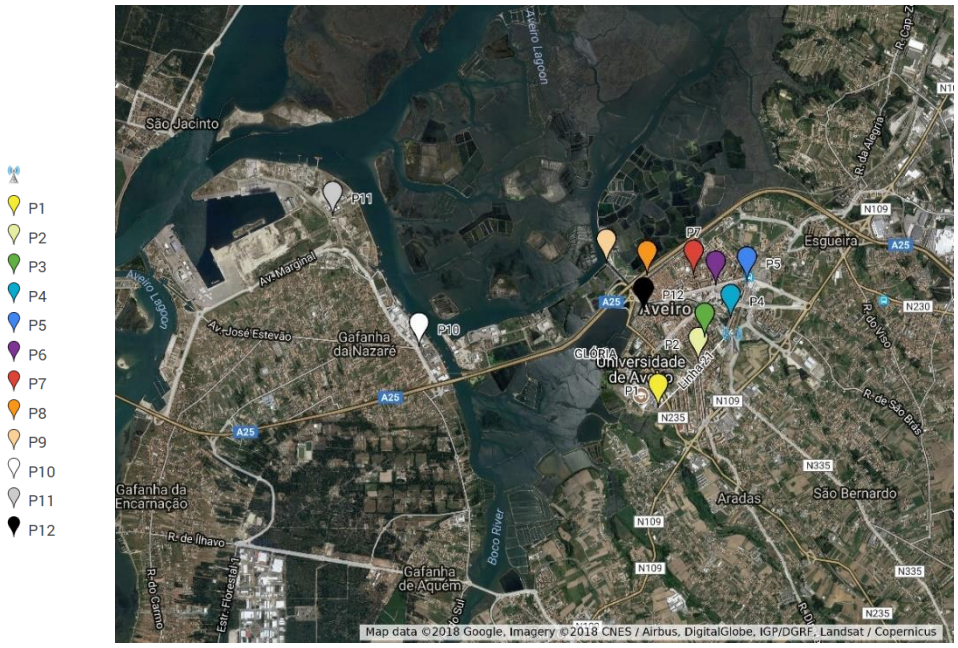

Figure 6.4 a) – Top-View of the locations defined

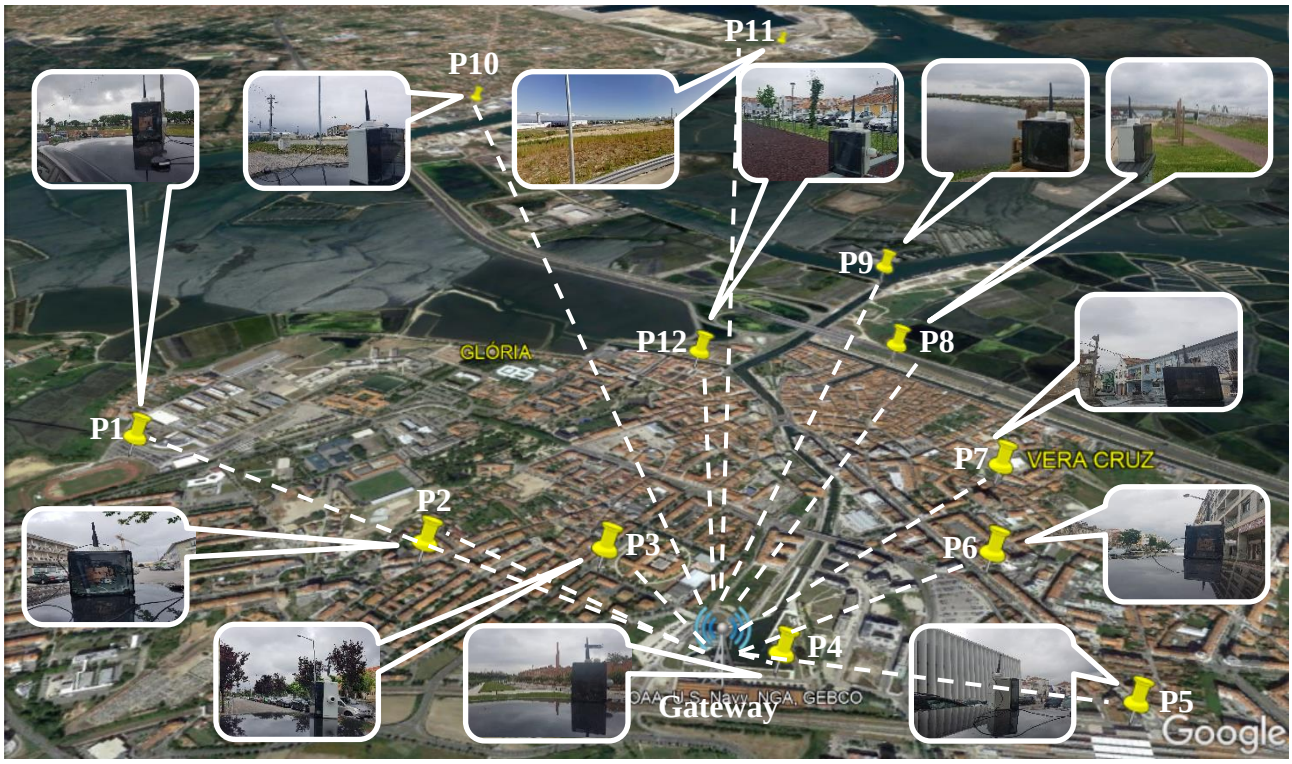

Figure 6.4 b) – Detailed view of the locations defined

For every reference point illustrated in the figures above, 50 packets of 255 bytes were transmitted in Uplink in order to have a conservative analysis. The size of the transmitted packets are considered to be higher than the usual for most of the IoT applications, however it will still give a better idea of the results since this is the maximum length of a LoRa packet and the scenarios are tested in the worst conditions. With this in consideration, all of the measurements were concluded and a *.log* file for each of the modes were stored in the gateway. This file has the format illustrated in Figure 6.3. After some analyses and calculations to the obtained results, the total number of transmitted and received packets, the PSR (Packet Success Ratio), SNR, RSSI and can distance between the end-device and the gateway can be extracted for each of the locations. The results for Mode 3, 7 and 10 are presented in Table 6.7, 6.8 and 6.9 respectively.

		Pkt. TX	Pkt. RX	PSR [%]	SNR [dB]	RSSI [dBm]	Lat [º]	Long [º]	d [m]
Mode 3	P1	50	49	98%	1,8	-107,8	40,628	-8,655	1400
	P2	50	50	100%	5,6	-101,3	40,634	-8,649	640
	P3	50	50	100%	7,0	-92,9	40,637	-8,648	400
	P4	50	48	96%	7,8	-76,7	40,639	-8,644	120
	P5	50	49	98%	4,7	-103,7	40,644	-8,641	615
	P6	50	45	90%	5,5	-102,3	40,643	-8,646	570
	P7	50	44	88%	-7,2	-122,9	40,644	-8,649	840
	P8	50	47	94%	1,5	-109,0	40,644	-8,657	1300
	P9	50	47	94%	7,0	-95,6	40,646	-8,663	1850
	P10	50	46	92%	-9,6	-122,3	40,636	-8,692	4100
	P11	50	47	94%	4,3	-104,9	40,651	-8,705	5400
	P12	50	38	76%	-6,0	-121,4	40,640	-8,657	1200

Table 6.7 – Reliability results for Mode 3

		Pkt. TX	Pkt. RX	PSR [%]	SNR [dB]	RSSI [dBm]	Lat [º]	Long [º]	d [m]
Mode 7	P1	50	48	96,00%	-2,1	-116,1	40,629	-8,655	1400
	P2	50	48	96,00%	2,7	-103,5	40,634	-8,649	640
	P3	50	49	98,00%	5,5	-97,2	40,637	-8,648	400
	P4	50	48	96,00%	6,9	-77,5	40,639	-8,644	120
	P5	50	46	92,00%	1,4	-105,6	40,644	-8,641	615
	P6	50	36	72,00%	0,0	-109,3	40,643	-8,646	570
	P7	50	35	70,00%	-10,4	-124,4	40,644	-8,649	840
	P8	50	36	72,00%	-10,3	-118,5	40,644	-8,649	1300
	P9	50	45	90,00%	3,5	-100,3	40,646	-8,663	1850
	P10	50	24	48,00%	-11,4	-125,4	40,636	-8,692	4100
	P11	50	48	96,00%	-3,3	-117,0	40,651	-8,705	5400
	P12	50	0	0,00%	-	-	-	-	-

Table 6.8 – Reliability results for Mode 7

		Pkt. TX	Pkt. RX	PSR [%]	SNR [dB]	RSSI [dBm]	Lat [º]	Long [º]	d [m]
Mode 10	P1	50	0	0%	-	-	-	-	-
	P2	50	0	0%	-	-	-	-	-
	P3	50	38	76%	3,0	-98,2	40,637	-8,647	400
	P4	50	50	100%	4,7	-81,1	40.639	-8,644	120
	P5	50	50	100%	1,3	-107,6	40,644	-8,641	615
	P6	50	49	98%	0,1	-102,5	40,643	-8,646	570
	P7	50	0	0%	-	-	-	-	-
	P8	50	0	0%	-	-	-	-	-
	P9	50	49	98%	2,7	-99,0	40,646	-8,663	1850
	P10	50	0	0%	-	-	-	-	-
	P11	50	0	0%	-	-	-	-	-
	P12	50	0	0%	-	-	-	-	-

Table 6.9 – Reliability results for Mode 10

For a more ease comparation, the results presented in the tables above, are divided in two parts: First, a comparation between the various values of the SNR and RSSI are presented in Figures 6.5 a), b) and c), and second, the relation between the received packets and transmitted packets (PSR) is presented in Figures 6.6 a), b) and c).

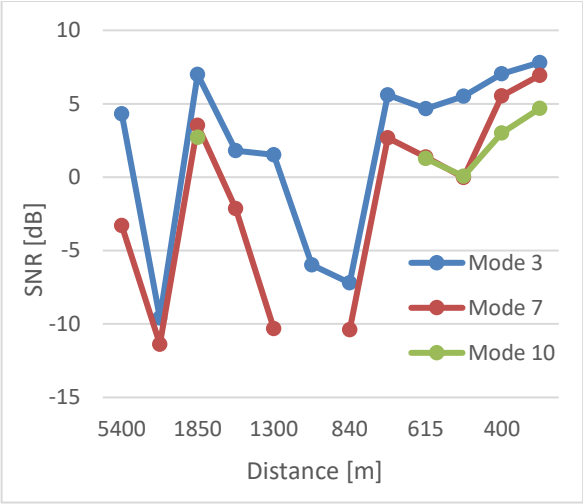

Figure 6.5 a) – SNR variation with the distance for the various LoRa modes

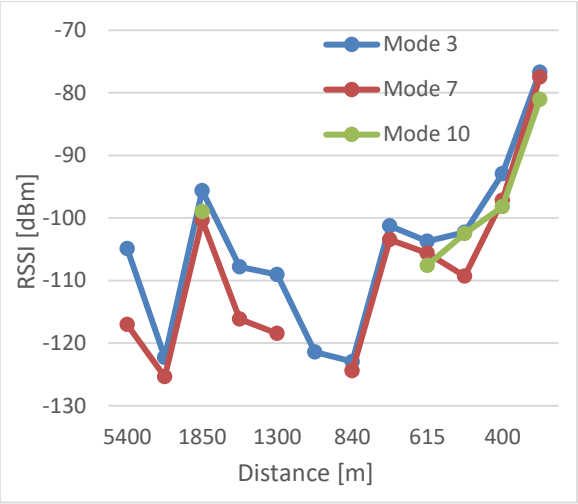

Figure 6.5 b) – RSSI variation with the distance for the various LoRa modes

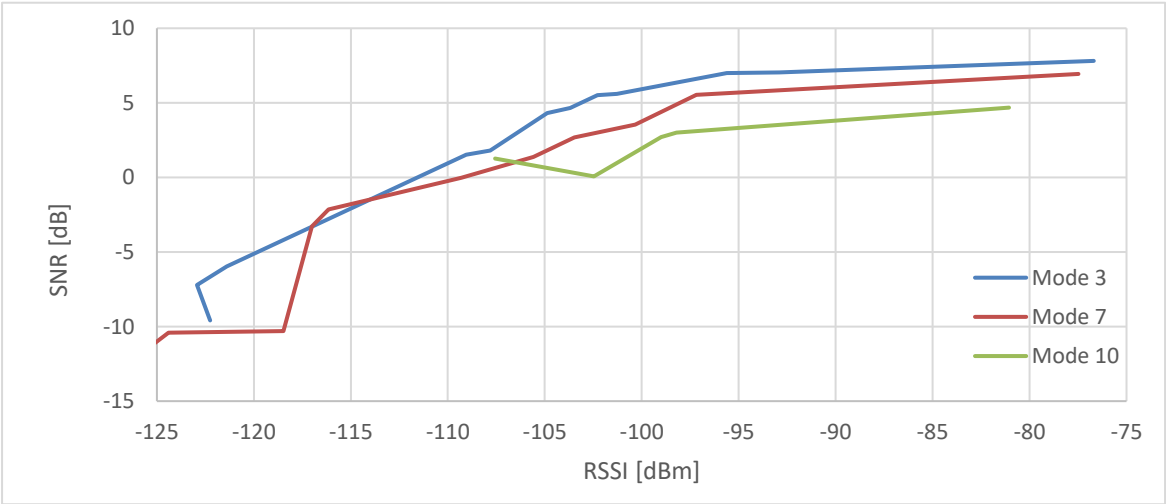

Figure 6.5 c) – SNR variation with RSSI for the various LoRa modes

Starting with the shorter-range mode (Mode 10), a maximum distance of 1850 meters was achieved with an SNR of 2.7 dB and an RSSI of -99 dB. If we consider just the value, this is indeed a very good coverage range for the mode in utilization, however, this was only possible because the location was in clear line-of-sight with the gateway. With this mode, only more 4 locations were possible to be classified as reliable: P3, P4, P5, P6. The longest location from

the gateway that the end-node was still able to receive packet was at P5, where an SNR of 1,27 dB and RSSI of -107,56 dBm was achieved. If we define this as the maximum range of Mode 10, then we can conclude that the results expected in chapter 3 are similar to the obtained, since we've determined a maximum range of 800m with an RSSI of -104,4 dBm for this configuration.

With Mode 7, at P11 which was located 5,4 km away from the gateway an SNR of -3,2 and an RSSI of -117 dBm was obtained. For the same location, Mode 3 got much higher values. This position is quite similar in terms of environment characteristics as P9, which explains why a bigger SNR and RSSI is obtained, regardless the mode of utilization. Among all the measurements, only 1 location was not covered by the gateway, which is an area fully surrounded by buildings, which caused the signal to drop below the receiver sensitivity (Figure 6.5 b)). From the theoretical calculations, an RSSI of -112,4 dBm was defined to be expected at a range of 1,4 km. From the results obtained in the measurements, -118,5 dBm was achieved at a similar distance (P8).

Finally, with Mode 3, similar results are obtained as with Mode 7. The only difference is that with Mode 3, in all of the locations defined, the node was able to communicate with the gateway (whereas in Mode 7 there was a blind spot at P12), and for all the locations, a better SNR/RSSI was received. As expected, this mode offered the best conditions in terms of propagation. In Chapter 3 we have estimated a maximum range of 2 km, with an RSSI of -117,9 dBm. On the results presented, the closer distance to this value of P9, however, since it is in an open area, a better RSSI was received ad therefore this comparation cannot be done.

In a comparative analysis between RSSI and SNR (Figure 6.5 c)), it can be concluded that for received power levels in the -100 to -122 dBm range, a fairly linear response is obtained for mode 1, and similarly for mode 7 and 10, where the range varies from -100 to -117 dBm and from -98 to -102 dBm, respectively.

In resume, two main conclusions can be taken from the figures above:

1) SNR/RSSI tends to decrease with the raise of a distance until a coverage area of around 700m is reached. After that, at bigger distances, the signal starts to be highly impacted by the buildings obstructions and presence of shadowing effect, and therefore the results for SNR/RSSI reduces drastically. This is the points where the difference among difference modes starts to be notorious. For more sensitive nodes (i.e Mode 3), the gateway

is still able to communicate with the node, however, this is the opposite for the less sensitive (i.e Mode 10);

2) Although it's clear that the distance between the gateway and the node highly affects the propagation signal in the city centre, this is not valid when the node starts entering locations with better propagation conditions (such as open areas, or areas where better LOS is achieved). In this case, SNR/RSSI values starts to increase, making possible a good reliable link at very significant distances, under those circumstances.

In regards to PSR comparation, the results among all the modes are illustrated in Figures 6.6 a), b) and c). The number of samples (50) is definitely not enough to get the proper results, which will be statistically meaningful. Unfortunately, the low data rate and limitations of the spectrum usage regulations on the duty cycle significantly hamper the measurements, since the nodes automatically take this in consideration upon transmitting a LoRa packet. Nonetheless, even the presented results can be useful and provide insight into the capabilities and limitations of the LoRa technology in terms of Packet Success Rate.

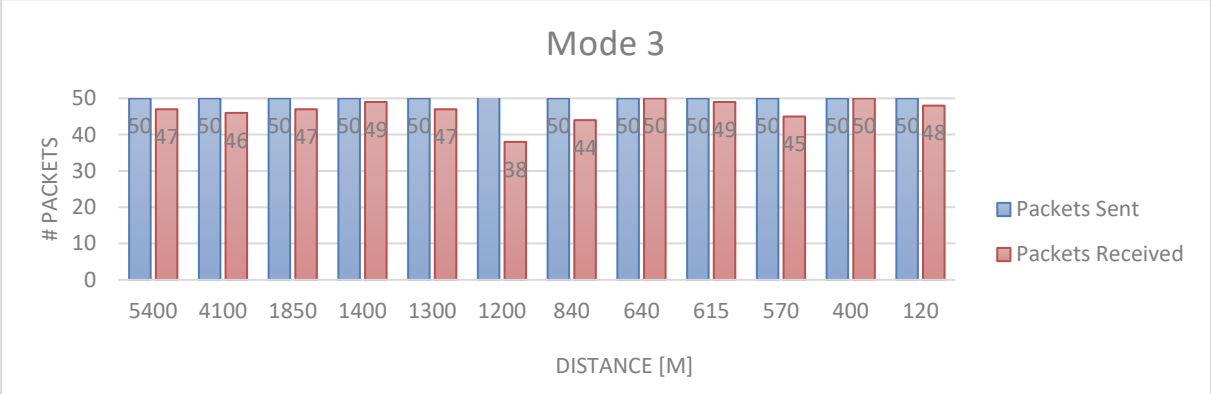

Figure 6.6 a) – Packet Data Rate for Mode 3

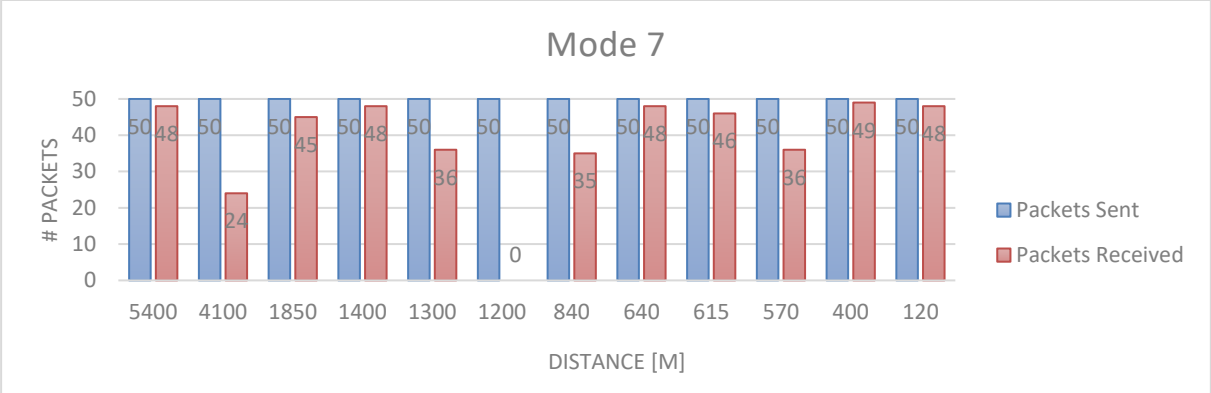

Figure 6.6 b) – Packet Data Rate for Mode 7

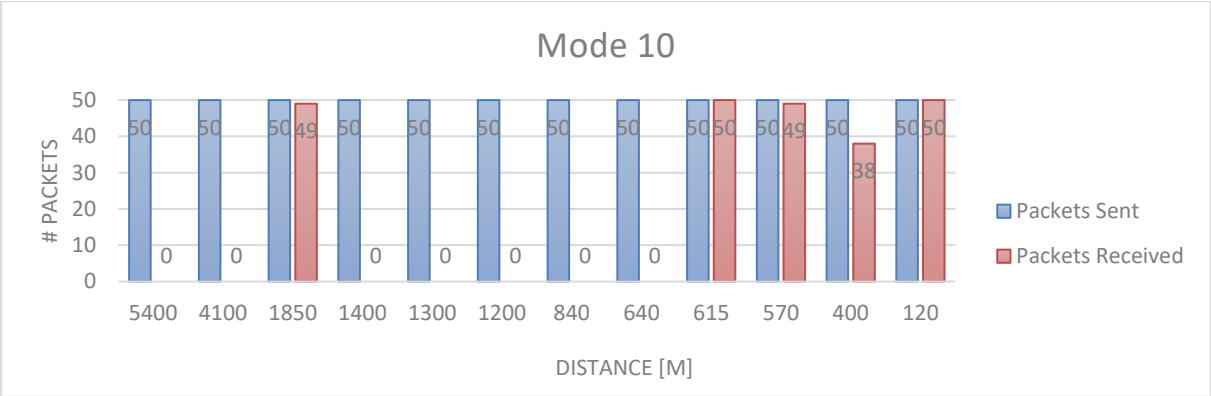

Figure 6.6 c) – Packet Data Rate for Mode 10

With Mode 3, most of the transmitted packets were received successfully with a pretty good PSR (above 90%), with an exception of P12, where a less number of packets was received (38), and consequently a less PSR was seen.

In Mode 7, it is seen that the PSR is about 90% for locations where the RSSI is high, and it decreases drastically where the RSSI is low.

Finally, in Mode 10 we can see that the PSR is quite consistent among all of the locations, which is due to the fact that the mean RSSI is above the minimum receiver sensitivity. In resume, we can conclude that the more the RSSI is close to the minimum receiver sensitivity, the higher is the chance of decoding the packets with errors or not detecting them at all.

6.3.2 Availability analysis

In order to test the availability of the LoRa network, multiple measurement runs using a car moving through the city of Aveiro were performed in the uplink scenario. During these measurements, the car was driven along the major roads following the speed limits (10 - 90 km/h) and the end-device was transmitting periodically a packet of 255 bytes for all the three modes configured. Figure 6.7 illustrates the route followed by the car, where the end-node was transmitting packets in all of the measurement runs. The path taken was of course not exactly the same among the three modes, but since the difference was not much among them, only one path is illustrated.

Figure 6.7 – Measurements path performed with the movement car

In the logs captured, there was a discrepancy between the transmitted packets and the received packets, meaning that various packets were included in the end-node *logs*, along with the GPS locations of the car, but not captured in the gateway *log-file*. This packet loss were due to several reasons, such as interference/collisions by other LoRa transmissions occurring at the same time, doppler effect caused by the speed of the car in some areas, strong NLOS and not enough sensitivity to decode some packets using lower SF/higher BW, and therefore they are not considered for the availability analysis. Also, multiple measurements existed for one location due to traffic and congestion of the roads, and therefore the mean value of RSSI for these locations was considered. This results in an useful *data-log* consisting 329 packets received in Mode 3; 259 in Mode 7 and 269 in Mode 10.

Finally, the RSSI of the useful packets results in an availability map of the network laid on the satellite image of the Aveiro region called Heat Map. This heat map was made using the *Google Maps* API in an *Android* application, and it was constructed with the ease of analysing the *.logs* captured by either by the end-node or the gateway, and easily attribute a scale based on the RSSI captured. For the sake of simplicity, nine different scales were considered in terms of evaluation of RSSI, each of them containing an interval of -15 dBm, where:

1) RSSI greater than -105 dBm gives a strong signal with a high anticipated reliability towards fading and interference effects;
2) RSSI between -105 dBm and -135 dBm gives a weaker signal, but depending on the mode in usage, it can still be decoded correctly.

The availability results obtained for each of the modes were extracted from the developed application, and placed on the top on *Google Earth* in order to have the same delimitations as presented in Chapter 5. This results in the illustration of Figures 6.8 a), b) and c).

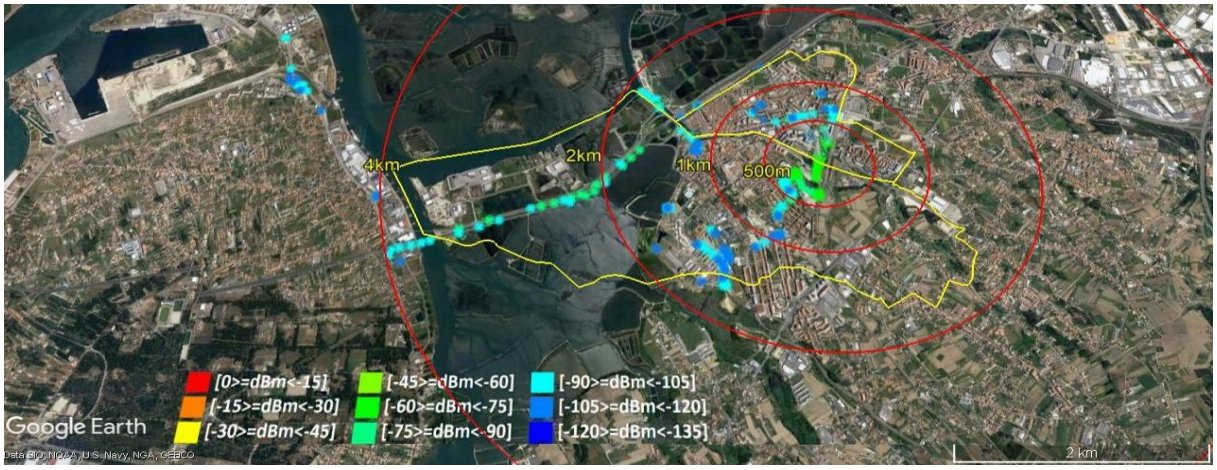

Figure 6.8 a) – Availability analysis for Mode 3

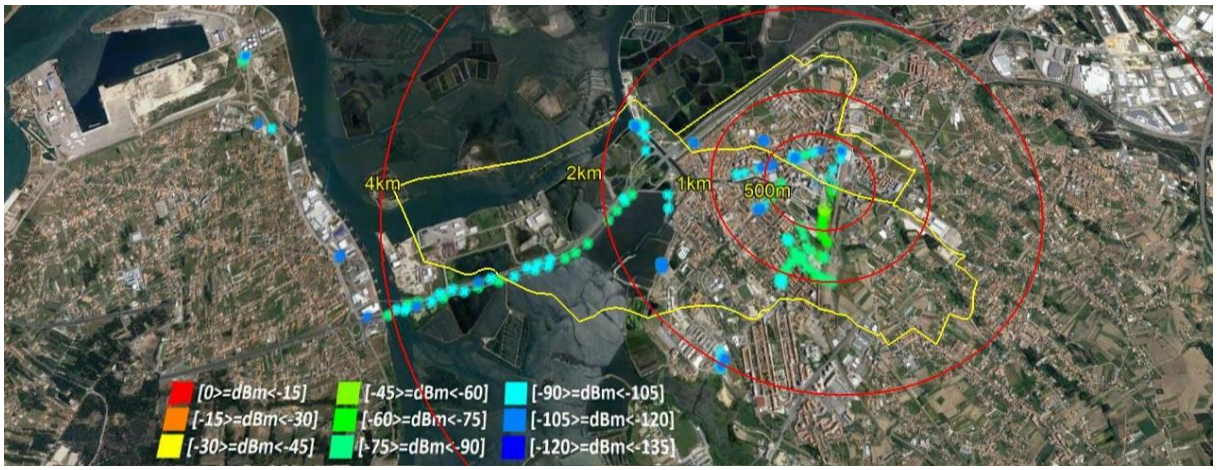

Figure 6.8 b) – Availability analysis for Mode 7

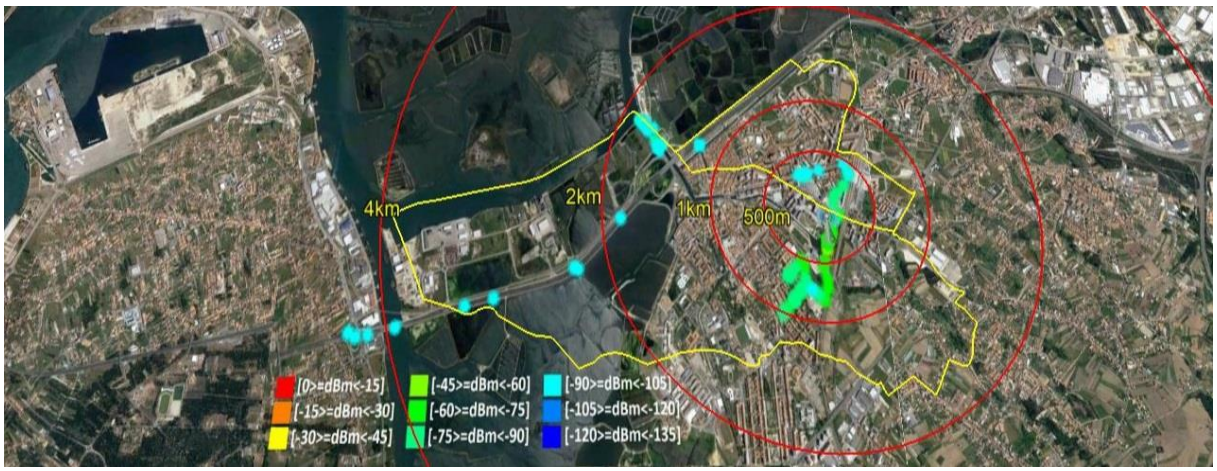

Figure 6.8 c) – Availability analysis for Mode 10

Starting with the analysis of Figure 6.8 a), Mode 3 reveals that within 500m range from the gateway, the signal mostly exceeds -90 dBm in the measured points, and between 500m and 1km of range, the signal drops slightly between -90 and -120 dBm. Until 500m of range, the distance between the gateway and the end-node is so small that an high RSSI is expected. After 500m, the signal power starts to decrease because of the "real" urban environment characteristics, such as a line of sight blocked by some obstacles. Between 1<km<2 some blind spots can be found, caused by elevations and obstacles and it starts to get difficult for the node to decode the packets. Despite that, still most of them are received with an RSSI between -105 and -120 dBm. A very good link over 2 km was also achieved, but in places where there was no major attenuations caused by the buildings and a better LOS was assured. Note, that few packets were also received from the distances exceeding 4 km (e.g., Gafanha da Nazaré area, on the west side of the city in study), but the communication at such distances is only possible in that kind of environment.

For this particular mode, 809 packets were transmitted and only 329 were received, giving an PER of 60%. From the *data-log* collected, it was clear that the impact of the distance between the gateway and the end-node (especially when the distance between the gateway and the end-node was bigger than 1km) truly affects the PER, but also the velocity of the car proved to play an important role in this analysis, especially for this mode. The maximum velocity registered by the end-node was 19.61 m/s, approximately 71 km/h, however after approximately 18 m/s (64,8 km/h) most of the packets started to be lost. This was similar to what was calculated in Figure 4.9, where it was proved that after 64 km/h, some Doppler Effect would be expected thus, the link would be affected.

Similarly, to this results, Mode 7 in Figure 6.8 b) shows that the coverage within 1km is pretty much similar. The difference between Figure 6.8 a) and b) starts to be highlighted after 1 km, where in some places the end-node is not able to receive the packets for the second option. This was also expected, since in the theoretical calculations, a range of 1,5 km was achieved (Table 4.6). Also, the maximum velocity of the car that the end-node was able to receive the packet was approximately 91,62 km/h. Accordingly to the calculations of Figure 4.9, the Doppler Effect would start to be visible at 208 km/h, however since the car didn't reach that velocity in any point, this couldn't be proved, but some packets were started to get lost when the car hit a speed of 85 km. In total, 889 packets were transmitted and 359 were received, giving a PER of 60% aswell.

Finally, for the weakest mode in terms of range, not much coverage was achieved, where most of the packets were not received due to the high distance between the end-device and the gateway. Until 1km pretty much all the packets are received with a good value in terms of RSSI, but with the exception of the packets on the east-side rural area (Gafanha da Nazaré), no other packets are received by the gateway with this configuration, which matches the expectations where a maximum range of 800m was computed. Also with this configuration, there was no packet loss due to the movement of the car, and the maximum registered velocity was approximately 76,94 km/h. Here 575 packets was transmitted, and 269 were received, resulting in a PER of 53%.

7

Conclusions and Future Work

7.1 Conclusions

As it was presented in the beginning of this dissertation, LPWAN technologies are the rising stars in the IoT networks. One of the most evolved ones is LoRa, which presents different trade-offs between coverage and data rate, making it a suitable and versatile technology to be used in any environment type. Spreading factor is one of the leading parameters that allows LoRa to have this versatile characteristic. By increasing the SF, a better robustness to interference and noise will be expected. However, it will increase the total Packet Air-Time (Equation 3.10) and therefore there will be a higher probability of collisions, which is a very important factor to take in consideration in a real-life network.

An IoT network planning involves a careful definition of factors and margins that are presented in a real-life environment and which influences the propagation signal, before proceeding with any Link Budget calculations. Some of these factors are for example long-scale fading and small-scale fading, which were taken in consideration upon estimating a network planning using LoRa technology for the city of Aveiro. Besides this, LoRa has a particularity of having different sensitivity values, depending of the configuration applied on the network and thus, four different configuration modes were evaluated in the theoretical coverage estimation. Here, a maximum PL of 142 dB and 127 dB was expected in the longer-range mode for an outdoor and indoor environment respectively, and also a maximum PL of 123.3 dB and 108.3 dB for the weakest-range mode, under the same circumstances. From this output, and with the usage of the empirical propagation model *Okumura-Hata*, the coverage area was estimated, which led to a maximum range in an outdoor environment of 2,9 km and 1 km in an indoor environment. For the worst-case scenario, a total area of coverage of 800m and 314m was achieved, also in outdoor and indoor environment respectively. From these results, it can be said that LoRa is not

suitable for indoor applications since it will introduce a very high attenuation, especially when it is configured in a low-range mode, instead it is more suitable in outdoor applications. In this analysis only the OH equations for urban environment was considered, however it is expected to reach an even higher range if the suburban or rural equations are used.

CloudRF has demonstrated to be a good choice for an IoT software simulator, although it is not meant for that. In most of the analysis driven, the coverage of the city in study was assured with only one gateway (as the expected theoretical results), however in the medium range mode it was necessary to add another one gateway to compensate the blind spots. The simulator estimates the coverage area essentially depending on the sensitivity of the device, and this is the key parameter for the simulator to distinguish between different LoRa configuration modes. For instance, for a fixed bandwidth, a configuration with SF=12 is more sensitive when compared to SF=7, and therefore the simulator will provide a wider coverage as a result. Two different propagation models were evaluated here: OH and ITM. Although both presented significant results in terms of range, ITM proved to be a more conservative model in urban areas, where the attenuation caused by buildings and other obstacles are higher. When comparing the output from the simulator with the calculated in the Link-Budget, it's difficult to reach the same results considering the fact that the propagation model equations consider the same characteristics and type of environment, and the simulator has a better view in terms of terrain and environment characteristics and doesn't apply the same data for all the points.

To evaluate the capabilities of LoRa in terms of its communication range and quality, several tests were performed in different conditions of the urban city of Aveiro in terms of reliability and availability. In both analysis, the results were performed with a LoRa gateway installed in 30 m height above ground and a LoRa end-device placed in a car at 1.5m height above the ground. The gateway used was a single-channel gateway, meaning that a fixed channel was always implicated, and therefore the results obtained are not provided by a fully capable gateway. When determining the reliability of the LoRa network, 12 locations were defined across the city, which resulted in a better reliability for the mode with the longest range (3), where the coverage was assured in all the points defined with a mean RSSI below the maximum receiver's threshold (-124 dBm). With the evaluation of the middle-range mode (7), it was concluded that, although the end-node was able to communicate with the gateway in all the points (except P9), some of the locations were to much closer to the cell boundary, which justifies the low PSR (less than 70%) in some of these locations. For the weakest mode in terms of range (10), only in a few of the locations within a range of approximately 600m, the sensor was able to reach

the gateway, however most of the packets were received successfully. Three main conclusions can be taken relative to Availability:

1) LoRa's coverage not only depends on the distance between the end-node and the gateway, but also depends on the type of environment, and both are not directly related. As an example, with mode 3, the end-device was able to communicate with the gateway in a distance greater than 5 km in an open-area (outside of the city center) but in an urban environment area, the maximum distance was approximately 1,5 km;
2) The packet reception ratio is highly influenced by the RSSI, where, the closer the RSSI is to the minimum receiver sensitivity, the higher is the chance of decoding the packets with errors or not detecting them at all;
3) For short communication distances (i.e bellow 500m), it is not necessary to use LoRa's maximum range mode, instead, the weakest mode might be a better choice, since not only it will offer the same coverage criteria, but also will provide a better data rate (Equation 3.5).

An availability analysis with a movement car following the legal speed limits inside an urban city showed that mobility introduces several attenuations to the received packets. In the case of the longest-range mode, the maximum velocity registered by the end-node was 64 km/h, and most of the packets transmitted when the node was having a speed over this limit were lost. This needs to be carefully addressed in any environment because in most of the practical real-life scenarios, the measurements are performed in a movement car, so Doppler will affect the quality of the measurements if previous evaluations (i.e estimation of the maximum velocity of the car – Figure 4.9) are not taken in consideration. For the remaining configuration modes, this effect was almost not experienced, however some of blind spots were present, mainly due to the short receiver sensitivity for the distance of communication. With this analysis no other packets were being transmitted apart from the node itself, so no packet collisions were seen. Although the availability with SF=12 is what provides the best output in terms of availability, is also the one who has more probability of collisions in case more packets are transmitted with the same configuration. It is recommended to use SF=7 when devices are located close enough to a gateway, approximately below 500 meters in an urban area. SF=10 should be enough for typical scenarios.

7.2 Future Work

Although the end-node used to perform the tests in Aveiro municipality presented good reliable results, is very expensive (approximately 300€). Since cost reduction is mandatory in any network implementation, the development of a LoRa sensor with a module designed by Microchip, RN2483 is proposed as future work. This module has the complete LoRa and LoRaWAN stack implemented, and it works with a simple list of commands available on its datasheet. For this solution, a maximum amount of 20€ would be needed, and the obtained results would be similar to the ones obtained with SX1272 by Libelium, since RN2483 also uses the same transceiver.

The RN2483 chip doesn't support any command to give the RSSI value as an output as SX1272 by Libelium does. Instead, it includes a register for reading out the SNR of the last successfully received packet, returning a value between −128 and 127 dB, according to it's the documentation. From the measures performed with the Libelium Hardware, these intervals were never reached. Instead, all the SNR values were varying between -12 dB and 8 dB (Figure 6.5 c)), meaning that a good RSSI approximation value can be extracted from the output of the SNR within this range.

Another approach for future work is the analysis of the capacity of a LoRaWAN network. As already stated in this dissertation, in order to take up all the potential of a LoRaWAN network, a proper gateway has to be used to (i.e with SX1301). In this dissertation, due to limitations in terms of cost and availability, only LoRa was considered, and therefore only coverage analysis was driven. In the area defined for the Aveiro municipality ($8{,}5km^2$) there are approximately 3500 inhabitants. It has been demonstrated in subchapter 4.4 that one gateway can cover the entire city in terms of coverage, meaning all the population would be connected to the same gateway. Although the coverage is assured with only one gateway, this doesn't mean this gateway can serve all of the IoT devices, and therefore, more than one gateway might be necessary to assure a proper network capacity, which depends essentially on the number of packets it receives, and is directly related the IoT application, since different applications have different transmissions average. If we assume Aveiro municipality is covered with SX1301 transceiver in the gateway design, then it can receive approximately 1.5 million packets per day [45]. In terms of Smart Cities, if for example one end-node transmits 100 packets/day, and if we consider a perfect synchronization on the gateway, then it would mean this single LoRaWAN gateway can carry about 15000 end-nodes per day, therefore each inhabitant in the city of Aveiro

connected to that gateway, could hold up to 4 IoT devices. This is still quite a low number when compared to the expectations of [5] for the current year (approximately 4 devices per person). However, accordingly to the same reference, by 2020 the number of things per person will be increased to 6, which will not be a problem considering the fact that the next generation of LoRa gateways will be released at the time, and it is expected to triple the current capacity (around 45000 nodes/gateway) by using multi directional antennas, instead of the a single omni directional antenna, as it is in the conventional setup. With this, the expectations for 2020 will be accomplished, and it can be assumed that 6-7 things per person can be considered more than adequate for the beginning of most of the Smart City applications. Thus, throughout the time, any further increase in the traffic demand can be easily addressed by installing additional gateways, a solution similar to densification in cellular networks.

References

[1] V. Galetic, I. Bojic, M. Kusek, G. Jezic, S. Desic, and D. Huljenic, “Basic principles of Machine-to-Machine communication and its impact on telecommunications industry,” *2011 Proc. 34th Int. Conv. MIPRO*, pp. 380–385, 2011.

[2] M. Mackenzie, “The automotive and transport sector will continue to drive growth in cellular M2M connections,” *Anal. Mason*, no. April, 2016.

[3] T. Hardwood, “Internet of Things (IoT) History,” *Postscapes*, 2018. [Online]. Available: https://www.postscapes.com/internet-of-things-history/.

[4] M. Mancini, “Internet das Coisas : História , Conceitos , Aplicações e Desafios,” pp. 1–9, 2018.

[5] J. Frahim, C. Pignataro, J. Apcar, and M. Morrow, “Securing the Internet of Things: A Proposed Framework,” *Cisco*, 2017. [Online]. Available: https://www.cisco.com/c/en/us/about/security-center/secure-iot-proposed-framework.html.

[6] J. Rivera and R. Van Der Meulen, “Gartner Says the Internet of Things Installed Base Will Grow to 26 Billion Units By 2020,” *Gartner*, 2013. [Online]. Available: https://www.gartner.com/newsroom/id/2636073.

[7] K. Panetta, “Top Trends in the Gartner Hype Cycle for Emerging Technologies,” *Gartner*, 2017. [Online]. Available: https://www.gartner.com/smarterwithgartner/top-trends-in-the-gartner-hype-cycle-for-emerging-technologies-2017/.

[8] R. Van Der Meulen, “Gartner Says 8.4 Billion Connected ‘Things’ Will Be in Use in 2017, Up 31 Percent From 2016,” *Gartner*, 2017. [Online]. Available: https://www.gartner.com/newsroom/id/3598917.

[9] R. Van Der Meulen, “Gartner Says 6.4 Billion Connected ‘Things’ Will Be in Use in 2016, Up 30 Percent From 2015,” *Gartner*, 2015. [Online]. Available: https://www.gartner.com/newsroom/id/3165317.

[10] T. Engineering, “Università degli Studi di Padova Network level performances of a LoRa system.”

[11] G. Margelis, R. Piechocki, D. Kaleshi, and P. Thomas, “Low Throughput Networks for the IoT: Lessons learned from industrial implementations,” *IEEE World Forum Internet Things, WF-IoT 2015 - Proc.*, pp. 181–186, 2015.

[12] U. Raza, P. Kulkarni, and M. Sooriyabandara, “Low Power Wide Area Networks : An Overview,” pp. 1–19, 2016.

[13] K. Mikhaylov, J. Petäjäjärvi, and K. Mikhaylov, “On the Coverage of LPWANs : Range Evaluation and Channel Attenuation Model for LoRa Technology On the Coverage of LPWANs : Range Evaluation and Channel Attenuation Model for LoRa Technology,” no. January 2016, 2015.

[14] Ericsson AB, “Cellular networks for Massive IoT,” *Ericsson*, vol. 1, no. January, pp. 1–13, 2016.

[15] I. C. Magazine and K. Zheng, “Low power wide area machine-to-machine networks : Key techniques and prototype L OW P OWER W IDE A REA M ACHINE - TO -M

ACHINE N ETWORKS :," no. September, 2015.
[16] L. Clavier, "A Study of LoRa Low Power and Wide Area Network Technology," no. November, 2017.
[17] M. Centenaro, L. Vangelista, A. Zanella, and M. Zorzi, "Long-range communications in unlicensed bands: The rising stars in the IoT and smart city scenarios," *IEEE Wirel. Commun.*, vol. 23, no. 5, pp. 60–67, 2016.
[18] "Bluetooth wireless technology based guidance system," no. December 2000, 2001.
[19] R. Want, B. Schilit, and D. Laskowski, "Bluetooth le Finds Its Niche," *IEEE Pervasive Comput.*, vol. 12, no. 4, pp. 12–16, 2013.
[20] M. Collotta, G. Pau, T. Talty, and O. K. Tonguz, "Bluetooth 5: a concrete step forward towards the IoT," pp. 1–17, 2017.
[21] A. Kumar and S. Gupta, "Study on ZIGBEE Technology," vol. 2, no. 10, pp. 297–301, 2013.
[22] U. Noreen, A. Bounceur, and L. Clavier, "Modeling Interference for Wireless Sensor Network Simulators," *Proc. Int. Conf. Futur. Networks Distrib. Syst. - ICFNDS '17*, pp. 1–6, 2017.
[23] R. Yasmin, J. Petäjäjärvi, K. Mikhaylov, and A. Pouttu, "On the integration of LoRaWAN with the 5G test network," *IEEE Int. Symp. Pers. Indoor Mob. Radio Commun. PIMRC*, vol. 2017–Octob, pp. 1–6, 2018.
[24] R. Sanchez-Iborra, J. Sanchez-Gomez, J. Ballesta-Viñas, M. D. Cano, and A. F. Skarmeta, "Performance evaluation of lora considering scenario conditions," *Sensors (Switzerland)*, vol. 18, no. 3, 2018.
[25] I. Com, "Low power wide area network," 2015.
[26] L. Power and W. Area, "Low Power Wide Area Connectivity GSMA INDUSTRY Paper."
[27] M. Mackenzie and T. Rebbeck, "The LPWA market has massive potential , but developing a sustainable business will be challenging Growth in LPWA connections is robust , but low connectivity revenue may not sustain a large number of network providers," no. August 2016, 2019.
[28] J. Petäjäjärvi, K. Mikhaylov, and T. Hänninen, "On the Coverage of LPWANs : Range Evaluation and Channel Attenuation Model for LoRa Technology," pp. 55–59, 2016.
[29] ETSI, "Final draft ETSI EN 300 220-1 V2.4.1 (2012-01)," *Etsi*, vol. 0, pp. 1–73, 2014.
[30] S. L. Joshi and C. Bhowmik, "An Overview of Ultra Wide Band Communication System and Its Components," *Imp. J. Interdiscip. Res.*, vol. 2, no. 8, pp. 930–933, 2016.
[31] R. Sanchez-Iborra and M. D. Cano, "State of the art in LP-WAN solutions for industrial IoT services," *Sensors (Switzerland)*, vol. 16, no. 5, 2016.
[32] Sigfox, "Sigfox." [Online]. Available: https://www.sigfox.com/.
[33] A. Augustin, J. Yi, T. Clausen, and W. M. Townsley, "A Study of LoRa : Long Range & Low Power Networks for the Internet of Things," pp. 1–18, 2016.
[34] Weightless, "Weightless." [Online]. Available: http://www.weightless.org/.
[35] On-Ramp Wireless Inc., "RPMA Technology for the Internet of Things," pp. 1–46, 2015.
[36] Semtech, "Semtech." [Online]. Available: www.semtech.com.
[37] "Lora Alliance." [Online]. Available: www.lora-alliance.org.
[38] I. Measurements, "LoRa Scalability : A Simulation Model Based on," 2017.
[39] K. Mikhaylov, J. Petäjäjärvi, and T. Hänninen, "Analysis of Capacity and Scalability of the LoRa Low Power Wide Area Network Technology," *Eur. Wirel. 2016*, pp. 119–124, 2016.
[40] J. Petäjäjärvi, K. Mikhaylov, M. Pettissalo, J. Janhunen, and J. Iinatti, "Performance of a low-power wide-area network based on lora technology: Doppler robustness, scalability, and coverage," *Int. J. Distrib. Sens. Networks*, vol. 13, no. 3, 2017.

[41] M. Cattani, C. A. Boano, and K. Römer, “An Experimental Evaluation of the Reliability of LoRa Long-Range Low-Power Wireless Communication,” *J. Sens. Actuator Networks*, vol. 6, no. 2, p. 7, 2017.
[42] Semtech, “SX1272/73 -860 MHz to 1020 MHz Low Power Long Range Transceiver,” no. Rev. 3.1, p. 129, 2017.
[43] LoRa Alliance, “LoRaWAN Regional Parameters v1.1 REV B,” pp. 7–11, 2016.
[44] B. Mir, R. Vidal, and C. Gomez, “Modeling the Energy Performance of LoRaWAN Llu í s Casals,” 2017.
[45] E. Aras, G. S. Ramachandran, P. Lawrence, and D. Hughes, “Exploring the Security Vulnerabilities of LoRa Exploring The Security Vulnerabilities of LoRa,” no. June, 2017.
[46] R. S. Sinha, Y. Wei, and S. Hwang, “A survey on LPWA technology : LoRa and NB-IoT ☆ , ☆☆,” vol. 3, pp. 14–21, 2017.
[47] LoRa Alliance, “LoRaWAN 1.1 Specification,” *LoRa Alliance*, no. 1.1, p. 101, 2017.
[48] D. Di and I. Dell, “Enabling relay-based communication in LoRa networks for the Internet of Things : design , implementation and experimental evaluation,” 2016.
[49] INE - Instituto Nacional de Estatística, *Censos 2011 Resultados Definitivos – Região Centro*. Lisboa, 2011.
[50] “União das Freguesias de Glória e Vera-Cruz - Dados Geográficos e Populacionais.” [Online]. Available: https://www.ufgloriaveracruz.pt/dados-geograficos-e-populacionais.
[51] J. Milanović, S. Rimac-Drlje, and I. Majerski, “Radio wave propagation mechanisms and empirical models for fixed wireless access systems,” *Teh. Vjesn.*, vol. 17, no. 2, pp. 43–52, 2010.
[52] S. R. Saunders and A. A. Zavala, *Antenna and Propagation for Wireless Communication Systems*. 2007.
[53] P. Vieira, A. Martins, and T. Cunha, “Introducing Redundancy in the Radio Planning of LPWA Networks for Internet of Things,” *Proc. 13th Int. Jt. Conf. E-bus. Telecommun.*, vol. 6, no. Icete, pp. 137–144, 2016.
[54] S. Y. Seidel, T. S. Rappaport, S. Jain, M. L. Lord, and R. Singh, “Path Loss, Scattering, and Multipath Delay Statistics in Four European Cities for Digital Cellular and Microcellular Radiotelephone,” *IEEE Trans. Veh. Technol.*, vol. 40, no. 4, pp. 721–730, 1991.
[55] A. Hoeller Jr, R. D. Souza, O. L. A. López, H. Alves, M. de Noronha Neto, and G. Brante, “Exploiting Time Diversity of LoRa Networks Through Optimum Message Replication,” *Iswcs 2018*, pp. 1–5, 2018.
[56] R. Theodore S., *Wireless communications: principles and practice. Vol. 2*. New Jersey, 1996.
[57] T. Schwengler, “Wireless & Cellular Communications, Class Notes for TLEN-5510 Fall 2018.”
[58] C. Prehofer, C. Bettstetter, and J. Widmer, “Mobile Communication Networks,” *Towar. 4G Technol. Serv. with Initiat.*, pp. 15–50, 2008.
[59] R. Baxter, N. Hastings, A. Law, and E. J. . Glass, *Radio System Design For Telecommunications*, vol. 39, no. 5. 2008.
[60] E. S. S. Suthersan, B. Raton, and C. R. C. Press, “Sklar , B . ‘ Rayleigh Fading Channels ,’” 1999.
[61] A. Note, “LoRa ™ Modulation Basics,” no. May, pp. 1–26, 2015.
[62] J. LEMPIÄINEN and M. MANNINEN, *Radio interface system planning for GSM/GPRS/UMTS*. Springer Science & Business Media, 2007.
[63] ETSI, “Digital cellular telecommunications system (Phase 2+); Radio network planning

aspects (GSM 03.30 version 6.0.1 Release 1997)," *ETSI Tech. Rep. 101 362*, vol. 1, pp. 1–36, 1998.
[64] "RF GUIDELINES 1800 MHz THE ERICSSON GSM SYSTEM R8," vol. 1, no. 44, 2000.
[65] B. Reynders, W. Meert, and S. Pollin, "Range and coexistence analysis of long range unlicensed communication," *2016 23rd Int. Conf. Telecommun. ICT 2016*, no. c, 2016.
[66] H. B. From *et al.*, "Understanding and Relating E b / N o , SNR , and other Power Efficiency Metrics," pp. 1–14, 2017.
[67] "TTN Gateways." [Online]. Available: https://www.thethingsnetwork.org/docs/gateways/.
[68] T. Petrić, M. Goessens, L. Nuaymi, L. Toutain, and A. Pelov, "Measurements, performance and analysis of LoRa FABIAN, a real-world implementation of LPWAN," *IEEE Int. Symp. Pers. Indoor Mob. Radio Commun. PIMRC*, 2016.
[69] K. B. Baltzis, "Hexagonal vs Circular Cell Shape : A Comparative Analysis and Evaluation of the Two Popular Modeling Approximations," *Cell. Networks-Positioning, Perform. Anal. Reliab.*, no. May, pp. 103–122, 2011.
[70] C. Splitting, "Lecture 10 : Frequency Reuse Concepts Improving Coverage and Capacity in Cellular Systems Lecture 10 : Frequency Reuse Concepts," *Communications*, no. 082, pp. 1–6.
[71] Y. Khaled, "LoRa simulation using ATDI's RF Solution," 2016.
[72] "CloudRF." [Online]. Available: https://cloudrf.com.
[73] NASA, "SRTM coverage." [Online]. Available: https://www2.jpl.nasa.gov/srtm/coverage.html.
[74] "Telewave." [Online]. Available: https://www.telewave.com.
[75] "Kathrein." [Online]. Available: https://www.kathrein.com/.
[76] S. Kasampalis, P. I. Lazaridis, Z. D. Zaharis, A. Bizopoulos, S. Zettas, and J. Cosmas, "Comparison of Longley-Rice, ITU-R P.1546 and Hata-Davidson propagation models for DVB-T coverage prediction," *IEEE Int. Symp. Broadband Multimed. Syst. Broadcast. BMSB*, no. June, 2014.
[77] S. Kasampalis, P. I. Lazaridis, Z. D. Zaharis, A. Bizopoulos, S. Zettas, and J. Cosmas, "Comparison of Longley-Rice, ITU-R P.1546 and Hata-Davidson propagation models for DVB-T coverage prediction," *IEEE Int. Symp. Broadband Multimed. Syst. Broadcast. BMSB*, no. July, 2014.
[78] N. Guide, "Waspmote LoRa 868MHz 915MHz SX1272 Networking Guide | Libelium."